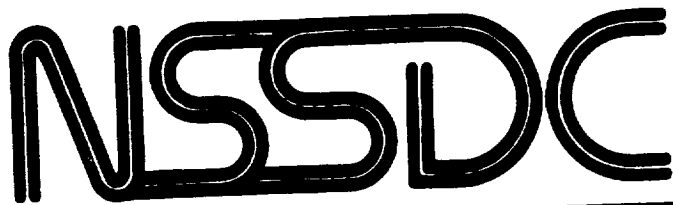


P-132

Scandola



NATIONAL
SPACE
SCIENCE
DATA
CENTER

WORLD DATA CENTER A for ROCKETS AND SATELLITES

88 - 10

Results from Alouette 1, Explorer 20, Alouette 2, and Explorer 31

July 1988

(NASA-TM-101822) RESULTS FROM ALOUETTE 1,
EXPLORER 20, ALOUETTE 2, AND EXPLORER 31
(NASA) 132 P CSCL 08P

N90-29690

03/43 Unclass
0204581



National Aeronautics and
Space Administration

Goddard Space Flight Center



RESULTS FROM ALOUETTE 1,
EXPLORER 20, ALOUETTE 2, AND EXPLORER 31

by

John E. Jackson

July 1988

National Space Science Data Center (NSSDC)/
World Data Center A for Rockets and Satellites (WDC-A-R&S)
National Aeronautics and Space Administration
Goddard Space Flight Center
Greenbelt, Maryland 20771



CONTENTS

	<u>Page</u>
PREFACE	vii
1. ALOUETTE 1 RESULTS.....	1
1.1 Introduction.....	1
1.2 The Topside Sounder Experiment.....	2
1.2.1 Introduction.....	2
1.2.2 Acquisition and Processing of Sounder Data.....	2
1.2.3 Scaling and Interpretation of Sounder Data.....	2
1.2.4 Analysis of Vertical Incidence Reflection Traces.....	3
1.2.5 Global Electron-Density Distribution (Quiet Ionosphere).....	8
1.2.6 Topside Ionosphere (Magnetically Disturbed).....	15
1.2.7 Ionospheric Electron-Density Models.....	18
1.2.8 Ionospheric Irregularities	21
1.2.9 Topside Sounder Resonances.....	24
1.2.10 Various Radio Propagation Factors.....	29
1.3 The Alouette 1 VLF Experiment.....	31
1.3.1 Introduction.....	31
1.3.2 LHR Noise	31
1.3.3 Proton Whistlers.....	34
1.3.4 Short Fractional-Hop Whistlers.....	34
1.3.5 Long-Path Whistlers.....	35
1.4 The Alouette 1 Cosmic Noise Experiment	35
1.4.1 Introduction.....	35
1.4.2 Galactic Noise.....	36
1.4.3 Solar Noise	36
1.5 The Alouette 1 Energetic Particle Experiment.....	37
1.5.1 Introduction.....	37
1.5.2 Average Properties of Outer Radiation Zone at 1000 km.....	38
1.5.3 High-Latitude Boundary of Outer Belt at 1000 km.....	38
1.5.4 Diurnal Intensity Variations of Outer Belt at 1000 km.....	39
1.5.5 Electron Fluxes Outside Outer Belt at 1000 km	39
1.5.6 Temporal Intensity Variations of Outer Belt at 1000 km.....	39
1.5.7 High-Altitude Nuclear Explosions and Inner Belt	39
1.5.8 Auroral Absorption and Precipitated Electrons.....	40
1.5.9 Polar Cap Absorption and Solar Protons.....	40
1.5.10 Auroral Substorms and Electron Fluxes at 1000 km.....	40
1.5.11 Pattern of Auroral Particle Precipitation.....	41
1.5.12 Ionospheric Effects of Precipitated Electrons.....	41
2. EXPLORER 20 RESULTS.....	43
2.1 Introduction.....	43
2.2 Topside Sounder Resonances.....	44
2.2.1 Introduction.....	44
2.2.2 Experimental Observations.....	45

CONTENTS (Continued)

	<u>Page</u>
2.2.3 Theoretical Explanations of Principal Resonances	46
2.3 Investigations of Ionospheric Irregularities	49
2.3.1 Introduction	49
2.3.2 Ducting and Scattering	49
2.3.3 Conjugate Ducts	50
2.3.4 Electron-Density Gradients in Topside Ionosphere	52
2.3.5 Sporadic E	52
3. ALOUETTE 2 RESULTS	53
3.1 Introduction	53
3.2 The Alouette 2 Topside Sounder Experiment	54
3.2.1 Introduction	54
3.2.2 Measurements of Very Low Densities at the Spacecraft	55
3.2.3 Calculations of Electron-Density Profiles	56
3.2.4 Investigations of the z-Trace	56
3.2.5 Global Electron-Density Distribution	57
3.2.6 The Upward Flow of Light Ions	58
3.2.7 Miscellaneous $N(h)$ -Related Studies	59
3.2.8 Medium-Frequency (MF) Ionospheric Ducts	61
3.2.9 Topside Sounder Resonances	64
3.3 The Alouette 2 VLF Experiment	69
3.3.1 Introduction	69
3.3.2 Ion Whistlers	70
3.3.3 Whistler-Mode Noise Emissions	71
3.3.4 Non-Guided Whistlers	72
3.3.5 Rendezvous Experiments	73
3.4 The Alouette 2 Cosmic Noise Experiment	73
3.4.1 Introduction	73
3.4.2 Galactic Noise	74
3.4.3 Solar Noise	74
3.4.4 LF Emissions at 200 kHz	74
3.5 The Alouette 2 Energetic Particle Experiment	75
3.5.1 Introduction	75
3.5.2 High-Latitude Boundary for $E > 35$ keV Outer-Zone Electrons ...	75
3.5.3 Outer Radiation Zone Morphology	77
3.5.4 Solar Proton Profiles	77
3.5.5 Solar Electron Profiles	78
3.5.6 Latitude Cutoff of Solar Particles vs. Rigidity	78
3.5.7 Solar Particles and Closed Field Lines	79
3.6 Cylindrical Probe/Sounder Compatibility Test	79
3.7 Ionospheric Studies with Alouette 2 Cylindrical Probe	80

CONTENTS (Continued)

	<u>Page</u>
4. EXPLORER 31 RESULTS.....	83
4.1 Introduction (General Objectives).....	83
4.2 Summary of Explorer 31 Experiments.....	83
4.3 Thermal Plasma Data from Explorer 31	85
4.4 Topside Morphology (Experiments A, B ₁ , and D).....	86
4.5 Conjugate Point Studies (Experiments A, B ₁ , B _A , and E).....	87
4.5.1 Introduction.....	87
4.5.2 Measurements of Conjugate Photoelectron Flux	88
4.6 Wake Effects (Experiments A, B ₁ , D, and E).....	89
4.6.1 Introduction.....	89
4.6.2 Wake Effects on Electron and Ion Distributions	89
4.6.3 Wake Effects on Electron Temperature	91
4.7 Rocket Rendezvous with ISIS X.....	91
4.8 Langmuir Probe vs. Incoherent Scatter Radar Data	92
4.9 Vertical Temperature and Composition Profiles.....	92
4.10 Suprathermal Electrons (Experiments B _A and B ₁).....	93
REFERENCES.....	95

10/1 INTENTIONALLY BLANK

PREFACE

This report is a continuation of the Alouette-ISIS Program Summary (Jackson, 1986). The concept of the program summary, as developed at the National Space Science Data Center (NSSDC), includes not only a description of the objectives, spacecraft, experiments, and flight performance, but also a complete experiment-related bibliography along with a comprehensive assessment of the technological and scientific accomplishments. The 1986 Program Summary includes all the above items except the discussion of the scientific accomplishments. The present report provides the scientific results from the first four of the six spacecraft of the Alouette-ISIS program, namely Alouette 1, Explorer 20, Alouette 2 and Explorer 31. These spacecraft were designed, built and launched during the first decade of NASA (1958-1968), a period during which the NASA space program experienced its highest rate of expansion. The first of the above spacecraft, the Canadian satellite Alouette 1 provides a perfect example of a very early space mission with rapid development, international prestige and worldwide participation.

In December 1958, a few months after the creation of NASA, the Defence Research Telecommunications Establishment (DRTE) in Ottawa, Canada proposed an ambitious and bold satellite program of ionospheric investigations to be carried out in cooperation with NASA. The Canadian proposal was ambitious because it would in effect assume the responsibility for much of NASA's planned effort in the ionosphere discipline. The boldness was in the experimental approach which required technology that did not exist in 1958. Because of the remarkable success of their program, the Canadians actually carried out space missions that NASA would otherwise have had to undertake. The Canadian competence was also a valuable addition to NASA's ionospheric team. Because of the Canadian leadership in ionospheric research, many NASA ionosphere scientists proceeded during the mid and late sixties to build their own programs around that of Canada. This is exemplified by the second spacecraft discussed in this report (Explorer 20) and by the fourth spacecraft (Explorer 31), which was launched simultaneously with Alouette 2. The scientific cooperation between Canada and the United States culminated in the two ISIS satellites which, however, are not discussed in the present report.

The organization of this report is by spacecraft in chronological order. Thus, the report begins with a discussion of Alouette 1, followed by Explorer 20, Alouette 2 and Explorer 31. The scientific results for the period September 29, 1962 to August 25, 1964 were based almost entirely on Alouette 1. Later publications, however, were frequently based on results from two or more spacecraft. Typically, these results are presented only once in this report and they appear with the discussion of an earlier spacecraft whenever this leads to a more logical organization of the text. This policy tends to make the Alouette 1 portion of the report slightly longer than it would have been otherwise. This procedure, however, has

also led to the inclusion of certain ISIS 1 and ISIS 2 results that appeared in publications based on both ISIS and earlier spacecraft. Because of its importance throughout the Alouette-ISIS program, and because it was by far the most important investigation on Alouette 1, the topside sounder technique is discussed in great detail in the beginning of the report under Alouette 1. This also lengthens the Alouette 1 discussion. The main factor, however, contributing to the length of the Alouette 1 portion of this report is the total number of Alouette 1 publications. This number exceeds by at least 60 percent the total publications for any of the succeeding spacecraft of the Alouette-ISIS program (Jackson, 1986, Fig. 1).

The compilation of the present report was made possible by the support of the NSSDC management, particularly Dr. James I. Vette and Dr. Joseph H. King, and by the use of the NSSDC resources, especially the Technical Reference File (TRF), a computerized space science literature file. This file contains some 38,000 literature citations coded according to satellite(s) and experiment(s). The task of producing a program summary and scientific overview can thus be greatly simplified with the help of appropriate computer printouts from the above NSSDC file. In this regard, the author is indebted to Patricia Ross for supervising the production from TRF of numerous printouts giving comprehensive bibliographies relevant to each experiment discussed in this report, and for supervising the computer compilation of the list of references at the end of the report. The author is also grateful for the extensive editorial assistance provided by Mary Elsen and Robert Richards.

1. ALOUETTE 1 RESULTS

1.1 Introduction

Alouette 1, the first satellite designed and built by a nation other than the United States or the Soviet Union, was constructed at a time when most satellites had a useful lifespan of a few months. Although Alouette 1 was as complex as any previously launched satellite, rapidly advancing technology and the extreme care exercised in all phases of the Alouette 1 development had led the Canadian builders to expect that their satellite would operate for at least 1 year. Their most optimistic prediction was 5 years of declining usefulness. No one, least of all the project team, would have dreamed of the 10-year life that was actually achieved by Alouette 1. Many, in fact, shared the more conservative view of John Chapman, the leader of the Canadian team, who stressed that even 3 months of operation should be considered a complete success, since this would contribute enormously to the then very limited knowledge of the topside ionosphere. In its first 3 months of operation, Alouette 1 produced some of the most exciting data obtained during the entire 50-year history of ionospheric research, and it continued to provide valuable information until its tenth birthday.

Alouette 1 is best known for its swept-frequency topside sounder experiment. The other experiments (VLF, cosmic noise, and energetic particle measurements) were, however, equally successful and they also remained operational for 10 years. The Alouette 1 mission resulted in over 300 publications¹ in refereed scientific journals. About 80 percent of the Alouette 1 publications were based on the ionograms obtained from the topside sounder experiment. In its first 3 years of operation, Alouette 1 obtained over a million ionograms, each equivalent to a snapshot of the ionosphere from the Alouette 1 altitude of 1000 km down to an altitude of about 300 km. These ionograms have provided data at all geomagnetic latitudes and at geographic latitudes ranging from 80 deg N to 80 deg S. After 10 years, Alouette 1 had produced two million ionograms.

The wealth of information provided by Alouette 1 (and to a lesser extent by the later satellites of the Alouette/ISIS program) also has led to an unusually large number of summary papers (Nelms, 1964; Davies, 1965; Bourdeau et al., 1965; Chapman, 1966; Calvert, 1966c; Paghis et al., 1967; Chapman and Warren, 1968; King, 1969a; Jackson and Warren, 1969; Eccles and King, 1970; Nelms and Chapman, 1970; Bowhill, 1970; Jackson et al., 1980; Cogger, 1982).

¹ This number includes about 60 publications based partly on Alouette 1 and partly on other satellites of the Alouette-ISIS program.

1.2 The Topside Sounder Experiment

1.2.1 Introduction

The data from the topside sounder have been processed into ionograms having essentially the same format as that used since the late thirties for ground-based soundings. The use of a data presentation that was familiar to ionosphericists throughout the world and the rapid availability of these data to the international scientific community were additional reasons for the extraordinary success of the Alouette 1 mission. Because of this extensive international participation, a considerable amount of effort was devoted to the development of data processing and data analysis techniques, resulting in a rather extensive literature on these topics. The discussion of the Alouette 1 topside sounder experiment will therefore include the technical and scientific contributions in the areas of data processing and analysis.

1.2.2 Acquisition and Processing of Sounder Data

The techniques used for the acquisition and processing of the data from a given satellite tend to be of very limited interest outside the small group directly concerned with the data handling responsibility. In the case of the topside sounder experiment, these techniques were of considerable interest to a dozen or so research institutions throughout the world who participated in the acquisition and processing of topside sounder data.

Most of the sounder data were acquired and processed using the system described by Franklin et al. (1969). Particularly helpful to the users of ionograms is the detailed analysis of range resolution and range accuracy given by Franklin et al. (1969). Further information on range accuracy has been given by Franklin and Bibby (1969) (Appendix E, Minutes of the 19th ISIS Working Group Meeting). A discussion of frequency calibration and frequency accuracy has been given by Benson (1969, 1972a, b). Although the format is basically the same for all Alouette-ISIS ionograms, significant differences exist in sounding ranges, frequency ranges, and sweep rates with corresponding differences in range and frequency calibrations. The various ionogram formats used for Alouette 1, Alouette 2, ISIS 1 and ISIS 2 have been described by Jackson (1988).

The elaborate system described by Franklin et al. (1969) was needed for maximum quality and reliability. Useful data have also been obtained using the much simpler arrangements described by Ferguson and Green (1969) and by Arendt et al. (1969).

1.2.3 Scaling and Interpretation of Sounder Data

An ionogram contains a wealth of information, typically 5×10^5 pixels, each with an associated intensity. Ionograms exhibit a great variety of electromagnetic phenomena, but only a small fraction of the available

information is used for any given application. Selection of the useful data is a problem in pattern recognition, a task which for many years was considered beyond the capability of existing digital computers,² but one that a trained operator can (in most cases) perform with relative ease (Hagg et al., 1969; Watt, 1967, 1969).

The features of interest in a topside ionogram can be classified in four broad categories, each category being the basis for a unique group of scientific investigations. These categories are (1) reflection traces that can be used to derive the electron density N as a function of the altitude h (see Sections 1.2.4.1 to 1.2.4.4); (2) reflection traces that are generally unsuitable for $N(h)$ analysis, but are instead either a measure of ionospheric irregularities such as spread-F echoes (see Sections 1.2.8.1 to 1.2.8.6) and sporadic-E echoes³ or a measure of the total electron content between the satellite and the ground such as ground echoes;³ (3) local resonances which can be used for a great variety of plasma physics studies (see Sections 1.2.9.1 to 1.2.9.6); and (4) radiofrequency signals, such as auroral kilometric radiation (observed mainly with ISIS 1), that are unrelated to sounder transmissions and therefore observable with the swept-frequency receiver whether or not the sounder transmitter is turned on.

1.2.4 Analysis of Vertical Incidence Reflection Traces

1.2.4.1 Simplified Analysis

Detailed scaling of a reflection trace (vertical incidence ionospheric echoes) and extensive computer processing are required to obtain vertical electron-density profiles. The scaling is at least one order of magnitude simpler, and a computer is not needed if only the density at the satellite and/or at the peak of the F2 region is desired. The simpler scaling procedure was the basis for a number of ionospheric studies, done mostly during the early days of topside soundings (Hagg, 1963; Thomas and Sader, 1964; Dayharsh and Farley, 1965). These studies typically involved the simplified scaling of a

² Routine computer scaling of topside ionograms has recently been achieved by Reinisch and Huang (1982). A variety of ISIS 1 and ISIS 2 ionograms was used to test this new scaling procedure.

³ At frequencies greater than the critical frequencies of the F2 region, topside ionograms occasionally exhibit echoes returned either from E-region irregularities known as sporadic E (see Section 2.3.5) or from the ground (see Section 1.2.4.4, 3rd paragraph). The retardation observed on the ground echo is a measure of $\int_0^{h_s} Ndh$, where h_s is the satellite height.

few thousand ionograms. The simpler scaling procedure was performed to a considerably greater extent by the topside sounder team at the Defence Research Telecommunications Establishment (DRTE)⁴ in Ottawa, Canada.

All Alouette 1 ionograms recorded between 1962 and 1968 have been scaled for the electron density at the satellite and at the peak of the F2 region. These measurements have been tabulated, together with appropriate orbital and geophysical parameters. The tables also include data concerning the presence (or absence) of spread F, sporadic E, and ground echoes. Performing the required manual scaling, data interpretation, and evaluation on about one and a half million ionograms was truly a monumental data analysis task. The results were published in the 114 volumes of Alosyn data (Alouette topside sounder synoptic data). The Alosyn books have been used as a source of reduced data for various synoptic studies (King et al., 1968d; Chandra and Krishnamurthy, 1968; Fatkullin, 1970a; Gondhalekar, 1973; Gondhalekar and King, 1973; Sharma and Hewens, 1976) or as a catalogue raisonné from which ionograms could be selected for further analysis (Soicher, 1973).

Titheridge (1976c) devised a very simple technique for obtaining the slope dN/dh of the vertical electron-density profile at the satellite height. This slope, according to the diffusive equilibrium theory (see Section 1.2.5.3), provides information on the plasma temperature and composition at the satellite height. Titheridge showed that the slope could be calculated with an accuracy of 5 percent from a simple formula that utilizes data routinely compiled for Alosyn and one additional parameter that is easily scaled from an ionogram. Titheridge used ISIS 1 ionograms to illustrate his technique because a wide variety of dN/dh values was thus available, and because the high quality of ISIS 1 ionograms made it possible to calculate the full electron-density profile from which dN/dh can be accurately determined.

1.2.4.2 Calculation of Vertical Electron-Density Profiles

Alouette 1 was initially planned as a topside sounder satellite as part of a topside sounder program conducted jointly by Canada and the United States. Although other experiments were added later, topside soundings remained the principal experiment on Alouette 1. The original purpose of topside soundings was to provide data from which the electron density N could be derived as a function of altitude h . The calculation of $N(h)$ from topside sounder data is a problem that has received considerable attention (Thomas et al., 1963; Fitzenreiter and Blumle, 1964; Doupnik and Schmerling, 1965;

⁴ DRTE became the Communications Research Centre (CRC) in April 1969.

Vasseur and Felstein, 1968; Jackson, 1969a, and other papers cited later). Since this type of calculation was required for a large number of Alouette/ISIS publications, an outline is given here of the basic concept involved and of the limitation of the procedure.

The basic measurement of a topside sounder is the time t required for a pulse radio signal to propagate to its reflection point and return to the sounder. The apparent path length P' defined as $ct/2$ (where c is the velocity of light in vacuum) is related to the propagation path p by the formula:

$$P'(f) = \int_{p_0}^{p_r(f)} n' [N(p), f, B(p), \phi(p)] dp$$

where

n' = group refractive index,⁵

B = magnitude of the terrestrial magnetic field,

ϕ = angle between the magnetic field vector and direction of propagation,

p_0 = location of sounder,

$p_r(f)$ = location of reflection point at frequency f .

and other terms have been previously defined. The basic sounder data are presented in the form of ionograms or $P'(f)$ records which show the apparent path length P' as a function of frequency. The equation was written in terms of a generalized propagation path p to indicate that the sounder data do not necessarily correspond to "vertical" incidence. The propagation path is, however, essentially a vertical path if the electron-density distribution is a function of altitude alone (spherically stratified ionosphere). In this case the variable p in the equation becomes the altitude h and the equation thus modified shows the relationship between the $P'(f)$ ionogram data and the desired vertical electron-density profile $N(h)$. The $N(h)$ function is obtained from the equation by an inversion procedure. Most $P'(f)$ to $N(h)$ inversion techniques assume that stratification is essentially spherical within the ionospheric region from which the sounding echoes are received, and that the propagation path is vertical.

⁵ See Equation 2.119 on p. 93 in Davies (1966).

The inversion techniques used with topside ionograms are similar to the techniques developed earlier for ground-based soundings (Special Issue of *Radio Science*, Oct. 1967). With topside data, however, much greater care must be exercised in the handling of the magnetic field parameters in the equation.

Since topside soundings are obtained from a moving platform, the continuous satellite motion also must be taken into consideration. The $P'(f)$ to $N(h)$ conversion for topside ionograms requires the manual scaling of a reflection trace (usually the extraordinary one) and extensive computer processing of the resulting $P'(f)$ data. This relatively laborious analysis has been carried out for over 60,000 Alouette 1 ionograms. Most of this work was done at DRTE (now CRC) in Ottawa. Other participating agencies included the Ames Research Center of NASA and the Radio and Space Research Station in Slough, England. An excellent summary of the available topside sounder data has been given by King (1969b).

1.2.4.3 The $P'(f)$ to $N(h)$ Inversion for Complex Ionograms

The investigations discussed in Section 1.2.4.3 were conducted to solve $P'(f)$ to $N(h)$ inversion problems met primarily with topside soundings from altitudes greater than 2000 km (high-altitude Alouette 2 and ISIS 1 ionograms). Although these investigations were caused primarily by Alouette 2 data, the resulting refinements in $P'(f)$ to $N(h)$ inversion techniques will be given here to provide greater continuity in the discussion of this topic.

On many high-altitude ionograms the low-frequency portion of the reflection trace is missing or cannot be scaled with adequate accuracy. Analysis techniques were developed to solve this problem (Jackson, 1972). It was also found that some of the iteration techniques developed for the analysis of Alouette 1 ionograms would not converge when applied to some of the very high-altitude Alouette 2 ionograms. More refined iteration procedures were developed to overcome this difficulty (Lockwood, 1970).

Nonvertical propagation tends to become a more serious problem with high-altitude ionograms. Oblique propagation can be caused by departure from spherical stratification, a problem investigated by McCulley (1972). Another common deviation from vertical propagation occurs when the soundings are guided by irregularities aligned with the terrestrial magnetic field. Techniques for analyzing the corresponding field-aligned traces have been developed by Jackson (1972) and Lockwood (1972).

On some ionograms either the direction of propagation or the scaled $P'(f)$ values may be uncertain. This difficulty has been overcome to some extent by using computer-aided scaling techniques in which the computer calculates and plots the ordinary trace based on the operator's extraordinary

trace scaling. The operator compares the computed and observed ordinary traces and uses this information to revise the original scaling. The procedure is repeated until satisfactory agreement is achieved (Lockwood, 1972).

1.2.4.4 Accuracy of the $P'(f)$ to $N(h)$ Inversion

Because of its complexity and underlying assumptions, the $P'(f)$ to $N(h)$ inversion techniques have been subjected to extensive theoretical and experimental tests.

It is well known that the geomagnetic field causes deviations from vertical propagation even in a spherically stratified ionosphere. It had also been known for at least two decades before the advent of topside soundings that these deviations can be ignored in the analysis of ground-based soundings. Much greater lateral deviations were expected in topside soundings where path lengths can be an order of magnitude greater than those occurring in ground-based soundings. The magnitude of the resulting errors were, however, unknown. The problem of lateral deviations in topside soundings was investigated theoretically in Canada and in the United States. The most complete documentation on this subject was presented by Colin et al. (1969a), who found that lateral deviations up to 500 km can occur for topside soundings from a height of 3000 km. Colin et al. (1969a), however, concluded that "the resultant effects on analysis accuracy were generally tolerable" for a spherically stratified ionosphere. Colin et al. (1969a) also investigated the effects of lateral deviations in the presence of modest horizontal gradients in the electron-density distribution and concluded that the combined effects could introduce serious errors in the analysis.

The accuracy of the $P'(f)$ to $N(h)$ inversion also was checked by a number of experimental procedures, the easiest one being to compare topside soundings with bottomside soundings obtained at the same location and time (Dot and Faynot, 1965; Arendt and Papayoanou, 1965; Bernard and Taieb, 1970; and Becker, 1971). Due to the difficulty of finding a statistically significant number of good space and time coincidences under quiet ionospheric conditions, the results tend to be inconclusive. The most detailed investigation of simultaneous topside and bottomside soundings was conducted by Jackson (1969b) using Alouette 1 and 2 ionograms obtained from altitudes ranging from 520 to 2200 km. He concluded that the $N(h)$ profiles deduced from topside soundings had a tendency to be too low. At the height of maximum density ($h_m F_2$) the error was found to increase with satellite altitude, resulting in an overlap between topside and bottomside profiles. The errors in the topside profiles, however, were usually found to be too small to detract from the general usefulness of topside ionograms. A unique aspect of Jackson's study was the use of the ground reflection traces to check the combined topside and bottomside profiles.

Incoherent backscatter soundings of the ionosphere were also used to check the accuracy of topside $P'(f)$ to $N(h)$ inversion (Calvert, 1966c; Cohen and Van Zandt, 1967). The most detailed study seems to be that of Fleury and Taieb (1971) who found that the topside profiles agreed with the incoherent scatter profiles in 17 out of the 20 cases investigated. The three other cases showed overlaps comparable to those found by Jackson (1969b).

One attempt was made to check an Alouette 1 profile with a sounding rocket measurement (Bauer et al., 1964). This measurement showed that the Alouette 1 profile was slightly lower than the rocket profile. The results of the various experimental comparisons discussed above can be summarized as follows: the profiles derived from topside ionograms are either correct or too low, they cannot be too high, if the ionograms have been properly scaled.

1.2.5 Global Electron-Density Distribution (Quiet Ionosphere)

1.2.5.1 Introduction

One of the most important results of the Alouette 1 mission was to provide the first worldwide picture of the electron-density distribution in the topside ionosphere. Previous data of this type had been limited to a few rocket measurements and incoherent backscatter soundings at three or four locations. The first week of topside soundings provided more information about the topside electron-density distribution than had been obtained from all sources prior to the Alouette 1 launch. The Alouette 1 orbit was such that (1) data were obtained at all geomagnetic latitudes and (2) a full diurnal cycle was achieved in 3 months; i.e., once for each season. These characteristics, combined with the extraordinary longevity of Alouette 1 (resulting in data for nearly a full solar cycle), led to the most comprehensive survey ever conducted of the topside ionosphere. A wealth of information was obtained on the global morphology of the topside ionosphere, resulting in approximately 125 publications on various aspects of this broad subject. Because of the very large number of publications, many of these have not been quoted in the overview. The overview summarizes the typical investigations that have been conducted and provides representative references in each case.

A few studies, based on early (1962-1963) observations, have provided the first information on the diurnal and seasonal variations of the "pole-to-pole" electron-density distribution in the topside ionosphere (Nelms, 1966; Thomas and Rycroft, 1970). The data provided by Nelms (1966) covered the region near 75 deg W longitude, under magnetically quiet ($K_p < 3$) conditions. Twelve "pole-to-pole" sets of data for different local times approximately 2 hours apart were given for a period near the June solstice. A similar group of data was given for a period near the March equinox. The "pole-to-pole" electron-density contours show that the quiet topside ionosphere can be divided into three geomagnetic latitude regions: equatorial ± 20 deg, midlatitude ± 20 to ± 70 deg, and high latitude ± 70 to ± 90

deg (Paghis et al., 1967). In addition to diurnal and seasonal variations, these regions exhibit (even under quiet magnetic conditions) a large number of irregularities (spread F, ducts, troughs, ledges, etc.) and anomalies.⁶ Most of the Alouette 1 publications on the topside morphology are concerned either with one of the three regions or with a specific ionospheric phenomenon (such as a given anomaly, a type of irregularity, eclipse effects, or storm behavior). The topics to be discussed in Section 1.2.5 are related primarily to the quiet undisturbed ionosphere. Results related to ionospheric storms are given in Section 1.2.6.

1.2.5.2 The Equatorial Ionosphere

The morphology of the topside equatorial ionosphere has been studied primarily in two longitude zones, the first one close to 105 deg E (Asian sector), the second one close to 75 deg W (American sector). The first investigation of the topside anomaly in the Asian sector was conducted by King et al. (1964). A similar study was carried out for the American sector by Lockwood and Nelms (1964). Both studies were based upon Alouette 1 data for the period October to December 1962. These early studies revealed essentially the same general diurnal development and decay of the equatorial anomaly in the topside ionosphere. Shortly after sunrise the constant-density contours exhibit a single peak centered above the magnetic equator. When the anomaly develops later during the morning, two peaks are observed, one on each side of the magnetic equator. When the peaks are first observed, they are present only at altitudes less than about 500 km. By midafternoon the peaks can be seen, typically up to an altitude of about 800 km. These peaks are aligned with a different magnetic field line at different local times. The peaks are usually not symmetrical (in either amplitude or location) with respect to the magnetic equator. The asymmetry, however, is more pronounced in amplitude than in location. The anomaly disappears gradually in the late afternoon. The main difference between the results of King et al. (1964) and Lockwood and Nelms (1964) was in the local times of initial appearance and decay of the anomaly. The anomaly seemed to develop earlier and decay sooner in the Asian sector than in the American sector. Additional information on the equatorial topside ionosphere, based on data for the period October 1962 to December 1963, has been provided by Rush et al. (1969), who showed that the topside anomaly was symmetric about the dip equator when the sun was over the dip equator. The

⁶ The term ionospheric anomaly is used when the electron-density variation departs significantly from simple solar control. Equatorial anomaly refers to the fact that N is not maximum at the equator when the sun is directly overhead. The ionospheric seasonal anomaly refers to electron densities being greater in winter than in summer.

asymmetry was most clearly developed at 75 deg W during the December solstice, the anomaly crest being more pronounced in the summer hemisphere. A more recent study by Sharma and Hewens (1976) using Alosyn density data at $h_m F_2$ for approximately 1120 equatorial passes during low sunspot years (1962-1964) at longitudes between 55 and 90 deg W showed that the anomaly develops essentially at the same local mean time in the Asian and American sectors. The discrepancy between the results of Lockwood and Nelms (1964) and the results of King et al. (1964) was due to insufficient data between 0930 and 1100 h LMT in the work of Lockwood and Nelms. Sharma and Hewens (1976) also found pronounced seasonal variations in the morphology of the topside anomaly. The evening disappearance of the anomaly occurs at an earlier local time during the months of November, December, January, and February than during other months of the year. The position and amplitude asymmetries of the anomaly peaks also were shown to depend upon the season. Topside sounder data also have been used to supplement aircraft and ground-based studies of the equatorial anomaly in the African sector (Vila, 1971).

The new information on the equatorial anomaly made possible the development of theoretical models. Most theories are based upon the interaction of the ionosphere with the earth's magnetic field via mechanisms involving drifts and currents. Some theories have considered control due to production, loss and temperature effects. Considerable success has been achieved by various authors in reproducing from basic theory the experimentally observed characteristics of the topside anomaly (Goldberg, 1969).

King and Eccles (1968) used topside sounder data to investigate the equatorial ionosphere during the annular solar eclipse of November 23, 1965. The eclipse day was very quiet magnetically. The equatorial region near 105 deg E was eclipsed from 0930 to 1230 h LMT; i.e., during a significant part of the anomaly development phase. An Alouette pass at the same longitude at 1500 h LMT showed that the eclipse had no effect on the development of the equatorial anomaly.

King and Reed (1968) showed that the topside electron densities in the equatorial ionosphere increased by a factor of between 2 to 5 during periods of enhanced 10.7 cm solar flux. The effect was found to be more pronounced at a latitude where the magnetic dip was 30 deg than it was above the magnetic equator. There was no corresponding effect on the critical frequencies of the F2 region. King and Reed concluded from these observations that the entire topside electron distribution was displaced upward during periods of enhanced solar flux.

1.2.5.3 The Midlatitude Ionosphere

The electron-density distribution in the topside ionosphere most nearly approximates spherical stratification under midlatitude, daytime conditions,

as can be seen in typical pole-to-pole constant density contours (Nelms, 1966). During the night, however, the contours tend to be irregular at all latitudes.

Bauer and Blumle (1964) have shown that the diurnal variation of the midlatitude ionosphere decreased with altitude, the amplitude of the variation being approximately four times greater at 400 km than at 1000 km. This behavior changed drastically north of the 70 deg magnetic dip line, where the normalized variations at 400 and at 1000 km were found to be basically the same. These observations led Bauer and Blumle to conclude that the 70 deg dip line represents an approximate northern boundary for the midlatitude ionosphere. Midlatitude diurnal variations also were studied by Legg et al. (1967) and by Dyson (1967c) using Alouette 1 data for the Asian sector (Southern Hemisphere). Each study included data for two seasons. Both studies showed that a secondary maximum was present near midnight at all altitudes between 400 and 1000 km. This secondary maximum could not be seen by Bauer and Blumle (1964) because their study did not include sufficient data for the period 2200 to 0200 h LMT.

The studies of Legg et al. (1967) and of Dyson (1967c) showed no evidence of the seasonal anomaly at heights above 400 km, in complete contrast to the ionospheric behavior below $h_m F2$. Dyson (1967c) noted a diurnal anomaly in winter (nighttime density values as large as or larger than daytime values). King et al. (1968c) showed that the seasonal anomaly was completely absent at 1000 km in the American sector at all geographic latitudes between 20 deg N and 60 deg N. Fatkullin (1970a) showed that the midlatitude seasonal anomaly extends to heights above $h_m F2$ in a manner that depends upon latitude. In the Northern Hemisphere in the American sector, the anomaly reaches its maximum height of 500 km at geographic latitudes between 46 and 53 deg N. Fatkullin (1970b) also found that the altitudinal extension of the seasonal anomaly was dependent on local time, the maximum upward extension being observed between 1400 and 1500 h LMT.

At midlatitudes the topside electron density decreases exponentially with altitude as would be predicted by the diffusive equilibrium theory (Johnson, 1960). In its simplest form this theory relates the slope of the vertical electron-density profile to the average ionic mass and to the effective plasma temperature (average of electron and ion temperature). In the more complete theory the height derivative of the effective temperature must be included in the slope formula. Since the ionic mass is basically 16 (O^+) for a few hundred kilometers above $h_m F2$, the diffusive equilibrium theory provides a way to derive the plasma temperature from a vertical electron-density profile (if temperature gradients are negligible). Conversely, if the temperature is assumed to be constant, one can infer changes in average ionic mass as a function of altitude. Early attempts to interpret midlatitude topside electron-density profiles in this manner have been made by Bauer

and Blumle (1964), Thomas and Dufour (1965), Watt (1965), and Smith and Kaiser (1967). Bauer (1969) has pointed out that these interpretations were not necessarily correct since they were based upon assumptions concerning the altitude variations of the parameters involved. In recent years, however, an increased understanding has been achieved of the many factors that control the shape of vertical electron-density profiles. This new knowledge has enabled Titheridge (1976a, b) to derive reliable O^+/H^+ ion transition height and plasma temperature information from a large number (60,000) of electron-density profiles obtained with Alouette 1. Titheridge has shown that his analysis techniques yield dependable results, not only at midlatitudes, but also at low and high geomagnetic latitudes. The work of Titheridge has yielded the diurnal and seasonal variations of ion-transition height and plasma temperature, for geomagnetic latitudes between 90 deg N and 75 deg S under solar minimum conditions. Although less accurate than direct measurements, Titheridge's results were useful because they filled gaps where direct measurements were not available.

The midlatitude topside ionosphere during sunrise also was investigated with the Alouette 1 topside sounder data. Initial studies of the sunrise behavior (King et al., 1968a; Watt, 1971) were based on a small number of Alouette 1 passes occurring near sunrise. On such passes, the solar zenith angle could vary from 105 to 95 deg over a latitude range of about 12 deg. The sunrise behavior could therefore be seen on a single pass if the latitudinal variation effects were negligible. Based upon a study of three satellite passes near sunrise, Watt (1971) concluded that the electron density exhibits a sharp decrease at all altitudes as the solar zenith angle decreases from 105 to 98 deg. Further decrease in solar zenith angle results in a rapid increase in density.

A more comprehensive study of midlatitude sunrise phenomena was conducted by Soicher (1973) in which latitudinal and solar zenith angle effects were separated by using data from 40 sunrise orbits. Soicher showed that the topside sunrise behavior exhibits a strong latitudinal control. South of 55 deg N the sunrise effects include temperature increases and ion mass changes. North of 55 deg N the sunrise variations are characterized mainly by temperature increases. Topside electron densities at fixed altitudes decrease with increased illumination at all altitudes and latitudes until the time of ground sunrise.

Alouette 1 topside sounder data were used by King et al. (1967b) and by Smith and King (1969) to investigate the effects of two solar eclipses upon the midlatitude topside ionosphere. Measurements were made during the annular eclipse of January 25, 1963, and during the partial eclipse of January 14, 1964, both of which occurred in the South Atlantic region during magnetically quiet days. The eclipse effects were presented as a function of magnetic dip to facilitate comparisons with control days. The electron-density was found to decrease, typically by a factor of 2, at all heights and locations investigated during an Alouette 1 pass on January 25,

1963, that occurred 20-70 min after the middle of the eclipse. Maximum effects were seen at a dip of 60 deg S (approximately 50 deg geomagnetic) due to a combination of percent obscuration and local time differences between the eclipse and the Alouette pass. For the eclipse of January 14, 1964, data were obtained 11 min before, 93 min after, and 200 min after the center of the eclipse. During both eclipses the greatest percent reduction in electron-density occurred at an altitude of 400 km. The data indicated that the topside ionosphere had returned to normal by about 3 hours after the center of the eclipse.

1.2.5.4 The High-Latitude Ionosphere

According to Paghis et al. (1967), the ± 70 deg geomagnetic latitude can be considered as the boundary between high-latitude and midlatitude ionospheres. This definition is consistent with the daytime contrast between the very irregular electron-density contours in the ± 70 to ± 90 deg (polar) regions and the smooth, low-gradient contours in the ± 20 to ± 70 deg (midlatitude) regions. Many characteristics of the polar ionosphere, however, are evident, particularly during the night, at geomagnetic latitudes between 50 and 70 deg. Thus, Bauer and Blumle (1964) have suggested that the 70 deg dip line (corresponding to 50 deg geomagnetic latitude) could be taken as the boundary between midlatitude and polar ionospheres. Many authors (Thomas et al., 1966; Nishida, 1967; Jelly and Petrie, 1969), have included the 50 to 70 deg geomagnetic latitude range in their discussions of the polar ionosphere. The topside ionosphere morphology discussed in Section 1.2.5.4 is based primarily upon Northern Hemisphere data obtained in the geomagnetic latitude range from +50 to +90 deg.

The high-latitude topside ionosphere was virtually unknown prior to the advent of the Alouette 1 satellite. The Alouette 1 topside sounder data has shown that this region exhibits a series of maxima (peaks) and minima (troughs) as a function of latitude⁷ (Thomas et al., 1966). According to Thomas et al. (1966), the principal features of the polar ionosphere are (1) the midday polar peak observed at about 75 deg geomagnetic; (2) the nighttime auroral peak seen around the auroral zone, and (3) the nighttime "midlatitude" trough found near 58 deg geomagnetic. In one of the most

⁷ The latitudinal maxima have been referred to as peaks in the literature. These maxima should not be confused with maxima in vertical profiles, which are also called peaks. The latitudinal minima have been called troughs, because of their east-west persistence on successive satellite passes.

quoted papers⁸ of the Alouette-ISIS program, Muldrew (1965) showed that troughs were a persistent feature of the nighttime high-latitude ionosphere. The midlatitude (or main) trough is first seen in the late afternoon at about 70 deg geomagnetic. It gradually moves to lower latitudes during the evening hours. At 2200 h LMT the main trough is at about 58 deg geomagnetic latitude, and it stays at that latitude until sunrise. Muldrew (1965) also showed that the high-latitude troughs (i.e., the low-density regions between the high-latitude peaks) were also centered on the geomagnetic poles. Muldrew (1965) suggested that the main trough was a low-altitude extension of the plasmapause, because the magnetic L lines (McIlwain, 1961) through the main trough were approximately the same as the L lines corresponding to the plasmapause. Later studies (Rycroft and Thomas, 1970; Rycroft and Burnell, 1970) have shown that the main trough and the magnetospheric plasmapause are located on the same L line for a given value of K_p .

The trough studies of Muldrew (1965) were based mainly upon topside sounder data for $h_m F_2$. The main features of the topside polar ionosphere as a function of altitude were obtained by Nishida (1967). Over 3000 Alouette 1 $N(h)$ profiles were used in this work. Nishida's results showed that the general characteristics of the main trough could be seen at all altitudes up to the height of Alouette 1 (1000 km). The overall complexity of the electron-density contours (at fixed heights) was found to decrease as a function of altitude. Because of the averaging process used in the analysis, Nishida's results tend to eliminate much of the complex structure of the polar ionosphere. Nishida's results, however, are useful as a smoothed average picture of the polar ionosphere.

Sato and Colin (1969) showed that the electron density peaks at 1000 km tend to cluster in three well-defined regions around the geomagnetic pole. Region 1 includes all geomagnetic latitudes greater than 80 deg and magnetic local times centered at 0500 and 1800. Region 2 is located between 75 and 80 deg, and region 3 extends typically from 60 to 70 deg geomagnetic. Peaks occur primarily in the daytime in region 2 and during the night in region 3. Sato and Colin (1969) showed that the peak clustering could be caused by particle ionization due to precipitation of low-energy electrons ($E < 1$ keV). From their study of the topside polar ionosphere, Thomas and Andrews (1969) have concluded that poleward of the main trough the ionization is due mainly to particle precipitation.

⁸ The paper by Muldrew (1965) was quoted 148 times during the period 1965-1977, according to the "Citation Classic" in *Current Contents*, 19, no. 2, p. 10, Jan. 8, 1979.

As mentioned earlier the main trough is a nighttime phenomenon. Consequently the excellent correlation between the main trough and the plasmapause is also a nighttime phenomenon. Titheridge (1976e) derived from the analysis of topside $N(h)$ profiles some features of the topside ionosphere at 1000 km that correlate with the plasmapause at all times of the day. Titheridge used the techniques discussed in Section 1.2.5.3 (4th paragraph) to calculate mean plasma temperatures and ion composition data. The resulting temperature versus latitude data exhibited a broad maximum corresponding to the plasmapause. The ion composition data also could be used to define the position of the plasmapause. A second and much sharper maximum in the daytime temperature data was located beneath the magnetospheric cleft at a geomagnetic latitude of about 77 deg (Titheridge, 1976d).

1.2.6 Topside Ionosphere (Magnetically Disturbed)

1.2.6.1 Introduction

The effect of magnetic disturbances on the ionosphere below $h_m F2$ has been investigated since the late thirties (Berkner et al., 1939). The early studies showed that a large decrease in electron density occurs near the peak of the F region during the main phase of a geomagnetic storm. In some cases (G-condition) the maximum density of the F2 region becomes less than the maximum density of the F1 region. Conversely, such ionospheric behavior is nearly always associated with magnetic storms.

1.2.6.2 Scale Heights vs. K_p

The data from Alouette 1 provided the first opportunity to investigate the behavior of topside $N(h)$ profiles as a function of geomagnetic activity. Watt (1966) found that the ionospheric scale height

$$H = N \frac{dh}{dN}$$

at 700 km decreases at night with increasing values of the magnetic index K_p . Watt found no correlation between K_p and daytime scale heights. Watt's study was limited to dip latitudes between 48 deg N and 72 deg N and to K_p values less than 4+ (which are hardly within the storm regime). Using Alosyn data for the period October 10, 1962, to March 31, 1963, Chandra and Krishnamurthy (1968) showed that the electron densities at the satellite, N_s , and at the peak of the F2 region, N_m , show a positive correlation with K_p only at magnetic dips between 45 and 50 degrees. Positive correlations were found for N_s at the dip zone 65-75 and for N_m at the dip zone 0-5. King et al. (1967a) have shown that abnormally small ionospheric scale heights occur in the region of the South Atlantic anomaly

during magnetic disturbances. King et al. suggested that this localized phenomenon was due to electrons dumped from the radiation belt.

1.2.6.3 Effects Below and Above 500 km

Ondoh (1967) showed that the effect of magnetic storms on topside profiles is often opposite below and above 500 km. King et al. (1967c) also reported this difference between low- and high-altitude behavior. In addition, King et al. observed latitude variations and the fact that the equatorial anomaly was less pronounced during storms. Sato (1968) extended considerably the scope of previous studies by describing the behavior of the topside ionosphere between 60 deg N and 60 deg S for 20 separate storms during 1962 and 1963. There was no severe storm during this period since the solar activity was near a minimum. The K_p values for the 20 storms were between 4 and 6. Sato's study revealed two types of disturbance patterns, D (daytime) and N (nighttime). The D type includes both increases and decreases in density, relative to the undisturbed vertical $N(h)$ profile; the N type shows only enhancements.

1.2.6.4 Effects Related to Storm Development

Bauer and Krishnamurthy (1968) were the first to relate storm-time effects in the topside ionosphere with the phase of the storms. They showed that the topside behavior during a geomagnetic storm varies not only with longitude (i.e., day and night sector) but also with the development of the storm through its initial (or positive) phase, its main (or negative) phase and its recovery phase. Bauer and Krishnamurthy suggested that the enhancements and depletions of the topside ionosphere are related to compressions and expansions of the magnetosphere. Another important contribution to the understanding of the complex storm phenomenon was made by Arendt (1969) who showed that the topside response to a geomagnetic storm depends upon the nature of the storm's commencement (sudden vs. gradual commencement).

1.2.6.5 Effects on Polar Ionosphere

In spite of its irregularity the topside polar ionosphere exhibits certain near-permanent structures, such as the polar peak, the auroral peak and the main trough. Nishida (1967) showed that these structures become accentuated during storms (i.e., higher peaks and deeper troughs). Herzberg and Nelms (1969) have shown examples of the G-condition (see Section 1.2.6.1) seen from the topside. A more unusual condition, first reported by Herzberg and Nelms, is the S-condition during which the ionosphere appears to contain a series of minitroughs with a nearly periodic spatial structure. The S-condition has been seen only following a solar proton flare.

1.2.6.6 Recent Storm Studies and Conclusions

The most recent Alouette 1 paper on ionospheric storms is by Fatkullin (1973) who obtained storm results agreeing with those of Bauer and Krishnamurthy (1968), provided the nature of the storm was taken into consideration as emphasized by Arendt (1969). Fatkullin's work also revealed a remarkable similarity between the altitude variation of storm effects and the altitude variation of the seasonal anomaly. This similarity led Fatkullin to suggest that both phenomena might result from the same major cause; namely, changes in neutral upper atmospheric composition. Fatkullin pointed out, however, that this approach may explain the height variation of storm effects, but not the other aspects of storm phenomena that are far more complicated than the seasonal anomaly.

In summary, topside sounder data from Alouette 1 have shown that the topside electron density changes during a geomagnetic storm in a manner that depends on altitude, latitude, local time, storm time, and type of storm.

1.2.6.7 Midlatitude Red Arcs

Topside sounder data have been used to study ionospheric effects associated with midlatitude red arcs, a phenomenon observed during magnetically disturbed periods around sunspot maximum. These red arcs occur at much lower latitudes ($L = 2$ to $L = 4$) than do the polar zone auroras ($L > 4$). These red arcs can extend several thousand kilometers in magnetic longitude, and they can last from several hours to several days. About 12 arcs per year were seen during 1957 and 1958. None was seen from September 1963 to September 1967. A midlatitude red arc reappeared on September 29, 1967, and was investigated by Alouette 1, Alouette 2, and Explorer 31. The Alouette 1 sounder data (Norton and Findlay, 1969) showed that the electron density increased at 1000 km as the satellite passed over the arc. At altitudes near $h_m F2$, i.e., close to the arc altitudes, the electron density was found to decrease. The Alouette 2 sounder data also presented by Norton and Findlay (1969) showed electron-density decreases both at $h_m F2$ and at 2000 km as Alouette 2 passed over the arc. Data from the electrostatic probe on Alouette 2 (Norton and Findlay, 1969) showed an increase by a factor of two in the electron temperature at 2000 km over the arc. The Explorer 31 data (Chandra et al., 1971) showed a similar increase in electron temperature and a decrease in ion density by a factor of 10. Alouette 1 sounder data obtained during the midlatitude red arc of July 10, 1968 (Lund and Hunsucker, 1971) substantiated the findings of Norton and Findlay (1969). These investigations collectively produced the first experimental evidence for accepting the thermal conduction mechanism proposed by Cole (1965b) and for rejecting the dc electric-field theory and the low-energy electron precipitating flux theory. Roble et al. (1970) used Cole's mechanism and the above experimental data from Alouette 2 and Explorer 31 to calculate theoretically the intensity and the extent of

the September 1967 red arc. Their results were in general agreement with the ground-based observations of the red arc.

1.2.7 Ionospheric Electron-Density Models

1.2.7.1 Introduction

One important objective of ionospheric investigations has been the development of models representing the typical variations of the ionosphere as a function of altitude, geographic location, time, geomagnetic conditions, and solar activity. This broad objective has received much attention during the past 50 years and considerable progress has been made. Theoretical investigations have led to analytical solutions that represent various approximations to the actual behavior of the ionospheric plasma. For example, the diffusive equilibrium theory (see Section 1.2.5.3) has provided useful representations of topside vertical electron-density profiles. The empirical approach consists typically of deriving representative "averages" based on extensive quantities of experimental observations. The compilation of global critical frequency maps (that are equivalent to maximum density maps) is one of the earliest examples of the empirical approach. Early studies, as illustrated by the two examples above, have been concerned with only a few aspects of the overall modeling problem. The results of these early studies, however, have provided valuable inputs for the more recent modeling effort.

1.2.7.2 Average Densities at h_mF2 and at 1000 km

As explained in Section 1.2.4.1, the Alosyn project has provided a wealth of information on the electron density at h_mF2 and at 1000 km (the Alouette 1 altitude). This information was obtained for about one and a half million Alouette 1 ionograms, and it has provided an important data base for ionospheric modeling efforts. Petrie and Lockwood (1969) used Alosyn data to show that the standard CCIR⁹ critical frequency predictions could be improved by supplementing the ground-based ionosonde data with topside sounder data. Thomas and Sader (1964) have used Alouette 1 data at the satellite to determine the diurnal, seasonal, and latitudinal variations of the electron density at 1000 km.

1.2.7.3 Average Vertical Profiles

A number of investigators have used Alouette 1 data to derive various "average" vertical electron-density profiles. Angerami and Thomas (1964)

⁹ CCIR: Comité Consultatif International des Radiocommunications

used the model of the ionosphere at 1000 km obtained by Thomas and Sader (1964) to calculate theoretical electron-density profiles for the exosphere to a geocentric distance of about $6 R_E$. These calculations were done for a variety of isothermal exospheric temperatures and for various composition models at 500 km. Best agreement with whistler data was obtained by using the electron density at 1000 km as measured by Alouette 1 on summer nights. This study was continued by Colin and Dufour (1968) who used temperature data from Explorer 22 to reduce the temperature uncertainty at 1000 km associated with the earlier work of Angerami and Thomas (1964). Colin and Dufour investigated five exospheric models and found that daytime temperature gradients of 1 to 2 K km^{-1} had to exist for the whistler data to be compatible with thermal equilibrium. For unequal electron and ion temperatures, agreement between theory and observations could be obtained with lower temperature gradients.

A standard midlatitude profile of the topside ionosphere was derived by Becker (1972). Becker's standard profile was based upon 521 high-quality midlatitude Alouette 1 profiles, and it was obtained by normalizing each individual profile first to the peak density, then by referring all altitudes to the peak altitudes, and finally by normalizing these altitudes to the half-layer thickness Y_m of a parabolic approximation to the peak. The peak density is representative of ionizing flux and Y_m is representative of the ionospheric scale height, which, under certain assumptions (Bauer, 1969), is related to the plasma temperature. A very high degree of uniformity was exhibited by these normalized profiles.

1.2.7.4 Average Pole-to-Pole Distributions

Chan and Colin (1969) published "average" daytime and nighttime electron-density distributions based on the $N(h)$ analysis of over 10,000 Alouette 1 ionograms collected under magnetically quiet conditions during the first year of operation. This period was close to sunspot minimum with an average sunspot number of 29. The data were separated into three seasons: December solstice, June solstice, and equinox. The ionograms selected for analysis were primarily from satellite passes yielding almost continuous data over North and South America. The resulting dip latitude coverage was from -60 deg S to $+90 \text{ deg N}$.

1.2.7.5 General Electron-Density Models of the Topside Ionosphere

The investigations summarized in Sections 1.2.7.2 to 1.2.7.4 have essentially been the precursors for the models discussed in this section. The general models are basically computer programs designed to provide vertical electron-density distributions (above and below $h_m F_2$) as a function of time, space, and geophysical conditions. Typical input parameters are position (altitude, latitude, longitude), time (day of year, local time), solar flux, and

geomagnetic activity. Only models based to a significant extent on topside sounder data are included in this section.

The model of Nisbet (1971) is a physical model for the altitude range 120 to 1250 km used mostly for theoretical investigations. In Nisbet's model the topside profile is represented by a very simple constant-temperature diffusive-equilibrium distribution adjusted to give densities at 1000 km in agreement with the densities measured by the Alouette 1 sounder.

The model of Bent (Bent et al., 1972) is a purely empirical model covering the altitude range from 150 to 1000 km. It is based on 50,000 Alouette 1 $N(h)$ profiles acquired during the period 1962 to 1966, and 400,000 bottomside soundings obtained from 1962 to 1969. The topside profile is represented by four segments; i.e., three exponential profiles and a parabolic layer. The prime objective of the Bent model was to keep the total electron content as accurate as possible in order to provide high-precision values of ionospheric delay and refraction for radio waves. The model has been used extensively by NASA (Schmid et al., 1973) to calculate ionospheric corrections for satellite tracking data.

Since 1969 an international steering committee established by URSI (Union Radio Scientifique Internationale) and COSPAR (Committee on Space Research) has been working on the development of an "International Reference Ionosphere" (IRI). The topside electron density portion of IRI is a refined version of the Bent model. The latest version, IRI 86 (Bilitza, 1986), is in the form of a computer program available from NSSDC.

The model of the polar ionosphere (Elkins, 1973) developed at the Air Force Cambridge Research Laboratories (AFCRL), was also based upon topside sounder data. The main emphasis of the AFCRL model was on radio propagation applications.

A global ionospheric electron-density model was developed at the University of Bonn (Köhnlein, 1978) for the altitude range 60-3500 km and for quiet geomagnetic conditions. Topside soundings obtained with Alouette 1, Alouette 2, ISIS 1, and ISIS 2 were used to provide a continuous data base for the period 1962 to 1973. This made it possible to extend the earlier models of Nisbet and Bent to one full solar cycle and also to higher altitudes. One objective of Köhnlein's model was to reduce the computer time required by the models of Nisbet and Bent, while preserving a sufficient degree of accuracy. This was done by "mapping" the global electron density at eight fixed altitudes (90, 110, 180, $h_m F_2$, 500, 1000, 2000, and 3500 km) and using appropriate interpolations to generate complete vertical profiles. Increased computer efficiency also was achieved by expanding the model into two parts. The general part describes the annual, semiannual, diurnal, and geographic structure. The differential part describes more localized structures as essentially a perturbation to the general structure.

1.2.8 Ionospheric Irregularities

1.2.8.1 Introduction

The ionospheric morphology discussed in Sections 1.2.5, 1.2.6, and 1.2.7 is concerned with the large-scale distribution of ionization. Superimposed on this broad background of ionization are small-scale density fluctuations known as ionospheric irregularities. The occurrence of spread echoes on bottomside ionograms provided some of the early evidence for these irregularities (Booker and Wells, 1938). The existence of irregularities aligned with the geomagnetic field was postulated by Booker (1956) to explain auroral radar echoes. It is now believed that most irregularities are aligned with the geomagnetic field. The work done prior to the satellite studies of the ionosphere showed that irregularities existed at all latitudes and longitudes as a normal feature of the ionosphere below $h_m F2$ under either quiet or disturbed conditions.

1.2.8.2 Field-Aligned Irregularities

The existence of irregularities aligned along the geomagnetic field and extending from one hemisphere of the earth to the other was demonstrated in a spectacular manner by the discovery of conjugate echoes on topside ionograms (Muldrew, 1963). Muldrew analyzed multiple traces observed on certain low-latitude ionograms and concluded that these traces were due to conjugate echoes corresponding to various combinations of north and south roundtrips along the earth's magnetic field. Muldrew supported his conclusions by showing that the observed traces had virtual heights consistent with ray-tracing calculations along a model field-aligned ionization duct with reflection occurring at the same height as the vertical incidence reflection level. Muldrew (1963) observed field-aligned traces on equatorial ionograms obtained during 0700 and 1400 and 2000 and 0300 local time. These traces were observed in 30 percent of the nighttime passes and 20 percent of the daytime passes. Calculations carried out for one particular ionization duct yielded a half-thickness of 0.6 km and a maximum electron density in the duct about 1 percent above the ambient ionization.

Muldrew (1963) also showed that in some special cases equatorial ionograms exhibit traces corresponding to waves, initially propagated at oblique incidence, which become subsequently trapped in field-aligned ducts. The waves propagate until the reflection level and return along almost the same path. Muldrew called this propagation mechanism a combination mode and suggested that it could explain certain spread echoes seen on equatorial ionograms. Combination mode ionograms have also been observed at midlatitudes (Dyson, 1967b).

A theory of ducted propagation, differing somewhat from Muldrew's (1963) treatment was given by Du Castel (1965). Ducted propagation according to

Du Castel can occur either inside the duct (duct density less than ambient) or at the lower surface of the duct (duct density greater than ambient). In the first case ducting is due to density variations; in the second case it is due to duct curvature. Du Castel's theory leads to typical duct widths of several kilometers and to density variations within the duct of a few percent.

1.2.8.3 Spread-F Mechanisms

Spread-F echoes seen on Alouette 1 ionograms have been attributed to three irregularity models. The first one is the combination mode of ducting discussed in Section 1.2.8.2. The second model also involves ionization irregularities aligned along the geomagnetic field. The irregularities in the second model, however, have a transverse thickness less than a wavelength, and there is no associated ducting. In this case, the spread echoes are due to aspect-sensitive scattering from these irregularities. The topside spread F corresponding to the second model is the most common type. It was first identified on equatorial topside ionograms by Lockwood and Petrie (1963) who were able to show conclusively that the minimum range of certain observed spread echoes was caused by overdense irregularities located below the satellite and aligned with the geomagnetic field. The third type of topside spread F is attributed to large scale irregularities that produce spread echoes as the result of refraction (Calvert and Schmid, 1964).

1.2.8.4 Morphology of Topside Spread F

Some very preliminary results concerning the morphology of topside spread F were given by Petrie (1963) and by Knecht and Van Zandt (1963). Petrie used Alouette 1 data obtained during the first week of operation (September 29 to October 4, 1962) and reached the following tentative conclusions. Spread F was (1) rarely seen at geographic latitudes between 25 and 45 deg N, (2) moderate between 45 and 60 deg N, and (3) severe at latitudes greater than 60 deg N. Petrie noted that spread F was frequently present at the satellite altitude for latitudes between 65 and 72 deg N. The appearance and disappearance of this spread F at the satellite altitude was attributed to patches of irregularities traversed by the satellite. Using data from 27 Alouette 1 passes during the first 2 weeks of operation, Knecht and Van Zandt (1963) concluded that topside spread F was almost always present for magnetic dips greater than 75 deg and rarely present at midlatitudes for dips less than 70 deg. The observations of Knecht and Van Zandt (1963) indicated that spread F was equally prevalent during mid-morning and during the evening. Both of these early studies of spread F stressed the abrupt transitions from a "no-spread" to a "spread" condition. More extensive studies by Petrie (1966) showed that spread F was a permanent feature of the topside ionosphere, at least during 1963-1964, for magnetic dip angles greater than 72 deg. Petrie (1966) showed that the intensity of topside spread F increased with increasing latitude, reaching a maximum near the auroral zone.

The worldwide distribution of topside spread F was investigated by Calvert and Schmid (1964) using 7000 Alouette 1 ionograms obtained between September 1962 and January 1963 over the American continents. Two zones of maximum occurrence were observed, one at high latitudes and one near the magnetic equator. These zones were separated by a region of minimum occurrence centered at 30 deg geomagnetic latitude. Equatorial spread F was seen mainly at night, while high-latitude spread F was seen at all hours, showing only a slight decrease near sunset and sunrise.

Hice and Frank (1966) extended the work of Calvert and Schmid (1964) by investigating the solstice periods of December 1962 and June 1963. Their spread-F results were classified according to the three models described in Section 1.2.8.3. The occurrence patterns for the three models were found to exhibit significant differences during the two periods of observation. Some differences were noted also by Hice and Frank (1966) between their December 1962 results and those of Calvert and Schmid (1964) for the same time period. These differences were attributed to the subjectivity that is involved in identifying the type of spread F exhibited on some ionograms particularly in distinguishing between ducting and scattering spread F. To avoid this problem, Dyson (1968) organized his midlatitude topside spread-F studies into only two categories, (1) refraction and (2) DS (indicating that either a ducting or a scattering mechanism was involved). Dyson's study was based upon 18,000 Alouette 1 ionograms recorded at Woomera, Australia, between September 1962 and October 1964. Dyson found the occurrence of DS spread F higher at night and during the local winter. Refractive irregularities were seen mainly during the daytime.

1.2.8.5 Comparisons Between Topside and Bottomside Spread F

Calvert and Schmid (1964) compared their topside spread-F results (obtained with sunspot minimum data) with the only ground-based survey available at that time, which unfortunately was based upon IGY (sunspot maximum) data. The two sets of results revealed very similar characteristics except that spread F was more frequent in the topside. Calvert and Schmid suggested that some difference in behavior could be due to differences in the criteria for spread F used in the two analyses. Singleton (1968) derived the morphology of bottomside spread-F occurrence at sunspot minimum using data obtained during 1964 at 13 stations distributed over the American sector. These bottomside results were then compared with the topside results of Calvert and Schmid (1964) to provide a legitimate sunspot minimum comparison of topside and bottomside spread-F distributions. The comparison of data obtained at the same point in the solar cycle led to more meaningful and consistent results than had previously been obtained. In particular there was considerable agreement between various details of the topside and bottomside spread-F morphology. The most significant difference between the occurrences of topside and bottomside spread F is that the percentage occurrences are greater in the topside ionosphere, particularly during daytime.

The comparisons discussed above were based upon statistical data concerning the occurrences of spread F. Dyson (1967a), using midlatitude data, investigated the simultaneous occurrences of topside and bottomside spread F for 99 cases of close coincidences (topside and bottomside ionograms within 3 deg of longitude, within 1 deg of latitude and typically within 10 minutes in time). This comparison included data for essentially all hours of the day. In 46 cases irregularities were present only on topside ionograms. In 23 cases irregularities occurred on both topside and bottomside ionograms. For the remaining 30 cases, the topside and bottomside data were free of irregularities. There was not a single case in which irregularities were observed on the bottomside only. At equatorial latitudes, however, Krishnamurthy (1966) found that the evening onset of spread F was about 2 hours earlier in the bottomside than in the topside. In the morning the bottomside spread F disappeared about 1 hour earlier than the topside spread F. Krishnamurthy's conclusions were based upon 36 topside-bottomside comparisons obtained also under conditions of close coincidences.

1.2.8.6 Topside Manifestations of Traveling Ionospheric Disturbances

Calvert and Schmid (1964) pointed out that the dimension and occurrence pattern of refractive spread F was consistent with (ground-based) observations of traveling ionospheric disturbances (TID). Further evidence of a close relationship between TID's on subpeak ionograms and refractive irregularities on topside ionograms was provided by Dyson (1967a, d). Du Castel et al. (1966), however, published one example in which the topside ionogram exhibited a combination-mode type of irregularity while the corresponding subpeak ionograms showed evidence of a TID. These observations show that TID's manifest themselves not only in the subpeak ionosphere, but also in the topside ionosphere. It is very difficult, however, to detect a TID with a topside ionogram (without the corresponding subpeak data) because the TID effects on topside ionograms are similar to effects produced by refraction or combination mode propagation.

1.2.9 Topside Sounder Resonances

1.2.9.1 Introduction

One of the unexpected benefits of topside soundings has been the vast amount of information obtained about "resonances" exhibited by the ionospheric plasma. Resonance-like phenomena are observed on topside ionograms as long-duration responses resembling the persistent ringing of resonances and occurring at characteristic frequencies of the ambient plasma. Because of their appearance on ionograms, these responses were initially called "splashes" or "spikes." The early theories, based on Alouette 1 data, attributed these responses to resonance phenomena, stimulated by the sounder in the ambient medium, and remaining close to the sounder for relatively long periods of time. Although it gradually became apparent

(partly as a result of additional information obtained with Explorer 20 and Alouette 2) that many of the observations could not be explained by resonance mechanisms, most authors have continued to use expressions such as "electron resonances," "plasma resonances," or "topside-sounder resonances," to designate the various types of long-duration responses seen on topside ionograms. This terminology will be used in the present text.

Resonance-like behavior was first observed in a rocket sounder experiment conducted to test the feasibility of topside soundings (Knecht et al., 1961). The rocket sounder operated on two fixed frequencies (4 and 6 MHz). Resonance-like "splashes" were seen at 4 and 6 MHz as the rocket passed through the levels corresponding to the three reflection conditions¹⁰

$X = 1$, ordinary (o)

$X = 1 - Y$, extraordinary (x)

$X = 1 + Y$, (z)

for each frequency. Extensive data on topside sounder resonances, however, became available only after the launch of Alouette 1.

It should also be emphasized that the Alouette 1 sounder was not designed to study resonances. The poor frequency resolution and the low radiated power at the low frequency end of the Alouette 1 sounder made it very difficult (if not impossible) to identify certain resonances. Spurious responses and magnetic contamination introduced further complexity in the analysis. In spite of these problems, however, much was learned from the Alouette resonance data and several new types of resonance were discovered.

1.2.9.2 Electron Cyclotron Resonances

Electron cyclotron resonances were first reported by Lockwood (1963) who showed that "spikes" occurred on topside ionograms at the electron gyrofrequency f_H and at harmonics of f_H . The frequencies f_n of the harmonics were found to agree within 1 percent with integer multiples of the fundamental. Barrington and Herzberg (1966) investigated specially selected Alouette 1 ionograms containing long series of cyclotron harmonic resonances and showed that the f_H values calculated from $f_H = f_n/n$ agreed

¹⁰ The X and Y nomenclature is as used in the standard magneto-ionic propagation theory; i.e., $X = (f_N)^2/f^2$ and $Y = f_H/f$ where f_N , f_H , and f are the plasma, cyclotron and sounding frequencies, respectively.

within their experimental accuracy of 1 percent. Benson (1970a) attained an accuracy of 0.2 percent by averaging the data from many ionograms, and found that the frequencies f_n of the higher harmonics were shifted by a maximum amount of -0.6 ± 0.1 percent between $4f_H$ and $12f_H$. Although the results of Benson revealed a small but systematic shift in the frequencies of the higher harmonics, these results do not disagree with those of Barrington and Herzberg (1966) since the shifts measured by Benson are smaller than the accuracy claimed by Barrington and Herzberg. Benson (1970a) suggested that the observed frequency shifts could be caused by magnetic contamination from the spring steel antennas used on Alouette 1, and pointed out that this hypothesis could be checked with data from Alouette 2 on which a nonmagnetic beryllium copper antenna was used.

Hagg (private communications) showed that the terrestrial magnetic field intensity derived from the Alouette 1 cyclotron resonances agreed within 1 percent with the intensity values calculated from the model of Jensen and Cain (1962). In view of this agreement the f_H data from Alouette 1 have been used to construct maps of the geomagnetic field intensity at 1000 km. A map of the geomagnetic field over North America at 1000 km (constructed by Hagg) has been shown in various review papers (Davies, 1964; Paghis et al., 1967). Muzzio et al. (1966) used f_H data from Alouette 1 to construct a similar map for the South Atlantic anomaly.

A very important property of the nf_H resonances was discovered by Lockwood (1965) who showed that the occurrence of these harmonics depends upon the angle between the sounder antenna and the terrestrial magnetic field. The number of harmonics observed was a maximum when the appropriate antenna was parallel to the geomagnetic field. Under these conditions Lockwood could observe harmonics up to the sixteenth.

The Alouette 1 data were used also to investigate the time duration of the various resonances in the nf_H series. The first investigation of resonant time durations was made by Fejer and Calvert (1964). They measured the durations of the f_H , $2f_H$, $3f_H$, and $4f_H$ resonances on several hundred Alouette 1 ionograms and showed the results as a function of f_N/f_H . The plasma parameter f_N/f_H was chosen because it influences the shape of the dispersion curves of the plasma waves, which were believed to be the cause of the resonances. Benson (1972a) extended this study to include the higher nf_H harmonics ($n = 5$ to $n = 12$). Benson's study included data obtained at all latitudes in order to investigate the effect of the angle β (angle between the geomagnetic field and the satellite velocity vector), and the effect of the dipole latitude. These parameters were chosen because they entered also in some of the nf_H resonance theories. The nf_H resonances did not exhibit a strong dependence on the parameter f_N/f_H . The most striking result was the strong peaking of the resonant durations as

$\cos \beta \rightarrow 1$, for $n = 3, 4$ and 5 (and to a lesser extent for $n = 6, 7$, and 8). There was no significant difference between the effect of β and the effect of dipole latitude. The apparent effects due to dipole latitude were actually caused by the corresponding changes in β . The amplitude of the $2f_H$ resonance was not related to the angle β .

1.2.9.3 Other HF Resonances

In addition to the nf_H resonances, Alouette 1 ionograms exhibit resonances near the sounder at the plasma frequency f_N and at the upper hybrid frequency

$$f_T = (f_N^2 + f_H^2)^{1/2}.$$

Except for a resonance seen occasionally at $2f_T$, there were no harmonics of either f_N or f_T . The existence of the f_N resonance was readily established from the initial analysis of Alouette 1 ionograms (Lockwood, 1963). The f_T spike, however, was incorrectly identified in this early study and believed to be the resonance at $X = 1-Y$ that had been seen by Knecht et al. (1961) in their rocket test (see Section 1.2.9.1). Actually this resonance occurred on Alouette 1 ionograms at a frequency slightly lower than that corresponding to $X = 1-Y$, but this displacement was believed to be the result of a perturbation in the local medium caused by the Alouette 1 satellite (Warren, 1963). This "displaced" resonance was recognized as a resonance at the frequency f_T by Calvert and Goe (1963), who then showed that there was no discrepancy between observed and computed resonances. Consequently, the perturbation theory of Warren (1963) was no longer needed to explain some of the resonance data. Calvert and Goe observed occasional spikes at $X = 1-Y$ and at $X = 1+Y$. Since these spikes were not seen consistently, Calvert and Goe concluded that the occasional spikes at $X = 1-Y$ and at $X = 1+Y$ were not related to the ambient plasma but due instead to some local irregularity.

The amplitudes of the f_N and f_T resonances were investigated by Fejer and Calvert (1964) who found the following. The amplitude of the f_N resonance is a minimum when the ratio f_N/f_H is close to unity. The amplitude of the f_N resonance is about one order of magnitude greater when $f_N > 1.5 f_H$. The amplitude of the f_T resonance is greatest when $f_N < f_H \sqrt{3}$. These results were confirmed by Benson (1972a).

1.2.9.4 The Remote Resonance

The resonances discussed in Sections 1.2.9.1 to 1.2.9.3 originate at zero range on Alouette 1 ionograms and appear to be excited in the vicinity of the

sounder. Hagg (1966) discovered a remote resonance that occurred well below the satellite, and showed that the spike for this resonance meets the extraordinary reflection trace at an altitude where the frequency of the extraordinary wave is equal to $2f_H$. Further characteristics of these remote resonances were given by Muldrew and Hagg (1966) who suggested that the remote resonances resulted from waves propagating along ionization irregularities aligned with the geomagnetic field. A more detailed discussion of the proposed generation mechanism was given by Muldrew (1967a). The mechanism described by Muldrew has successfully explained the detailed structure of remote resonances.

1.2.9.5 Proton Gyrofrequency Effects

The resonances discussed in Sections 1.2.9.1 to 1.2.9.4 have all been electron effects. The electron plasma resonances f_N on Alouette 1 occasionally exhibit a distinctive spur that seems related to the proton gyrofrequency at the satellite position (King and Preece, 1967). King and Preece offered no explanation for this phenomenon.

1.2.9.6 Theoretical Explanations of the Principal Resonances

The resonances that are consistently seen on topside ionograms (f_N , f_T , f_H , and the harmonics of f_H) have been called the "principal resonances." They occur at frequencies that are simple functions of the local electron density and of the local geomagnetic field intensity. The resonances at f_N and f_T were initially associated with stationary electrostatic waves (Calvert and Goe, 1963) because their frequencies agreed with resonances predicted for collective electron oscillations parallel and perpendicular to the geomagnetic field, respectively. The cyclotron resonances were naturally attributed to electron gyrations about the geomagnetic field. In the first published theory of electron gyroresonances, Lockwood (1963) invoked phase-bunching of individual electrons caused by the nonuniform radiation field of the sounder antenna. Fejer and Calvert (1964) showed that all the principal resonances could be attributed to plasma wave resonances if the effect of thermal particle motions were included in the electromagnetic wave equations. In this warm plasma treatment the harmonic cyclotron resonances were attributed to the "Bernstein modes" (Stix, 1962).

In addition to explaining the observed frequencies, the mechanisms proposed had to account for the long durations of these resonances. At first the wave group velocity was assumed to be zero, and the oscillations were viewed as standing waves remaining near the satellite (Fejer and Calvert, 1964). It was difficult to explain the long durations on this basis, and new theories were developed based on the concept of matching the group velocity of the waves to the velocity of the satellite (Shkarofsky, 1968).

The resonance phenomena discovered with topside soundings have opened new areas of theoretical and experimental investigations. A full account of these related investigations is beyond the scope of this overview. Thus, only a few of the theoretical studies have been mentioned here. As examples of the experimental investigations that have been inspired by the Alouette 1 resonance observations, one can cite the laboratory work of Crawford et al. (1967) and the rocket experiment of McAfee et al. (1972).

The resonance theories discussed in this section are indicative of the level of understanding that could be achieved with the Alouette 1 observations alone. Although some questions were left unanswered (such as why the resonance frequencies should be essentially unaffected by wake perturbations and by the plasma sheath around the sounder antenna), the early theories provided adequate explanations for the Alouette 1 observations. The improved data obtained with the later Explorer 20 and Alouette 2 satellites led to major revisions of the early theories of topside sounder resonances. The improved data and their impact on resonance concepts will be discussed under the Explorer 20 and Alouette 2 results.

1.2.10 Various Radio Propagation Factors

1.2.10.1 Introduction

The Alouette 1 topside sounder data have provided valuable information concerning (1) the radio noise level at the satellite, (2) the reflectivity of the earth's surface, and (3) the performance of HF radio propagation equipment in the terrestrial ionosphere. This information has been useful in the design of space HF and VHF telecommunication systems. A specific application of the information obtained has been in the greatly improved design of the subsequent topside sounders of the Alouette-ISIS program.

1.2.10.2 Radio Noise Level at the Satellite

The examination of early Alouette 1 ionograms indicated that the ionogram quality was much poorer at night than during the day. This decrease in quality was directly related to the unexpectedly large increase in radio noise level at night, as indicated by the AGC voltage in the sounder receiver. The source of this radio interference was investigated by Hartz (1963) who showed that the nighttime increase was not due (as initially assumed) to whistler mode propagation associated with the nighttime disappearance of D-region absorption. The most probable cause of the nighttime interference according to Hartz was the nighttime reduction in critical frequencies permitting a greater number of ground transmissions to reach the satellite. Some of these signals can beat together and produce an interfering signal at the frequency of the sounder IF amplifier.

Hartz (1963) showed also that the radio noise level at the satellite varied considerably with geographic location. The most severe noise level was

observed over Western Europe, where about 99 percent of the nighttime and 66 percent of the daytime ionograms were no better than "fair." In isolated regions, such as the South Atlantic, the radio noise levels were very low and little difference was observed between nighttime and daytime ionograms.

1.2.10.3 Reflectivity of the Earth's Surface

As mentioned in Section 1.2.3, echoes returned from the earth's surface are often seen on topside ionograms at frequencies greater than the critical frequencies. The strength of these echoes depends not only on the reflectivity of the earth's surface, but also upon the noise level at the satellite (see Section 1.2.10.2) and upon the directivity of the sounder transmissions. Thus the statistics of occurrence of ground echoes must be interpreted keeping in mind the worldwide distribution of radio noise. Conversely the worldwide occurrence of ground echoes can provide information concerning the radio noise distribution.

Keeping in mind the close relationship between noise and ground echoes, Muldrew et al. (1967) found an unusually low percentage of ground echoes over Greenland, suggesting that the radio waves were absorbed by the thick ice sheet. A very high percentage of ground echoes near the north magnetic pole was attributed to focusing by field-aligned ionization irregularities. There also were indications that sea was a better reflector than land.

The investigation conducted by Muldrew et al. (1967) yielded contour maps showing the worldwide occurrence of ground echoes on Alouette 1 ionograms for various seasons, local times, and sunspot numbers. Since the sea reflectivity is probably independent of geographic location, the contours over the oceans provide a measure of the noise level at 1000 km at low and midlatitudes.

Chia et al. (1965) used Alouette 1 ground echo data to calculate reflection coefficients for various locations over Australia and the Pacific Ocean. The general conclusion of this study was that the sea was a better reflector than the land conditions (sand and forests) found in Australia.

1.2.10.4 HF Radio Propagation from Earth Satellites

Many phenomena associated with either the ionospheric medium (troughs, ducts, spread F, etc.) or with the Alouette 1 sounder (resonances, interference, etc.) have an important bearing on the design of satellite HF and VHF telecommunications systems. Information of this type has been compiled by Paghis (1967) and Hartz (1972).

1.3 The Alouette 1 VLF Experiment

1.3.1 Introduction

Very low frequency (VLF) and extremely low frequency (ELF) signals have been used extensively in ionospheric investigations conducted from the ground. Naturally occurring VLF emissions known as whistlers have been attributed to electromagnetic impulses radiated from lightning discharges and propagating along field-aligned ducts of enhanced ionization. These whistlers can propagate along these ducts between hemispheres, sometimes making several round trips. From these long-path whistlers, electron-density information has been obtained at heights of several earth radii (Smith, 1961). VLF signals had not been observed in space at the time the Alouette 1 experiment was being planned. It was anticipated, however, that whistlers similar to those seen on the ground would be commonly observed with the Alouette 1 experiment. It was also expected that the satellite experiment would exhibit short fractional-hop (SFH) whistlers that had propagated directly from the lightning discharge to the satellite without crossing the magnetic equator.

The expected whistlers were seen in the Alouette data. These whistlers have not been used to calculate electron densities in the magnetosphere because of uncertainty in the propagation paths. The satellite data showed that the usual assumption of field-aligned propagation could be incorrect in many cases (Carpenter and Dunckel, 1965). The great value of the Alouette 1 VLF experiment was in the discovery of two unexpected phenomena, namely the lower hybrid resonance (LHR) noise and the proton whistler, both of which exhibit the influence of ions upon the propagation of VLF and ELF waves and both of which provide information about the concentration of positive ions in the vicinity of the spacecraft.

1.3.2 LHR Noise

1.3.2.1 Discovery of LHR Noise

Early VLF data from Alouette 1 revealed intense ELF and VLF noise bands that were not seen by ground stations located near the same geomagnetic field line. A surprising feature of these noise bands was the systematic changes in their spectral distribution with the satellite latitude (Barrington and Belrose, 1963). The VLF data typically showed (Barrington et al., 1963): a steady band of noise between 0.4 (the lower edge of the VLF receiver pass band) and 2.5 kHz in regions where the geomagnetic parameter L was greater than 9; erratic noise when L was between 4 and 9; and smooth noise when L was less than 4. Two well-defined noise bands were usually seen for L values between 4 and 2.6, with the upper band exhibiting a lower frequency cutoff that increased in value as L decreased. Brice et al. (1964) found that this latitude-dependent upper noise band (initially called the Alouette hiss band) could be triggered by atmospherics propagating upward

and by whistlers propagating downward. From these two observations it was concluded that the Alouette hiss band had to be generated near the satellite.

Brice and Smith (1964) suggested that the lower frequency cutoff f_r of the Alouette hiss band was due to the lower hybrid resonance, namely that

$$f_r = \frac{k f_N f_H}{f_T M^{1/2}}$$

where M is the effective ionic mass, k is a constant

$$k = \left(\frac{\text{electron mass}}{\text{proton mass}} \right)^{1/2}$$

and the other terms are as previously defined (see Sections 1.2.9.1 and 1.2.9.3). From the above relationship it is seen that the effective mass can be determined by using the VLF data to measure f_r and simultaneous sounder data to measure f_N , f_H , and f_T . This theory was developed further by Brice and Smith (1965) who showed that the effective mass values derived from the Alouette hiss band were consistent with the information on effective mass values available at the time of their study. Since the Alouette hiss band was also seen in the Injun 3 VLF data, it was recommended that the name "Alouette hiss band" be changed to "lower hybrid resonance hiss band." The name "LHR hiss band" and equivalent names such as "LHR emissions" or "LHR noise" are now the generally accepted terms for the very unusual noise band discovered in the VLF data from Alouette 1.

1.3.2.2 Morphology of LHR Noise and Source Mechanisms

The occurrence of LHR noise has been investigated as a function of latitude and time by McEwen and Barrington (1967). Their study included all VLF data recorded at Ottawa (250 passes) during 1963, and all VLF data recorded at Resolute Bay (300 passes) and South Atlantic (125 passes) during 1963 and 1964. Two distinctly different types of LHR noise were observed, the erratic polar LHR noise occurring mainly in the region 70-80 deg invariant latitude and the smooth midlatitude hiss occurring mainly in the 50-60 deg region. The polar LHR noise was seen approximately 50 percent of the time throughout the year day and night with two slight maxima at midnight and at 6 a.m. The midlatitude LHR noise was observed about 20 percent of the time and primarily during the night. The maximum occurrence surprisingly was found to be during the same months (May-October) in both hemispheres.

McEwen and Barrington (1967) suggested that the polar hiss was probably related to particle precipitation. Since the Alouette 1 examples of midlatitude LHR noise were mostly whistler-triggered hiss bands, McEwen

and Barrington (1967) suggested that whistler mode energy radiating from lightning discharges could be the sole source of midlatitude LHR noise.

Another mechanism for the generation of midlatitude hiss was proposed by Smith et al. (1966), who showed that VLF propagation ducts associated with the LHR frequency can form in the ionosphere when two or more ions are present with different height profiles. The presence of these ducts suggests that the midlatitude LHR noise need not be generated near the satellite. Thus the midlatitude LHR noise could be caused by particle precipitation in the nearby auroral regions with subsequent ducting to midlatitude regions.

Additional support for the LHR duct theory was provided by Gross (1970) who showed that north-south horizontal ducts are physically possible and can exist at altitudes well above 2000 km. The maximum bandwidth of these ducts was found to be typically 3 kHz. McEwen and Barrington (1967) had rejected the duct mechanism because midlatitude LHR noise had been seen (on Alouette 2) at altitudes near 3000 km and because they did not believe that LHR ducts could extend to such altitudes. The LHR duct theory was further refined by Gross and Larocca (1972) who showed that experimental observations were consistent with theoretical predictions. The experimental data used in this study were the 1963 and 1964 Alouette 1 records from the Ottawa telemetry station. Gross and Larocca (1972) extended the polar and midlatitude LHR noise classification of McEwen and Barrington (1967) to provide a distinction between three types of midlatitude hiss, all of which have narrow bandwidth (in contrast to the wide-band polar hiss): (1) hiss with smooth lower frequency cutoff (S-type); (2) whistler-associated hiss; and (3) erratic-cutoff hiss. Gross and Larocca (1972) pointed out that the S-type hiss is the LHR noise best explained by the duct theory.

1.3.2.3 Use of LHR Noise to Measure Ion Composition and Temperature

As explained in Section 1.3.2.1, the effective ionic mass M at the satellite can be calculated from a measurement of the lower frequency cutoff f_r of the LHR noise band and from a topside sounder measurement of the plasma resonance frequency f_N . In a two-ion ionosphere the effective ion mass yields directly the fractional abundance of these two ions. In the more general topside ionosphere situation where three ions (atomic oxygen, helium, and hydrogen) must be considered, the value of M can be used only to set lower and upper limits for the fractional abundances. In some cases narrow limits can be placed on at least one of the three fractional abundances. The effective plasma temperature T_p , the average of electron and ion temperatures, also can be derived from simultaneous VLF and topside sounder data from the relationship $T_p = AMH$, where A is a constant and H is the scale height, a quantity derived from the slope of the $N(h)$ profile. These basic procedures have been used by Barrington et al. (1965) to calculate M and T_p .

Because of mutual interference, the Alouette 1 sounder and VLF experiments normally were not operated at the same time. Simultaneous data were obtained, however, on about 1 percent of the satellite passes due to telemetry command errors. From an analysis of all the simultaneous sounder and VLF data obtained during the first 2 years of Alouette 1 operation, Barrington et al. (1965) were able to calculate about 400 values of effective mass M . The observations were divided into four local-mean-time periods, one centered at noon (0900-1500 LMT), one centered at midnight (2100-0300 LMT), and two corresponding to the twilight hours (0300-0900 and 1500-2100 LMT). The results were presented as a function of the magnetic parameter L . In all cases the calculated values of M were, as they should be, between 1 and 16. In general, M was found to be greater during the day than during the night and to increase with latitude. The composition of the polar ionosphere at 1000 km was found to be about 60 percent O^+ at midnight and about 95 percent O^+ at noon. At middle latitudes the effective mass values were between 1.8 and 7. At low latitudes, the lowest value observed for M ($M = 1.3$) would require that the hydrogen concentration be at least 68 percent. An effective plasma temperature of 1200 K was obtained for middle latitudes, increasing to about 2500 K at high latitudes.

1.3.3 Proton Whistlers

The proton whistler is another VLF phenomenon that was first observed in the VLF data from Alouette 1. The proton whistler appears as a rising tone that starts immediately after the reception of a SFH whistler (see Section 1.3.1) and that approaches asymptotically the gyrofrequency for protons in the plasma surrounding the satellite (Smith et al., 1964). This discovery was soon confirmed by similar observations in the VLF recordings from Injun 3. A theory for the production of proton whistlers was developed by Gurnett et al. (1965) who suggested that the proton whistlers are a dispersed form of the original lightning impulse that can be explained by considering the effects of ions upon the propagation of whistler waves. The frequency at which the triggering SFH whistler meets the proton whistler (crossover frequency) was shown to be a relatively simple function of the ambient proton density. From this relationship a method was developed for calculating proton densities in the plasma surrounding the satellite (Gurnett and Shawhan, 1966).

1.3.4 Short Fractional-Hop Whistlers

The VLF data from Alouette 1 provided the first examples of short delay whistlers that had traveled directly from their lightning source to the satellite without crossing the magnetic equator. Called short fractional-hop (SFH) whistlers, they sometimes can be partially reflected at altitudes near 1000 km, returned to earth, reflected upward again, and returned to the satellite. An example of a whistler with two components corresponding to one and three trips through the ionosphere, respectively, was first reported

by Barrington and Belrose (1963). Because such whistlers tend to be confined to altitudes less than 1000 km; i.e., below the heights where hydrogen is the main ionic constituent, they have also been called "subprotonospheric" or "SP" whistlers. Carpenter et al. (1964) used Alouette 1 data to investigate the properties of SP whistlers. This study showed that the SP phenomenon occurs typically at night within a few hours of sunset, near sunspot minimum, and at dipole latitudes greater than 45 deg.

1.3.5 Long-Path Whistlers

As indicated in Section 1.3.1, the long-path whistlers observed with Alouette 1 have not been used to calculate electron densities in the magnetosphere. Carpenter et al. (1968), however, have shown that the Alouette 1 data on long-path whistlers could be used to locate the plasmopause. Typically, as the Alouette 1 satellite moved poleward, the rate of occurrence of long-path whistlers was observed to drop abruptly to zero near invariant latitudes of about 60 deg. The location of this satellite whistler cutoff was found to be in good agreement with the location of plasmopause derived from simultaneous ground whistler data at Eights, Antarctica. A systematic small difference between the two determinations of the plasmopause position was attributed to some uncertainty in the magnetic field model used to calculate the plasmopause position from the ground observations. These simultaneous satellite and ground observations were obtained for 12 Alouette 1 passes. To obtain additional statistics, the plasmopause position as a function of K_p was derived from the whistler cutoff at the satellite for a total of 27 Alouette 1 and 2 passes. The results were found to be consistent with the well-known relation between plasmopause position and magnetic disturbance, namely that the plasmopause moves to lower L values as the value of K_p increases.

1.4 The Alouette 1 Cosmic Noise Experiment

1.4.1 Introduction

Cosmic noise has been studied extensively with a variety of ground-based instruments since the discovery of radio waves from the Milky Way (Jansky, 1933). These studies, which soon became known as radio astronomy, have led to the discovery of numerous radio sources both inside and outside the solar system. The frequency spectrum over which radio astronomy observations can be made from the ground is restricted at the low-frequency end by the terrestrial ionosphere. One purpose of the cosmic noise experiment on Alouette 1 was to extend the knowledge of extraterrestrial noise to lower frequencies; a second purpose was to determine the noise background against which the topside sounder had to operate. Thus, before the Alouette 1 sounder was completed, the cosmic noise at 3.8 MHz was measured on the Transit 2A satellite by the topside sounder design team (Molozzi et al., 1961). The subsequent 1 to 10 MHz cosmic noise

measurements from Alouette 1 were much more comprehensive than the Transit 2A data and they constitute the first major radio astronomy experiment conducted on a satellite.

The cosmic noise experiment on Alouette 1 consisted simply of monitoring the automatic gain control (AGC) voltage of the sweep-frequency sounder receiver. The receiver gain had been calibrated before launch, but there was no provision for inflight calibration. A comparison of the cosmic noise data obtained over a period of 2 years showed sufficient consistency to suggest that significant changes in receiver gain had not occurred. The sounder antenna had too broad an aperture for a direct identification of sources, and it was necessary to locate sources by inference. The effective antenna beam width (half-cone angle) was shown to decrease from 90 to 60 deg as the ratio of operating frequency to plasma frequency decreased from 5:1 to 2:1 (Hartz and Roger, 1964). Thus additional antenna directivity was provided by the ionospheric plasma. The data from the cosmic noise experiment were used for two major purposes, (1) to conduct a survey of the galactic noise over the celestial sphere and (2) to study solar noise emissions.

1.4.2 Galactic Noise

The spectrum of the galactic radio emission was determined fairly reliably for frequencies between 1.5 and 5.0 MHz. Data of lesser accuracy also were obtained in the frequency range 5.0 to 10.0 MHz. The Alouette 1 data showed that the galactic noise varied systematically over the celestial sphere. The highest flux density was measured for a region centered approximately on the south galactic pole, and the minimum was found for the region centered on RA 9 hr, dec +75 deg. At 2.3 MHz the brightness temperatures for these two regions were 1.8×10^7 K and 5×10^6 K, respectively. At the same frequency the brightness temperature versus frequency curve had a slope of -1.7; at 1.5 MHz the slope was -1.3; and at 5.0 MHz the slope was -2.2 (Hartz, 1964b).

1.4.3 Solar Noise

Once the galactic noise level in a given direction had been established, detectable increases in the receiver noise above this level were shown to be entirely of solar origin. Solar noise events were frequently observed (Hartz, 1964a), but only the type III bursts¹¹ could be readily identified because of their short durations. Solar noise events of longer durations could not be

¹¹ The classification of solar bursts is based upon their frequency-vs.-time characteristics. The type III burst is characterized by a short duration (typically 10 seconds at 20 MHz) and by a rapid drift from high to low frequencies.

classified (based upon the satellite data alone) and were simply noted as enhanced solar noise. In some cases, simultaneous ground-based data were used to identify these enhancements. The type III bursts seen in the Alouette 1 records had frequency-vs.-time characteristics very similar to those of type III bursts at higher frequencies. Type III bursts and other types of solar noise enhancements appeared to be a low-frequency extension of the corresponding events seen with ground-based equipment. The source velocities computed from some 20 type III bursts observed with Alouette 1 ranged from $0.1c$ to $0.15c$ (where c is the velocity of light in free space). Long duration solar events (type IV bursts) have been used on several occasions to measure the effective aperture of the satellite dipole antenna in the ionospheric plasma. The results were found to agree with theoretical expectations (Hartz and Roger, 1964).

Dynamic spectra of a number of type III bursts obtained with Alouette 1 have also been analyzed by Bradford and Hughes (1974). From over 60 type III bursts observed during the period September 1962 to March 1966, 27 were selected for analysis. These were isolated bursts, each having a useful frequency range of at least 4 MHz and representing an enhancement over the galactic noise background of at least 3 dB. Bradford and Hughes employed an improved method of analysis, which utilized the measured moments of the shapes of the bursts up to the third moment, and which permitted a more detailed interpretation of the events producing the bursts. The apparent source velocities derived from the frequency drift data ranged from $0.05c$ to $0.20c$ for 22 of the 27 bursts. The velocities for the remaining five bursts were between $0.25c$ and $0.50c$. The mean value was $(0.17 \pm 0.01)c$. The coronal temperature at 2 MHz calculated by Bradford and Hughes was $1.7 \times 10^5 K$, compared with the value of $3 \times 10^5 K$ obtained by Hartz (1964a).

1.5 The Alouette 1 Energetic Particle Experiment

1.5.1 Introduction

The main purpose of the energetic particle experiment on Alouette 1 was to study the outer Van Allen belt ($3 < L < 10$) at high latitudes and its relationship to geophysical phenomena such as auroral activity and ionospheric absorption. At the Alouette 1 altitude of 1000 km, the L values over Canada are typically between 3 and 20. Most of the Alouette 1 particle studies were based on data obtained over Canada since these data were so well suited for the main scientific objectives. Data obtained at lower latitudes ($L < 3$) were used to investigate the effects of high-altitude nuclear tests upon the inner Van Allen belt. The measured particles were separated into two categories, trapped and precipitated. Particles with pitch angles in the range 90 ± 20 deg were considered trapped. Particles with smaller pitch angles were considered precipitated. Within each category the data were separated into two groups, one corresponding to K_p less than 4, and

the other corresponding to K_p greater than 4. The most useful data were obtained during the first year of operation. By the middle of the second year of operation, the satellite spin had decayed to such an extent that stabilization was lost, and a tumbling motion followed. This made the particle data too difficult to analyze.

1.5.2 Average Properties of Outer Radiation Zone at 1000 km

McDiarmid et al. (1963b) analyzed the data from several hundred passes over Canada and Alaska during the period October 1962 to mid-January 1963. The analysis was used to calculate average intensities as a function of (1) particle type and energy (protons in the range 1-7 MeV; electrons with energies greater than 40 keV, 250 keV and 3.9 MeV), (2) invariant latitude and the L parameter, (3) pitch angle (trapped and precipitated particles), and (4) magnetic activity.

A maximum omnidirectional intensity of 3×10^2 particles $\text{cm}^{-2}\text{s}^{-1}$ was found at $L = 4.4$ for trapped electrons with energies greater than 3.9 MeV for both $K_p < 4$ and $K_p > 4$. The directional intensity was maximum at $L = 4.7$ for trapped electrons with energies greater than 250 keV. The maximum values were $3 \times 10^4 \text{ cm}^{-2}\text{s}^{-1}\text{sr}^{-1}$ for $K_p < 4$ and $2 \times 10^4 \text{ cm}^{-2}\text{s}^{-1}\text{sr}^{-1}$ for $K_p > 4$. The trapped electrons with energies greater than 40 keV had a maximum directional intensity near $L = 6$. The maximum values were $3 \times 10^5 \text{ cm}^{-2}\text{s}^{-1}\text{sr}^{-1}$ for $K_p < 4$ and $6 \times 10^5 \text{ cm}^{-2}\text{s}^{-1}\text{sr}^{-1}$ for $K_p > 4$.

The average intensity of precipitated electrons with energies greater than 40 keV was maximum around $L = 6$ with a value of $3 \times 10^4 \text{ cm}^{-2}\text{s}^{-1}\text{sr}^{-1}$ for $K_p < 4$ and $3 \times 10^5 \text{ cm}^{-2}\text{s}^{-1}\text{sr}^{-1}$ for $K_p > 4$. Precipitated electrons were observed at $L = 6$ on about 20 percent of the passes when K_p was less than 4 and on about 70 percent of the passes when K_p was greater than 4.

1.5.3 High-Latitude Boundary of Outer Belt at 1000 km

McDiarmid and Burrows (1964a) analyzed data from about 1000 Alouette 1 passes for the period October 1962 to March 1963 to determine the high-latitude boundary of the outer belt. The boundary for electrons with energies greater than 40 keV was found to be symmetrical with respect to the noon-midnight meridian and to occur at the highest latitude (75 deg invariant) near local noon. The lowest latitude of the boundary (70 deg invariant) occurred at midnight. The high-latitude boundary was essentially the same for trapped and for precipitated electrons. The other electron energy ranges ($E > 250$ keV and $E > 3.9$ MeV) were not included in this study.

1.5.4 Diurnal Intensity Variations of Outer Belt at 1000 km

McDiarmid and Burrows (1964b) investigated the variability of the flux of trapped and precipitated electrons with energies greater than 40 keV as a function of local time and latitude under conditions of low to moderate magnetic activity. The diurnal variability was greatest near the high-latitude boundary of the outer zone. The shape of the distribution of average intensity versus local time was similar for both trapped and precipitated electrons in the range $L = 5$ to $L = 11$ with a daily maximum value occurring around 0800 hours local time.

1.5.5 Electron Fluxes Outside Outer Belt at 1000 km

Intense fluxes of electrons with energies greater than 40 keV were observed by McDiarmid and Burrows (1965) at latitudes higher than the normal outer belt boundary. The latitude profiles of these electron fluxes were usually in the form of narrow spikes and in some cases these events exhibited extremely high intensities. A total of 38 high-latitude electron spike events were included in this study, and these were found to occur preferentially on the night side of the earth and for values of K_p greater than 3. These electron spikes were located on magnetic lines connected to the tail of the magnetosphere and they occurred at times when enhanced fluxes are observed in the outer belt. This correlation led McDiarmid and Burrows (1965) to suggest that electrons generated in the tail of the magnetosphere may constitute an important source of electrons for the outer belt.

1.5.6 Temporal Intensity Variations of Outer Belt at 1000 km

The intensities of electron fluxes in the outer radiation belt were investigated as a function of time for the period December 1962 to May 1963 during which several moderate magnetic storms occurred (McDiarmid and Burrows, 1966). The quantities observed were the maximum values for electron fluxes in the three ranges $E > 3.9$ MeV, $E > 250$ keV and $E > 40$ keV which occur typically (see Section 1.5.2) at $L = 4.4$, $L = 4.7$, and $L = 6$, respectively. The electron intensities in the range $E > 40$ keV increased consistently after the onset of a magnetic storm. No consistent storm pattern was found for the other two energy ranges. During quiet periods the electron flux intensity decayed with a time constant of 4 ± 1 days for $E > 40$ keV and 14 ± 2 days for $E > 3.9$ MeV.

1.5.7 High-Altitude Nuclear Explosions and Inner Belt

McDiarmid et al. (1963a) have studied the spatial distribution and the time decay of artificially injected particles following the Starfish high-altitude nuclear test of July 9, 1962. Since Alouette 1 was launched on September 29, 1962, the earliest Alouette data were for a time approximately 3 months subsequent to the Starfish explosion. The Alouette 1 data for the period 3 to 6 months after Starfish revealed no decay

in the region $1.20 < L < 1.25$, where the initial Starfish effects had been the most intense. In the range $1.25 < L < 1.70$, a marked softening of the spectrum with increasing L was observed. A decay with a time constant of 550 days was measured at $L = 1.32$ for electrons with energies greater than 3.9 MeV.

The effects of the nuclear explosions of October 22 and 28 and November 1, 1962, could be studied more completely because the explosions occurred after the launch of Alouette 1. These explosions occurred at higher latitudes resulting in particle injection into the region $1.75 < L < 5.5$. Measurements of the flux intensities of electrons with energies greater than 3.9 MeV for L values ranging from 2 to 3 yielded decay time constants between 1.0 and 1.4 days (Burrows and McDiarmid, 1964). A total precipitation of 3×10^{21} electrons with energies greater than 3.9 MeV was estimated to have occurred at $L = 2.95$ during the first 525 hours following the explosion of October 22, 1962.

1.5.8 Auroral Absorption and Precipitated Electrons

Auroral absorption data from various riometer stations in Canada and Alaska were compared statistically with precipitated electron data from Alouette 1 (Jelly et al., 1964). Although the statistical approach led to considerable spread in the results, the absorption was in general found to increase with increasing flux.

1.5.9 Polar Cap Absorption and Solar Protons

Alouette 1 measurements of solar protons were correlated with absorption recorded by two networks of riometers, one located across the northern polar cap, the other located across the southern polar cap (Chivers and Burrows, 1966). The data were obtained during the two principal solar events that occurred during September 1963. A close correspondence was found between the latitudinal profiles of absorption and the latitudinal variations of the proton flux.

1.5.10 Auroral Substorms and Electron Fluxes at 1000 km

Counting rates of electrons with energies greater than 40 keV were measured by Alouette 1 during and after the onset of a substorm, as indicated by a nearby network of ground-based riometers (Lin et al., 1968). The Alouette 1 data corresponding to the beginning of the storm revealed intense electron fluxes extending to latitudes well beyond the normal northern boundary. For the two subsequent Alouette 1 passes (2 and 4 hours later), the boundary had returned to its normal latitude. The Alouette 1 observations were consistent with a typical substorm duration of less than 2 hours.

1.5.11 Pattern of Auroral Particle Precipitation

Using data from many sources, including the Alouette 1 energetic particle measurements discussed earlier, Hartz and Brice (1967) concluded that the auroral particle precipitation pattern was a two-zoned one. Both zones were found to be roughly circular, approximately centered on the geomagnetic pole, and about 10 deg of latitude apart. The inner precipitation zone (70 to 75 deg geomagnetic) exhibits a maximum intensity just prior to midnight; it is associated with discrete auroral events corresponding to short duration bursts of intense soft electron fluxes with energies of the order of a few kiloelectron volts. The outer precipitation zone (60 to 65 deg geomagnetic) exhibits a maximum intensity in the morning hours; it is associated with diffuse auroras corresponding to moderate electron fluxes with energies greater than 40 keV.

Hartz and Brice (1967) summarized their results on a diagram showing the two zones of precipitation and the relative flux intensities as a function of geomagnetic latitude and geomagnetic time. This diagram has been extensively quoted and reproduced in subsequent papers on the subject of auroral particle precipitation. The morning and the nighttime maxima of auroral particle precipitation have been shown to exhibit closely correlated variations, particularly after the onset of a nighttime polar substorm (Jelly and Brice, 1967). The correlation found between these phenomena at widely separated longitudes was considered a strong indication that substorms are not spatially isolated phenomena but, instead, a manifestation of large-scale magnetospheric processes.

1.5.12 Ionospheric Effects of Precipitated Electrons

The effect of precipitated electrons upon the ionosphere was investigated at the South African Antarctic base, SANAE. Because of its location within the region of the South Atlantic magnetic anomaly, it was expected that the effects of particle precipitation would be more pronounced at SANAE than at other stations. The particle data used for the initial study (Gledhill and Torr, 1966) were obtained by Alouette 1 in the Northern Hemisphere in the region magnetically conjugate to SANAE. It was found that a high precipitated electron flux ($E > 40$ keV) in the conjugate region was always accompanied by an ionospheric disturbance at SANAE.

This work was extended by Gledhill et al. (1967) to other stations located close to the magnetic shell through SANAE ($L = 4$). It was found that a higher flux level (as measured by Alouette 1) was required to produce ionospheric disturbances comparable to those seen at SANAE. A calculation of the electron flux, actually dumped at the various ionospheric ground stations, revealed a remarkable consistency. To obtain a more direct measurement of the precipitated flux at SANAE, Greener and Gledhill (1972) used Alouette 1 data acquired in the vicinity of SANAE. These measurements, however, were not correlated with ionospheric effects. A

comparison with earlier results based upon conjugate point measurements therefore is not possible.

2. EXPLORER 20 RESULTS

2.1 Introduction

The U.S. Explorer 20 mission has made significant contributions to the Alouette-ISIS program in several technical and scientific areas. The first technical achievement of this mission was to establish the feasibility of topside soundings under both quiet and disturbed ionospheric conditions. The rocket experiments (see Jackson, 1986, p.16) used for this feasibility study yielded design parameters that were used in the development of Explorer 20 and of Alouette 1. The rocket tests revealed the existence of plasma resonance phenomena associated with topside soundings (Calvert et al., 1964). These tests also provided the first experimental evidence for the existence of ionospheric irregularities aligned with the terrestrial magnetic field (Calvert et al., 1962).

The Explorer 20 satellite (Russell and Zimmer, 1969) operated for the period August 25, 1964, to December 29, 1965, and provided 1450 hours of data. Although its operation was much shorter than that of the Alouette and ISIS satellites, the Explorer 20 mission lasted long enough to achieve its objectives and to meet the relatively small demand for its data. Because of its limited usefulness (compared to that of Alouette 1), the Explorer 20 data created considerably less international interest than the Alouette 1 data. Thus, it appears doubtful that a longer life for Explorer 20 would have increased significantly the scientific output derived from its 16 months of operation.

The Explorer 20 mission led to several advances in spacecraft technology. The Explorer 20 data contributed to the understanding of spacecraft spin decay and to the solution of the plasma sheath problem on spacecraft carrying long dipole antennas. Explorer 20 was spin stabilized with an initial spin rate of 1.53 rpm after antenna deployment. By the end of the first year of operation, the spin rate had decayed to about 0.47 rpm. The investigation of the spin-decay problem initiated with the Alouette 1 spin history (see Jackson, 1986 p. 18, 2nd paragraph) was extended using the spin data from Explorer 20 (Hughes and Cherchas, 1970). Furthermore, in spite of its failure to yield scientific data, the ion probe experiment on Explorer 20 was an important step in the development of the Alouette-ISIS spacecraft. It was the first attempt to place a direct measurement experiment on a spacecraft carrying the long antennas required for topside soundings. The information obtained contributed materially to the subsequent success of experiments of this type on Alouette 2, ISIS 1, and ISIS 2.

In addition to making valuable contributions to spacecraft technology, the Explorer 20 mission demonstrated the importance of fixed-frequency soundings for the study of ionospheric irregularities and for the investigation of plasma resonances. Our present understanding of the f_N and f_T resonances is due to a large extent to the information first provided by the Explorer 20 data.

2.2 Topside Sounder Resonances

2.2.1 Introduction

When Explorer 20 was launched, topside resonances had been investigated for almost 2 years using Alouette 1 data. The studies based upon Alouette 1 have been described in Sections 1.2.9.1 to 1.2.9.5, and the theories resulting from these studies have been summarized in Section 1.2.9.6. It was the Explorer 20 data, however, that first revealed the unsuspected complexity of the resonance patterns. All the major resonances seen on Alouette 1 could be seen in spectacular detail on the Explorer 20 data, except the resonance at f_H since it always occurs (at the satellite altitude) at a frequency lower than 1.5 MHz, the lowest of the six fixed sounding frequencies used on Explorer 20. A given resonance could be observed by Explorer 20 whenever the plasma parameters were appropriate for one of the six fixed frequencies. Because the plasma parameters usually changed very slowly compared with the sounding rate, a single resonance could be observed continuously for an extended period of time. It was as if the Alouette 1 frequency scale had been expanded by a factor of 1000. This long viewing period made it possible to examine in detail the resonance features and the effects of antenna orientation.

The identification of the nf_H resonances was quite simple since the nf_H frequencies depend only on the (known) terrestrial magnetic-field strength at the satellite location. The resonances at f_N , f_T , $2f_T$ were initially more difficult to identify because these resonances depend on the (unknown) local electron density. A special procedure, devised for the identification of f_N , f_T , and $2f_T$ used observations at several of the fixed frequencies and required that the interpretation yield internal consistency (Calvert and Van Zandt, 1966). It was soon discovered, however, that each type of resonance (nf_H , f_N , f_T , and $2f_T$) exhibited a characteristic pattern on ionograms and could therefore be recognized by its unique signature.¹² In addition to being convenient for identification purposes, the resonance patterns contained the clues that led to the currently accepted theories of topside resonances.

The great resolution of the Explorer 20 data at various critical conditions (whenever the plasma parameters had the proper values for observations at the available sounder frequencies) made it possible to show conclusively that there was no resonance at $X = 1-Y$ and at $X = 1+Y$ (see Section 1.2.9.3). The Explorer 20 data was also used to demonstrate that the satellite wake had

¹² At high latitudes the rapid variations in local electron density tended to obscure the characteristic patterns of resonances making the identification unreliable. When this happened it was necessary to use the special procedure based on consistency at several fixed frequencies.

no detectable effect on the resonances. Because of its limited resolution, the Alouette 1 data had left some uncertainty concerning wake effects and resonances at $X = 1-Y$ and at $X = 1+Y$.

2.2.2 Experimental Observations

2.2.2.1 Introduction

The most complete description of the fixed-frequency observations of topside resonances has been given in a paper by Calvert and Van Zandt (1966). The paper was the basis of the nonpictorial summary given here. For a better appreciation of the complexity of the resonance patterns one should refer to the illustrations given by Calvert and Van Zandt. Additional examples have been shown by Calvert and McAfee (1969) and by King et al. (1968b). The paper by King et al., incidentally, seems to be the only one in which simultaneous observations at all six fixed frequencies have been presented.

2.2.2.2 The $2f_H$ resonance

The Explorer 20 data showed that the $2f_H$ resonance pattern was characterized by an unusual degree of complexity. Although these patterns exhibited a certain amount of variability, some features appeared quite consistently. Peaks in the resonance amplitude could be observed two or four times per roll period. Simple peaks with broad and shallow fringes were seen when the antenna was parallel to the geomagnetic field. When the antenna was perpendicular to the geomagnetic field, the peaks exhibited deep and narrow fringes. Sometimes on different days (when the geophysical conditions were nearly identical) the patterns would repeat with an amazing degree of similarity. The variability and occasional repeatability of the $2f_H$ fringe patterns indicated that these patterns were closely related to the ambient ionospheric conditions. The significance of this statement is better appreciated if one recalls that the frequency of the $2f_H$ resonance is controlled uniquely by the strength of the geomagnetic field at the satellite. Thus the $2f_H$ resonance pattern was evidently controlled by additional parameters, such as perhaps electron density, electron temperature, or other ionosphere characteristics.

2.2.2.3 The $n f_H$ resonances ($n > 2$)

Higher harmonics of the f_H resonance have also been observed on the Explorer 20 data. The third, fourth, and fifth harmonics exhibited resonance patterns similar to that of $2f_H$, but intensity became rapidly weaker as the harmonic number increased. When n was greater than 5, the $n f_H$ resonances were too weak to reveal the features of their patterns.

2.2.2.4 The f_N resonance

The f_N resonance was found to consist of two parts, a broad short-delay part and a narrow long-delay part. The short-delay response was usually finely fringed and exhibited narrow gaps when the antenna was perpendicular to the geomagnetic field. The long-delay response usually occurred as two very narrow columns of fringes. An important feature of the f_N resonance was the presence of thin, short, slanted lines emanating from the center of the f_N resonance and exhibiting a subsequent time delay about one order of magnitude greater than that of the ordinary reflection echoes. This little feature turned out to be the Rosetta stone of the resonance kingdom. Its interpretation (see Section 2.2.3.1) was the first step in unravelling the mysteries of topside resonances.

2.2.2.5 The f_T and $2f_T$ resonances

The f_T and $2f_T$ resonances were frequently observed in the Explorer 20 data. The f_T resonance was always very strong for $f_T < 2f_H$ (or equivalently for $f_N < f_H \sqrt{3}$). Under these conditions the f_T resonance had a striking characteristic fringe pattern, often resembling huge modulated arches merging at their peaks into a strong but relatively featureless continuum. When $f_T > 2f_H$ the f_T resonance was weak and finely fringed. The $2f_T$ resonance was always weak, fringeless, and slightly spin modulated.

2.2.3 Theoretical Explanations of Principal Resonances

2.2.3.1 Introduction

Our present understanding of the principal resonances (nf_H , f_N , f_T , $2f_T$) is based to a large extent on the interpretation of the Explorer 20 data. A major breakthrough occurred with the explanation of the long-delay traces originating from the center of the f_N resonance. Calvert (1966d) showed that these traces were oblique z-mode echoes propagating between the satellite and the ordinary-mode reflection level. These oblique echoes are made possible by the shape of the extraordinary (z-mode) refractive index surfaces in the vicinity of f_N . The properties of refractive index surfaces used in Calvert's analysis were previously known (Poeverlein, 1949). It was Calvert, however, who first realized that these properties could explain the very puzzling long-delay echoes seen on topside ionograms near f_N . Calvert's theory of the oblique z-mode echo may seem unrelated to the subject of topside resonances, until one realizes that the same basic theory (i.e., oblique z-mode propagation near f_N) was later used to explain the resonance at the plasma frequency. Calvert's work was therefore a major milestone in the development of topside resonance theories.

2.2.3.2 The Plasma Resonance ($f_N > f_H$)

Calvert's analysis of the oblique z-mode yielded a second solution which he discarded because the corresponding delays were excessively large. McAfee (1968) discovered that the delay times corresponding to this second solution have reasonable values when the operating frequency f is sufficiently close to f_N . McAfee found that the corresponding waves could be obliquely reflected after traveling short distances and that the resulting echoes could account for the f_N resonance. These waves were shown to be highly dependent on plasma parameters, particularly the electron temperature, indicating that the waves might be useful as an experimental tool. McAfee's initial analysis was based upon a simplified geometry (horizontal magnetic field, vertical electron-density gradient, and propagation in the magnetic meridian) and the assumption $f_N > f_H$ was made. In a subsequent paper McAfee (1969a) showed that slowly propagating waves near the plasma frequency can also reflect obliquely and intercept the satellite when the magnetic field is not horizontal and when propagation is out of the magnetic meridian. McAfee (1969a) also found that there are in general two waves that can return to the satellite for a given set of plasma conditions. By taking into consideration (1) the pulsed nature of the transmitted signal, (2) the bandwidth of the receiver, and (3) the motion of the satellite, McAfee showed that the two waves received at the satellite must be transmitted at slightly different frequencies in order to have the same time delay (and reach the moving satellite at the same time). McAfee showed that these two waves could produce an interference pattern consistent with the fringes exhibited by the f_N resonances seen in the Explorer 20 data. McAfee also pointed out that the observed beat frequency was dependent on the electron temperature and could therefore be used to measure this particular plasma parameter. Warnock et al. (1970) used data from an ISIS 1 ionogram (displaying consecutive fixed-frequency and swept-frequency soundings) to show how such a measurement could be made. The ionogram was obtained at an altitude of 1380 km, and an electron temperature of 4500 ± 300 K was calculated from the ionogram data. The plasma resonance beat frequency was measured from the fixed-frequency sounding; the electron-density scale height, a quantity needed in the calculations, was derived from the swept-frequency sounding. McAfee's theory of the topside sounder plasma resonance is still the currently accepted explanation.

2.2.3.3 The Upper Hybrid Resonance

McAfee (1969b) showed that the behavior of waves near the upper hybrid frequency f_T is similar to the behavior found near the plasma resonance f_N (see Section 2.2.3.2) when f_T is less than $2f_H$. Under these conditions ray paths almost identical to those calculated near f_N are found that can return energy to a moving satellite and account for the observed resonance at f_T . When f_T is greater than $2f_H$, the behavior of the waves near f_T is such that an

efficient return path no longer exists. However, the possibility of return paths producing weak echoes was found. This theoretical behavior is in excellent agreement with experimental observations.

2.2.3.4 The Plasma Resonance ($f_N < f_H$)

The theoretical explanation of the plasma resonance initially provided by McAfee (1968 and 1969a) assumed that f_N was greater than f_H . McAfee (1970) repeated his analysis for the condition $f_N < f_H$ and found that a difference in behavior occurs that is similar to the change in the upper hybrid resonance mechanism as f_T becomes less than $2f_H$. The theoretical predictions could not be verified with the Explorer 20 data because the lowest sounder frequency (1.5 MHz) was always greater than f_H . A few observations made with the fixed-frequency sounder on ISIS 1 have shown f_N resonances of short duration when f_N was less than f_H , as expected from McAfee's analysis. These observations, however, were all at high latitudes where other factors may have been more important.

2.2.3.5 Concluding Remarks

A number of authors have introduced various mathematical refinements to McAfee's treatment of the f_N and f_T resonances (Fejer and Yu, 1970; Graff, 1971; Parkes, 1974). In all cases, however, the assumed physical mechanism was the same as that originally proposed by McAfee. Thus, the subsequent analyses have confirmed McAfee's explanation of the f_N and f_T resonances. An experimental confirmation of McAfee's model of the f_T resonance was provided by a rocket test (McAfee et al., 1972), in which it was observed that the variation of the f_T echo versus frequency was according to McAfee's predictions. McAfee (1974) found that the mechanism that he had used so successfully to explain the f_N and f_T resonances could not be readily applied to the ηf_H resonances. He was unable to find any wave mechanism near f_H that could explain the f_H resonance. There were no data from Explorer 20 at the frequency f_H , but the fixed-frequency data from ISIS 1 showed that the f_H resonance has a fringe pattern, suggesting that a wave mechanism might still be responsible. Very refined calculations of refractive index surfaces for frequencies near f_H were performed by Muldrew and Estabrooks (1972). These calculations made fewer approximations than had been used in previous refractive index surface studies. This work did not resolve the f_H mystery; it simply led to the suggestions that three separate mechanisms could contribute to f_H . Further details on these unproven ideas seem unwarranted since a satisfactory explanation for the f_H resonance has not yet (1988) been published. McAfee (1974) pointed out that the refractive surfaces at frequencies near ηf_H are much more complicated than those near f_N and f_T . He suggested that the fringe patterns in the ηf_H resonances were probably

also due to wave mechanisms. With these concluding remarks we reach the point where further studies of topside resonances were based to a large extent upon data obtained by later satellites of the Alouette-ISIS program, particularly Alouette 2 (see Section 3.2.9).

2.3 Investigations of Ionospheric Irregularities

2.3.1 Introduction

The Explorer 20 mission has yielded new information on the structure and distribution of ionospheric irregularities for essentially the same reasons that it has yielded the improved observations of ionospheric resonances discussed in Sections 2.2.2.2 to 2.2.2.5. The Explorer 20 sounder cycled through all six of its sounding frequencies in 0.105 s during which time the satellite moved approximately 0.8 km. It was therefore well suited for measuring irregularities down to that size. In the case of the Alouette 1 sounder, the complete frequency sweep was repeated every 18 s, during which time the satellite moved about 130 km. The greatly improved spatial resolution of Explorer 20 was in the horizontal direction and more specifically along the circular orbit of the satellite. The vertical resolution was very poor, and the acquisition of vertical electron-density profiles was not practical. Useful electron-density information could, however, be obtained at the satellite altitude by using the data (at the lower sounder frequencies) on resonances and on x -mode cutoffs at the spacecraft. At the higher frequencies, whenever layer penetration occurred, f_oF_2 and sporadic-E data could sometimes be obtained. This made it possible, for example, to acquire new information on electron-density gradients at various latitudes and on the spatial extent of intense sporadic E.

2.3.2 Ducting and Scattering

The Explorer 20 data have supported the previous theories of ducting and scattering that had tentatively been formulated to explain certain sounding rocket and Alouette 1 observations (see Sections 1.2.8.2 and 1.2.8.3). Explorer 20 data have provided numerous examples of direct-ducted and combination-mode ducted echoes.

The direct-ducted echoes occurred when the satellite passed through a ducting irregularity. Since ducted signals were confined to the relatively small space of a duct, the geometrical losses were very small and the echoes were very intense. From the duration of the echoes and from the speed of the satellite, the ducts were found to be 2 to 4 km thick in the North-South direction (Calvert et al., 1964). Since this thickness was comparable to the East-West thickness measured with the topside sounder rocket test (Calvert et al., 1962), it was concluded that the ducts were circular and not laminar. This conclusion was also consistent with the intensity of the ducted echoes. The total delay through a duct for a direct-ducted signal was found to be consistent with the assumption of propagation along the geomagnetic field whenever such a detailed comparison was made.

Combination-mode echoes could be observed only when the satellite passed through the vertical plane containing a ducting irregularity. In this case the refraction of the ambient ionosphere is required to bring the wave to parallelism with the duct after which the wave is guided by the duct to the reflection level. The wave is then returned along the same path. The echo paths give rise to a trace starting at the normal ionospheric trace and gradually increasing in range as an increasingly greater portion of the path becomes ducted. Explorer 20 data on combination-mode ducted echoes have been discussed by Calvert (1966a).

Scattered echoes can be produced when an abrupt change in refractive index occurs perpendicularly to the path of a radio wave. Scattered echoes produced by field-aligned irregularities have frequently been observed on Explorer 20 ionograms. The scattered echoes are usually of two types, direct scattering and scattering after ionospheric reflection. Both types of scattering produce unique signatures on Explorer 20 ionograms that assist in their identification. These signatures are also consistent with the interpretation that the irregularities are field aligned. At high latitudes the direct echo pattern also goes to zero range, indicating that the field-aligned irregularities are distributed in sheets. Otherwise the minimum echo range would be that corresponding to the distance between the orbit and an isolated field-aligned irregularity (Calvert 1966a). The distribution in sheets tends to terminate southward in the region of the main ionospheric trough (see Section 1.2.5.4). Legg and Newman (1967) have suggested that this trough provides a path for the 1.95 MHz Loran signals that are frequently observed on the low-frequency (2 MHz) Explorer 20 records.

2.3.3 Conjugate Ducts

2.3.3.1 Introduction

A conjugate duct is a duct extending from one hemisphere to the magnetically conjugate region in the opposite hemisphere. Conjugate ducts are of considerable interest because of their importance to the theory of VLF radio wave propagation and to the theory of HF long-delay echoes.

A very comprehensive investigation of conjugate ducts was done by Loftus et al. (1966) using some 600 conjugate duct observations obtained with the Explorer 20 sounder. Since the sounding period of 15 ms (corresponding to a vertical range of 2250 km) was repeated every 105 ms, it was possible to observe echoes corresponding to the following virtual ranges in km: 0-2250, 15,750-18,000, 31,500-33,750, etc. Although echoes corresponding to the next virtual range window (47,250-49,500 km) were theoretically possible, only echoes corresponding to the first three windows have been reported.

2.3.3.2 Latitudinal Distribution

All observations of conjugate ducts occurred in regions where the magnetic dip angle was less than 65 deg. The very sharp decrease in duct occurrence

seen when the dip angle became greater than 65 deg may have been partly due to the observation windows indicated in Section 2.3.3.1. Making allowance for window and diurnal effects, the frequency of ducting seemed to be independent of latitude between dip angles 60 deg S and 30 deg N, except near the dip equator where the occurrence of ducting dropped to zero (Loftus et al., 1966).

2.3.3.3 Diurnal Variation

The diurnal variations of conjugate ducts were obtained for two equinoctial periods: August 25-November 20, 1964 (292 ducts) and February 14-May 12, 1965 (224 ducts). Data for the two periods were consistent in showing a minimum occurrence near midnight, a sharp rise near 2 a.m. local time, a maximum near sunrise, a second minimum near noon, and a small secondary maximum near sunset (Loftus et al., 1966).

2.3.3.4 Thickness and Separation of Ducts

A study of the North-South thickness of conjugate ducts, based on 567 observations, yielded thickness values ranging from 1 km (the smallest observable thickness) to 40 km. The data were summarized in a graph showing the number of observations (in steps of approximately 1 km) versus the logarithm of the duct thickness. The best fitting logarithmic normal distribution was centered at 4.2 km. For this logarithmic distribution curve the standard deviation corresponded to a thickness variation by a factor of 2.1 (Loftus et al., 1966).

Center-to-center duct separations were measured for 390 observations, and the results were presented in the same manner as the thickness data. The distribution was centered at 42 km, and the standard deviation corresponded to a factor of 4.3 (Loftus et al., 1966). The only previous measurement of duct thickness and separation was by Calvert et al. (1962), and it was based upon the data from the second rocket test of the fixed-frequency experiment (Jackson, 1986, p.16).

2.3.3.5 Electron Density in Ducts

The fractional enhancement of electron density within a duct was estimated from the latitude at which the duct was observed and from the highest frequency that was trapped by the duct. This study showed that in most cases the enhancement was less than 1 percent. The maximum enhancement observed was between 5 and 8 percent (Loftus et al., 1966).

2.3.4 Electron-Density Gradients in Topside Ionosphere

2.3.4.1 Gradients at Low- and Mid-Latitudes

The North-South electron-density gradient ($\Delta N/N$) per unit distance at the edge of the equatorial bulge was found to be about $5 \times 10^{-4} \text{ km}^{-1}$. A gradient of $1 \times 10^{-4} \text{ km}^{-1}$ was found to be typical at midlatitudes (Calvert, 1966b).

2.3.4.2 Gradients at High Latitudes

The scale of the electron-density structure at high latitudes was sometimes found to be smaller than the 0.8 km resolution of the Explorer 20 sounder. Consequently, the Explorer 20 data often yielded a lower limit to the actual gradient. Gradients measured were typically 6 percent per km within the high-latitude trough and 60 percent per km in the auroral zone (Calvert, 1966b).

By comparing Explorer 20 data with auroral backscatter data, Lund et al. (1967) showed that the electron density in the auroral zone exhibits fluctuations that are large in amplitude (of the order of 2 to 5 times the ambient values) but small in geographic size (about 1 to 10 km). These observations indicated that the backscatter echoes were produced by irregularities in the form of field-aligned sheets. A study by Jorgensen and Bell (1970), based on 14 Explorer 20 passes through the polar ionosphere, led to the conclusion that the Explorer 20 data could be used as an indicator of auroral activity and could provide a rough mapping of the auroral zone.

2.3.5 Sporadic E

New information on the North-South length of sporadic-E clouds was obtained by Cathey (1969) using Explorer 20 data. About 130 midlatitude sporadic-E clouds were measured during this study. Cathey found that the average length of a sporadic-E cloud was 170 km on the 7.22 MHz records and 250 km on the 5.47 MHz records. In approximately 97 percent of the observations, the sporadic-E clouds were transparent at 7.22 MHz as evidenced by the presence of ground echoes. The average length of nontransparent (blanketing) clouds at 7.22 MHz was found to be 80 km for the ordinary mode and 100 km for the extraordinary mode. Cathey found the lengths of sporadic-E clouds to be independent of latitude. The lengths measured by Cathey agreed quite well with estimates based upon ground-based observations (Thomas and Smith, 1959).

3. ALOUETTE 2 RESULTS

3.1 Introduction

The most significant aspect of the Alouette 2 mission was the major breakthrough in technology that was accomplished; namely, the successful combination on the same spacecraft of topside soundings and of local ionospheric measurements. There was no assurance prior to launch, however, that the necessary "breakthrough" in technology would indeed be achieved. In fact, to ensure that the scientific (if not the technological) objectives could be met, two satellites were launched simultaneously in the same orbit; namely, Alouette 2 with the topside sounder aboard and Explorer 31 carrying the ionospheric experiments that might not be compatible with the sounder. One of the Explorer 31 experiments was duplicated on Alouette 2, and comparisons between the results of the two identical experiments showed that the Alouette 2 design was compatible with the local measurements of ionospheric parameters in the immediate vicinity of the spacecraft. The success of the techniques first tried on Alouette 2 made it possible to combine all the desired ionospheric measurements on a single spacecraft in the subsequent ISIS 1 and ISIS 2 missions.

The ionospheric experiments making local measurements yield, typically, electron and ion densities, electron and ion temperatures, and ion composition. Since these measurements are made at the surface of the spacecraft, they yield data only at the altitude of the satellite. Had experiments of this type been performed on Alouette 1, all the resulting data would have been for an altitude of 1000 km. The eccentric orbit selected for the joint Alouette 2-Explorer 31 mission (also known as the ISIS X mission) made it possible to measure these additional ionospheric parameters over an altitude range of 500 to 3000 km. This orbit also made it possible to extend the altitude range of topside soundings by including the previously unexplored 1000 to 3000 km altitudes. Similarly, a new altitude region could also be explored by the VLF and Energetic Particle experiments that were repeated on Alouette 2.

The analysis of the high-altitude ionograms from Alouette 2 required that a number of refinements be made to the methods developed for the much simpler Alouette 1 ionograms. For continuity of presentation, however, the entire topic of ionogram analysis was given under the Alouette 1 overview. For similar reasons papers based either partly or entirely on Alouette 2 were quoted in other sections of the Alouette 1 overview. From the 200 references given in the Alouette 1 overview, a total of 34 references was based partly (and in some cases, mostly) on Alouette 2. The results related to Alouette 2 occur in Sections 1.2.2, 1.2.3, 1.2.4, 1.2.5.4, 1.2.6.5, 1.2.6.7, 1.2.7.4, 1.2.7.5, 1.2.9.2, 1.2.10.4, and 1.3.5. About five of the references given in the Explorer 20 overview were based partly on (or inspired by) the Alouette 2 results. To avoid repetition, the previously quoted Alouette 2 results will not be included again in the Alouette 2 overview. It is hoped that this policy and the resulting shorter Alouette 2 overview will not minimize the importance and the success of the Alouette 2 mission. Alouette 2

matched the longevity record of Alouette 1 by staying fully operational for 10 years. The Alouette 2 mission resulted in over 175 publications in refereed scientific journals.

3.2 The Alouette 2 Topside Sounder Experiment

3.2.1 Introduction

The Alouette 2 sounder was redesigned to measure electron-density concentrations much lower than the concentrations that could be measured with the Alouette 1 sounder. This redesign was based upon considerations similar to those given in the following discussion. Thomas et al. (1966) have shown that electron densities as low as $1000 \pm 700 \text{ cm}^{-3}$ were occasionally detected by the Alouette 1 sounder at the satellite altitude (1000 km). A density of 1000 cm^{-3} was about the lowest that could be detected with the Alouette 1 sounder, and the error was then comparable to the quantity measured. The density N_s at the satellite altitude was derived from the analysis of the extraordinary trace. Thomas et al. (1966) showed that the accuracy improved rapidly as N_s became greater, the error being 30 percent at $N_s = 3000 \text{ cm}^{-3}$, 12 percent at $N_s = 10^4 \text{ cm}^{-3}$ (a typical N_s value at 1000 km) and less than 5 percent for $N_s > 4 \times 10^4 \text{ cm}^{-3}$. The density at the satellite can also be derived from the value of the plasma resonance f_N . On Alouette 1 the minimum sounder frequency was 0.5 MHz (corresponding to $N_s = 3000 \text{ cm}^{-3}$). For a reliable measurement of f_N , however, the full frequency spectrum of the resonance should be displayed on the ionogram. This requires that f_N be at least 0.6 MHz with a corresponding N_s of about 4500 cm^{-3} . Consequently, the low densities encountered by Alouette 1 could not be measured with the plasma resonance. Considerations of this type, showed that (1) densities much lower than 10^3 cm^{-3} could be expected during the upper portions of the Alouette 2 orbit, in view of its 3000-km apogee; (2) the low-frequency resolution should be improved on Alouette 2; and (3) the minimum sounder frequency should be much lower on Alouette 2 than it was on Alouette 1. The study of resonance phenomena indicated also that an improved low-frequency resolution would be very helpful.

The minimum sounding frequency was lowered to 0.12 MHz on Alouette 2. The plasma frequency, however, could not be reliably measured at 0.12 MHz because the full f_N resonance spectrum could not be seen when $f_N = 0.12$ MHz and also because the minimum frequency calibration marker was at 0.2 MHz. An accurate measurement of f_N could be made, however, at $f = 0.2$ MHz, corresponding to $N_s = 500 \text{ cm}^{-3}$. Thus the range over which accurate density measurements could be made was extended downward by an order of magnitude on Alouette 2. The improved low-frequency performance of the Alouette 2 sounder (compared to the Alouette 1 sounder) was due not only to the extended low-frequency range but also to a substantial increase in power output and in resolution at the low frequencies.

The sounder resolution below 2 MHz was eight times greater on Alouette 2 than it had been on Alouette 1. To ensure that frequency measurements could be made below 2 MHz with an accuracy comparable to the resolution, Benson (1970b) developed a frequency interpolation correction procedure for Alouette 2 ionograms. Although the low-frequency resolution of the extraordinary trace had been increased by a factor of 8, the corresponding improvement in the measurement of low N_s values was no greater than that achievable with the improved plasma resonance data. It should be noted that the frequency resolution below 2.0 MHz on the ISIS 1 and ISIS 2 ionograms is about one-third that of Alouette 2. Thus the Alouette 2 resolution below 2.0 MHz is significantly better than that of the other sounders of the Alouette-ISIS series. Consequently, the Alouette 2 data have been found very desirable not only for low-density measurements, but also for the study of resonance phenomena. The improved low-frequency resolution (and output power) of the Alouette 2 sounder made possible many studies that could not be done with the Alouette 1 data.

3.2.2 Measurements of Very Low Densities at the Spacecraft

Although the Alouette 2 sounder could measure electron densities accurately down to 500 cm^{-3} ($f_N = 0.2 \text{ MHz}$) and estimate electron densities down to 280 cm^{-3} ($f_N = 0.15 \text{ MHz}$), it was soon discovered that in the polar regions at altitudes near apogee the electron density was frequently less than 280 cm^{-3} (Nelms and Lockwood, 1967). Hagg (1967) noted that the overlap of the f_H and f_T resonances in these very low density regions seems to produce an interference pattern. By assuming that the f_H and f_T resonances occur at their nominal (cold plasma) frequencies, a simple relationship can be derived that relates the interference or "beat" frequency to the ambient electron density. Using this beat-frequency technique Hagg (1967) made electron-density measurements in the 8 to 100 cm^{-3} range, which corresponds to the range over which the beat-frequency could be accurately measured on Alouette 2 ionograms. There is an upper limit of about 250 cm^{-3} to the density that can be measured by the beat-frequency method, and this was too low to permit a comparison with measurements based upon the plasma resonance (or upon the cylindrical probe that was also included on Alouette 2). Since the theory of the f_H and f_T resonances was not sufficiently well understood to justify the assumptions underlying Hagg's beat-frequency technique, and since independent checks were not possible, the accuracy of Hagg's technique could not be determined.

Jackson (1972) and Lockwood (1972) found that the Hagg technique yielded values of N_s (in the 8 to 100 cm^{-3} range) approximately one-third the values derived by $N(h)$ analysis techniques. These results were not conclusive, however, because for very low N_s values the $N(h)$ analysis has to

be initiated by assuming the scale height¹³ to be constant or monotonically decreasing as a function of distance below the satellite. A partial check of the Hagg technique was done by Whitteker (1978) using ISIS 1 sounder data. The minimum sounder frequency on ISIS 1 was slightly less than 0.1 MHz and a frequency calibration was provided at 0.1 MHz ($f_N = 0.1$ MHz corresponds to $N_s = 125 \text{ cm}^{-3}$). Thus the ISIS 1 data provided a density range of about 125 to 250 cm^{-3} where the f_N and the Hagg methods overlapped. Using the data from 77 ISIS 1 ionograms (for which both methods could be used), Whitteker (1978) showed that the beat method yielded values of density lower than those derived from f_N by an average of 10 percent and with a dispersion of about 10 percent. Although the results do not apply to Hagg's measurements in the 8 to 100 cm^{-3} range, they do lend some support to Hagg's technique.

3.2.3 Calculations of Electron-Density Profiles

Many refinements in ionogram reduction techniques were the results of efforts made to solve various problems presented by the Alouette 2 data. These refinements have been discussed in Section 1.2.4.3 and are therefore not repeated here. The Alouette 2 ionograms obtained during the higher portion of the orbit (altitudes between 2000 and 3000 km) tend to be very difficult and often impossible to reduce to electron-density $N(h)$ profiles. The Alouette 2 ionograms obtained near perigee (500 km) are in general easy to analyze, but they yield profiles over a very restricted altitude range. Thus the Alouette 2 ionograms were not as well suited as the Alouette 1 ionograms for large-scale routine reductions. Consequently, the number of Alouette 2 ionograms reduced to $N(h)$ profiles is only about one-third the corresponding number for Alouette 1. Electron-density profiles derived from Alouette 2 data have been published in Canada by CRC and in Japan by RRL (Radio Research Laboratories).

3.2.4 Investigations of the z-Trace

The high-resolution z-trace data on Alouette 2 ionograms made possible some investigations that were not possible with the Alouette 1 data. The z-trace on an ionogram is basically a low-frequency extension of the x-trace. The frequency f_z where the z-trace begins is related to the frequency f_x where the x-trace begins by the formula:

$$f_z = f_x - f_H$$

where f_H is the gyrofrequency at the satellite. For the Alouette and ISIS orbits f_H varies from 0.2 MHz to 1.6 MHz. The high-frequency end of the z-trace is always less than f_x . The frequency range of the z-trace is therefore

¹³ See Section 1.2.6.2 for the definition of scale height.

less than f_H . Thus, in contrast to the o - and x -traces, which can extend over a frequency range of 10 MHz or more, the frequency range of the z -trace seldom exceeds 0.8 MHz. Since f_X values of 2.0 MHz or less are fairly common on topside ionograms, the corresponding z -trace occurs at frequencies less than 2.0 MHz. Consequently, the great improvement in resolution below 2.0 MHz on Alouette 2 ionograms has been very helpful for the investigation of z -trace characteristics. Jackson (1969a) showed that the z -trace data on Alouette 2 could be used to check the results of the conventional x -trace analysis of topside ionograms. Colin and Chan (1969) conducted a comprehensive study of z -trace characteristics and concluded that the z -trace data on many Alouette 2 ionograms could be used to improve the accuracy of electron-density profile calculations.

3.2.5 Global Electron-Density Distribution

3.2.5.1 Introduction

The Alouette 2 sounder data were used to extend the knowledge of the topside ionosphere to altitudes between 1000 and 3000 km. In their study of the global electron-density distribution, Chan and Colin (1969) have shown Alouette 2 $N(h)$ data for two pole-to-pole passes, one in March 1966, and one in July 1966. This should be contrasted with the pole-to-pole data shown in the same study but based upon Alouette 1 ionograms. The Alouette 1 pole-to-pole data represent averages from over 100 separate pole-to-pole passes. This illustrates the point made earlier that the large-scale reduction of ionograms to $N(h)$ profiles was less extensive with the Alouette 2 data than with the Alouette 1 data.

3.2.5.2 Equatorial and Midlatitude Studies

Walker and Chan (1976) used Alouette 2 and ISIS 1 ionograms recorded at Singapore to conduct a comprehensive study of the equatorial anomaly in the topside ionosphere at sunspot maximum. All previously reported results had been for low-solar-activity conditions (see Section 1.2.5.2). Walker and Chan used data for the period November 1969 to January 1970 (Zurich sunspot number $R_Z = 100$, $K_p \leq 2$). Walker and Chan compared their results with those obtained for $R_Z = 30$ and found that the electron density had increased by a factor of 2.2 at all heights (up to 1000 km) at 30 deg S dip latitude and by a factor of 3.0 at 1000 km over the geomagnetic equator. The anomaly at sunspot maximum was found to begin at 1000 h (local time) and to be fully developed at 1600 h, which is very similar to the diurnal development of the topside anomaly observed at sunspot minimum.

Matuura and Ondoh (1969) used Alouette 2 ionograms to derive average $N(h)$ profiles for equatorial latitudes and midlatitudes. This study was based on 76 nighttime passes over Japan during the period October 1966 to September 1967 and when K_p was less than 4. The data corresponded to geomagnetic latitudes from -20 deg to +68 deg. Matuura and Ondoh

presented their results for the two consecutive 6-month periods. They published average densities at selected altitude levels (up to 3000 km) and at 10-deg intervals over the geomagnetic latitude range of the data.

Pandey and Mahajan (1973) have used Alouette 2 $N(h)$ profiles published in Canada by CRC to investigate the electron-density distribution at mid- and high latitudes for altitudes up to 3000 km. The main conclusions from this study were related to the occurrence of the "main" or "midlatitude" trough (i.e., the electron-density depression that occurs at geomagnetic latitudes of about 60 deg). They found that the trough is always seen at night. During the daytime, the trough is seen only during winter conditions and at heights above 1000 km. The trough was found at higher geomagnetic latitudes during the day than during the night.

3.2.5.3 The High-Latitude Ionosphere Above 1000 km

The Alouette 1 data on electron densities at high latitudes were extended by the Alouette 2 data to include the altitude range from 1000 to 3000 km. The principal new results obtained at these higher altitudes were related to the mapping of extensive regions where the electron density was less than about 100 cm^{-3} . Since these density values were less than could be measured by conventional topside sounder techniques, the beat-frequency technique of Hagg (1967) had to be used for the measurements. Timleck and Nelms (1969) examined 400,000 Alouette 2 ionograms for evidence of the beat phenomenon and found approximately 800 that contained clearly resolvable beats. In spite of some uncertainty concerning the accuracy of the beat technique (see Section 3.2.2) the presence of a clear interference pattern for the combined f_H and f_T resonances is a fairly reliable indication of ambient densities being less than approximately 100 cm^{-3} . Using basically this criterion, Timleck and Nelms (1969) found that $N_s \leq 100 \text{ cm}^{-3}$ occurred mainly at altitudes greater than 2000 km and at geomagnetic latitudes greater than 60 deg. The lowest altitude and latitude where these low densities were seen were 1400 km and 45 deg respectively. In the northern hemisphere winter and near sunspot minimum, the low densities were observed at all local times.

3.2.6 The Upward Flow of Light Ions

The existence of densities well below 100 cm^{-3} at altitudes as low as 2000 km (see Section 3.2.5.3) was a very surprising result. Axford (1968) showed that the low-density results from Alouette 2 were consistent with the concept of an outward flow of helium and hydrogen ions in the region of open magnetic field lines (i.e., outside the plasmasphere), which he called the "polar wind." At about the same time Hoffman (1968) using his data from the Explorer 31 mass spectrometer found that a high flux of H^+ ions was observed in high-latitude regions when the mass spectrometer was pointed downward. This observation, interpreted as an upward flow of H^+

ions (with a velocity of 10 to 15 km s⁻¹), provided the first experimental evidence of the polar wind.

The concept of the polar wind was developed further by Banks and Holzer (1969) and shown to be the result of the topside ionosphere being exposed to the general magnetospheric electric field. According to Banks and Holzer, the hydrogen ion flow velocity becomes supersonic (with values of about 20 km s⁻¹) at altitudes between 2000 and 4000 km and continues to increase at greater altitudes. Mahajan and Pandey (1974) used Alouette 2 electron-density profiles to estimate the H⁺ fluxes in the polar regions. The calculations of Mahajan and Pandey, which were based upon a comparison between typical $N(h)$ profiles at low-, mid-, and high latitudes, led to a value of 22 km s⁻¹ for the H⁺ ion velocity in good agreement with the theoretical results of Banks and Holzer (1969).

Banks and Doupnik (1974) used Alouette 2 electron-density profiles extending up to about 2500 km to show that a large upwards H⁺ ion flow occurs in the sunlit morning sector at invariant latitudes as low as 48 deg ($L = 2.2$); i.e., in regions considered well inside the plasmasphere. The light ion flow within the plasmasphere was tentatively attributed to a diurnal refilling process.

3.2.7 Miscellaneous $N(h)$ -Related Studies

3.2.7.1 The G-Condition

Herzberg et al. (1969) conducted a general survey of topside sounder data to determine the occurrence rate and other characteristics of the ionospheric G-condition (see Section 1.2.6.1). Approximately 100,000 Alouette 1 and Alouette 2 ionograms obtained between January 1966 and August 1967 were examined and the G-condition was seen on about 200 of these, corresponding to about 100 satellite passes. In agreement with earlier investigations, the G-condition was observed only at high latitudes and during the daytime. However, in contrast to previous results which had shown that the G-condition was associated with magnetic storms, the investigation of Herzberg et al. (1969) revealed many cases of G-conditions occurring in the absence of magnetic disturbances; for example, when K_p was as low as 1-. In fact, the most clearly defined cases of this G-condition were found to occur during periods of only mild magnetic disturbances.

Usually the G-condition was seen only on a single ionogram or on very few successive ionograms. However, three passes were found, each containing a series of about 10 consecutive ionograms indicating the presence of a G-condition over a path of about 1000 km. The $N(h)$ distribution versus latitude for one of these long sequences of G-condition ionograms showed very clearly the formation and recovery pattern. The electron density at fixed altitude in the F2 region and up to about 1000 km decreased as a function of latitude down to about half the normal value and then returned to

normal. Above 1000 km an opposite but somewhat less pronounced variation was observed.

3.2.7.2 Midlatitude Red Arcs

The investigation of the stable auroral red arc (SAR arc) of September 1967, which was based upon Alouette 1, Alouette 2, and Explorer 31 data, has been discussed in Section 1.2.6.7. Similar investigations were carried out by Roble et al. (1971) for the SAR arcs which occurred during the periods of October 29 to November 2, 1968, May 14-15, 1969, and March 8-9, 1970. Electron-density data from the topside sounder and electron-temperature data from the electrostatic probes on Alouette 2 and ISIS 1 were used for these studies. Data from five Alouette 2 passes were used for the first period above (October 29 to November 2, 1968). Two ISIS 1 passes and two Alouette 2 passes provided the data for the second and third periods, respectively. Theoretical calculations were carried out for these nine passes, again using the thermal conduction model of Cole (1965b) as had previously been done for the September 1967 event (see Section 1.2.6.7). The results were in general agreement with the emission features of the SAR arcs observed during each of the nine satellite passes.

3.2.7.3 Steep Vertical Electron-Density Troughs

A significant number of Alouette 2 ionograms exhibit prominent "nose-shaped" traces at frequencies slightly above that at which the extraordinary trace begins. Typically, these traces extend only a few tenths of MHz and they would be hardly noticeable on Alouette 1 ionograms. Clark et al. (1969) has shown that these "nose-shaped" traces occur when the sounder is inside a steep vertical depression of electron density. Oblique echoes are then reflected from the vertical side of the depression. Although these steep vertical "electron-density walls" were found more commonly at high latitudes, the Alouette 2 example investigated by Clark et al. (1969) occurred at 35 deg North.

A concurrent investigation by Shmoys (1969)¹⁴ of the "nose-shaped" traces on Alouette 2 ionograms led to a theoretical interpretation similar to, but somewhat more general than that of Clark et al. (1969). Shmoys used the term "duct" to describe the electron-density depression that caused the "nose-shaped" traces. Perhaps it would have been more appropriate to call the depression a "steep vertical trough," since the term duct is more commonly associated with the very extensively investigated field-aligned

¹⁴ The near-simultaneity of the two investigations can be judged from the submission and publication dates. The manuscript by Clark et al. was received by the Proceedings of the IEEE on October 30, 1968, and published in April 1969. The manuscript by Shmoys was received by the Journal of Geophysical Research on November 25, 1968, and published in May 1969.

irregularities (see Section 1.2.8.2). A further distinction was eventually made between the broad ducts responsible for the low-frequency whistlers and the narrow medium-frequency (MF) ducts responsible for the conjugate echoes seen on topside ionograms.

3.2.8 Medium-Frequency (MF) Ionospheric Ducts

3.2.8.1 Introduction

Because of their improved low-frequency resolutions, the Alouette 2, ISIS 1, and ISIS 2 ionograms have been used extensively for the study of medium-frequency ionospheric ducts. The results quoted in Sections 3.2.8.1 to 3.2.8.5 were in all cases based upon Alouette 2 data. In several cases, however, as indicated in the subsequent text, investigators have broadened their data bases by including ISIS 1 and ISIS 2 data.

As pointed out in Section 3.2.7.3, the use of the term "ionospheric duct" has not been limited to the field-aligned ionospheric irregularities that produce the conjugate echoes seen at medium frequency on topside ionograms. The guiding properties of these MF ducts are usually restricted to a tubular region having a width of the order of a few kilometers. The width over which MF radio waves are trapped in a duct is usually given as the measure of the duct width. Field-aligned irregularities having effective cross sections much broader than those of MF ducts include the low-frequency whistler ducts and the more recently identified equatorial bubbles. Equatorial bubbles have been investigated with Alouette 2 and ISIS 1 ionograms (Dyson and Benson, 1978; Benson, 1981). The concept of the equatorial bubbles, however, did not originate from the Alouette-ISIS program. Equatorial bubbles are large-scale regions of depleted equatorial plasma. These regions, which can exhibit decreases in electron density of as much as three orders of magnitude below the normal ambient values, were first discovered in OGO 6 data by Hanson and Sanatani (1973). Kelley et al. (1976) suggested that these depleted regions must move upward. The term "bubble" was first used by McClure et al. (1977) to represent such a depleted region and to suggest its upward motion.

Many of the above comments could have been given earlier when the subject of ducts was first introduced in the Alouette 1 overview (see Section 1.2.8.2). The above comments, however, apply more directly to the investigations of HF ducts based on Alouette 2 data, than to those based on Alouette 1 data.

The expanded low-frequency scale of the Alouette 2 ionograms not only has facilitated the study of MF ducts, but also it has produced some truly spectacular data. Many examples of the beautiful symmetric patterns that are sometimes formed by conjugate echo traces have been shown by Ramasastry and Walsh (1969). They have also published a remarkable sequence of 36 consecutive Alouette 2 ionograms exhibiting conjugate echoes. Ramasastry and Walsh pointed out that long sequences of 10 or

more conjugate echo ionograms were fairly frequent in the Alouette 2 data recorded at Singapore during 1966.

Various percentages have been quoted concerning the occurrence rate of conjugate echo ionograms. For example, Muldrew (1967b) stated that a sampling of 60,000 Alouette 2 ionograms from eight low-latitude stations yielded 3000 ionograms (5 percent) containing conjugate echoes. Ramasastry and Walsh (1969) found that 50 percent of the 1966 Singapore ionograms contained ducted echoes. It was soon realized, however, that these overall percentages were not particularly meaningful because the occurrence rate of ducted echoes depends critically on location, local time and season; i.e., on the selected data base. Magnetic activity, however, has apparently little or no effect on the occurrence rate of ducted ionograms. The occurrence rate was found to be either independent of K_p or to decrease very slightly with increasing K_p (Muldrew, 1967b; Ramasastry and Walsh, 1969).

3.2.8.2 Physical Characteristics of MF Ducts

From an inspection of 400,000 Alouette 2 ionograms, Ramasastry (1971) selected 2100 ionograms containing conjugate echoes and representing a broad range of latitudes and local times. The selected ionograms were used to calculate the average width of the ducts (as indicated by the duration of the ducted echoes on the ionograms). Ramasastry obtained an average width of 6.51 km and a median value of 4.66 km in general agreement with the most probable value of 4.20 km obtained by Loftus et al. (1966) from the Explorer 20 data (see Section 2.3.3.4). Ramasastry also calculated, from his data on ducts, the peak fractional deviation in electron density $\Delta N/N$, which he found to be typically a 1 percent enhancement inside the duct. This result was also consistent with those obtained from the Alouette 1 (Muldrew, 1963) and Explorer 20 studies (Loftus et al., 1966).

Some information on duct cross section was derived by Muldrew and Hagg (1969) from multiple-hop traces on Alouette 2 ionograms. Multiple-hop traces are frequently seen on ground-based ionograms where they are produced by two or more round trips between the ground and the ionospheric reflection levels. Although multiple echoes are not nearly as common on topside ionograms, two-hop echoes are sometimes observed, the second round trip being initiated by scattering from the sounder antennas. This topside phenomenon was investigated by Muldrew and Hagg (1969) using the high-resolution Alouette 2 data. From the strength of the two-hop signals, it was concluded that the propagation took place in field-aligned tubes having a cross section of about 0.1 km^2 and where the electron density was less than ambient. The ducted propagation was found to be considerably less efficient for the ordinary wave than for the extraordinary wave.

3.2.8.3 Diurnal and Latitudinal Effects

Diurnal and latitudinal effects on the occurrence rate of conjugate-echo ionograms were investigated by Muldrew (1967b) using as a data base 60,000 Alouette 2 ionograms recorded at eight equatorial stations during the period November 1965 to October 1966. The diurnal variation was found to exhibit a broad peak around midnight (with an occurrence rate of about 10 percent) and a broad minimum near noon (with an occurrence rate of about 1 percent). A similar diurnal variation was observed by Ramasastry and Walsh (1969) in their study of the Alouette 2 ionograms recorded at Singapore. Muldrew (1967b) found the occurrence rate to be very strongly dependent on the L value, exhibiting a sharp peak of about 20 to 30 percent at $L = 1.35$ and decreasing to about 1 percent at $L = 3$.

3.2.8.4 Lunar, Seasonal and Longitudinal Effects

From a study of 110,000 Alouette 2 ionograms and 85,000 ISIS 1 ionograms recorded at low-altitude stations from December 1965 to November 1971, Sharma and Muldrew (1973) found that the occurrence rate of conjugate-echo ionograms exhibited a lunar semimonthly oscillation reaching a maximum at 6 and 21 days after the new moon.

Sharma and Muldrew (1975) investigated the seasonal and longitudinal variations in the occurrence of conjugate echoes using all the ionograms (280,000) recorded at low-latitude stations by Alouette 2, ISIS 1, and ISIS 2 during the period December 1965 to August 1972. The results were rather surprising. At American longitudes the occurrence rate was found to exhibit a single maximum (of about 10 percent) at the December solstice and a single minimum (of about 2 percent) at the June solstice. At Asiatic longitudes an opposite behavior was observed; i.e., the maximum was in June and the minimum was in December. Sharma and Muldrew noted, however, that a common feature was present in what appeared to be a completely opposite behavior. In both American and Asiatic sectors the maximum rate of ducted-echo ionograms occurred when the conjugate points on magnetic field lines were the most asymmetric with respect to the earth-sun line.

3.2.8.5 Theory of MF Duct Formation

A theory of duct-formation mechanism must be consistent with the observations described in Sections 3.2.8.3 and 3.2.8.4, particularly the midnight peaking in the duct occurrence rate and its very strong L dependence. To determine even more precisely the effects of local time and L values, Muldrew (1980) conducted a further study based upon 200,000 Alouette 2 ionograms. From this study Muldrew concluded that two mechanisms were involved in the formation of MF ducts. Ducts for $L > 1.2$ were attributed to the mechanism proposed by Cole (1971), according to which ducts are produced by magnetospheric currents flowing from the dynamo region in one hemisphere of the earth to the dynamo region in the other hemisphere. The ducts for $L > 1.2$, however, seemed to be associated with the formation of ionospheric bubbles, and appeared to be

embedded in such bubbles. The observed lunar effects (see Section 3.2.8.4) led Sharma and Muldrew (1975) to conclude that the lunar semimonthly oscillations could be caused by electric fields induced in the dynamo region by lunar tides. The mismatch of conjugate ionospheric potentials, which is assumed in Cole's theory, is also consistent with the observed longitudinal effects discussed in Section 3.2.8.4.

3.2.9 Topside Sounder Resonances

3.2.9.1 Introduction

The study of topside sounder resonances is another area that has benefited substantially from the greatly expanded low-frequency scale of the Alouette 2 ionograms. The principal resonances (f_N , f_T , nf_H) that were discussed in connection with the Alouette 1 sounder were investigated further using the improved Alouette 2 ionograms. More importantly, the Alouette 2 data led to the discovery of many new resonance phenomena such as the Bernstein resonances (f_Q series), the diffuse resonances (f_D series), the floating spikes, and the resonance echoes.

3.2.9.2 The Principal Resonances

Benson (1971) used Alouette 2 data to provide experimental support for McAfee's oblique echo model of the f_N resonance (see Sections 2.2.3.2 to 2.2.3.4). McAfee (1970) predicted from his model that the duration of the f_N resonances should be much shorter for $f_N < f_H$ than for $f_N > f_H$. Benson (1971) found that the duration of f_N resonances on Alouette 2 ionograms was in full agreement with McAfee's predictions. Benson (1971) also showed that the Alouette 2 f_N resonances exhibited a rippled structure for $f_N > f_H$ but not for $f_N < f_H$. However, when f_N was less than f_H , the f_N resonance exhibited a clear Fourier spectrum which was not the case for $f_N > f_H$. These two additional observations were also what would be expected from McAfee's model.

Benson (1970a) had detected a very slight shift in the frequency of the nf_H resonances on the Alouette 1 data. The effect was barely noticeable on the Alouette 1 data, but on Alouette 2 ionograms greatly improved observations could be anticipated. From an initial study of the Alouette 2 data, Benson (1969) concluded that the frequency shifts seen on the Alouette 1 data were due to magnetic contamination by the steel antenna used on Alouette 1. The shifts observed on Alouette 1 were not observed on Alouette 2 where a nonmagnetic beryllium copper antenna had been used. A fairly large shift of about 1 percent, noted near f_H and $2f_H$ on Alouette 2 (Benson, 1969), was found to be instrumental (Benson, 1972b). After making allowance for this instrumental effect, a small residual shift was identified for the $2f_H$ resonance and attributed to plasma-wave dispersion effects (Benson, 1972b).

Muldrew (1972b) used Alouette 2 observations to show that the resonance at $3f_H$ can be explained by an oblique-wave mechanism similar to that used by McAfee to explain the f_N and f_T resonances (See sections 2.2.3.1 to 2.2.3.5). The nf_H resonances observed at $n = 2, 3, 4$ and 5 with a rocket-borne sounder were also explained by the same oblique-wave mechanism (Bitoun et al., 1975).

3.2.9.3 The Bernstein Resonances (f_Q series)

The analysis of the o , x , and z traces on ionograms (see Sections 1.2.4.1 to 1.2.4.3) is based upon the theory of wave propagation in a cold ionospheric plasma; i.e., in a plasma where the thermal motions of electrons are neglected. The electron temperature was taken into consideration (hot plasma theory) to explain the f_N and f_T resonances (see Sections 2.2.3.1 to 2.2.3.5). The theory of wave propagation in a hot plasma also predicts that additional wave modes are possible near the harmonics of f_H . These wave modes have been investigated theoretically by Bernstein (1958), and they are called the Bernstein modes. Dougherty and Monaghan (1966) predicted that the Bernstein modes should produce resonances on topside ionograms.

The Bernstein resonances were first identified on Alouette 2 ionograms by Warren and Hagg (1968). The frequencies at which the resonances occurred were labeled f_{Qn} where

$$nf_H < f_{Qn} < (n+1)f_H \quad \text{and } n \geq 2.$$

Warren and Hagg investigated the behavior of f_{Q2} , f_{Q3} , and f_{Q4} as a function of f_N/f_H . They found that the frequency of f_{Qn} increased monotonically with f_N/f_H within the range nf_H to $(n+1)f_H$. They also showed that f_{Qn} was always greater than f_T as predicted by theory. Muldrew (1972a) showed that the f_{Qn} resonances were due to waves generated in the Bernstein modes and having a group velocity nearly equal to the satellite velocity. The resonance is produced by the component of this wave traveling in the direction of the satellite velocity.

3.2.9.4 The Diffuse Resonances (f_D series)

A diffuse resonance occurring at a frequency approximately equal to $3f_H/2$ was identified in Alouette 2 ionograms by Nelms and Lockwood (1967). Nelms and Lockwood showed that the frequency of the diffuse resonance could deviate from the value $3f_H/2$ by an amount several times greater than the uncertainty of the measurements.

The frequency and occurrence of this diffuse resonance on Alouette 2 ionograms were investigated in considerably more detail by Oya (1970) who

showed that the diffuse resonance occurred when $1.8 < f_N/f_H < 3.7$, and that its frequency f_D varies almost linearly with the parameter f_N/f_H with

$$f_D = 1.4f_H \text{ when } f_N/f_H = 1.8$$

and $f_D = 1.8f_H$ when $f_N/f_H = 3.7$

Oya called this resonance f_{D1} because his study had also revealed three additional series of diffuse resonances which he named the f_{D2} , f_{D3} and f_{D4} resonances. These diffuse resonances satisfy the relationship

$$nf_H < f_{Dn} < (n+1)f_H \text{ with } n \geq 1$$

The relationship between f_{Dn} and the harmonics of f_H is very similar to the relationship given in Section 2.3.9.3 for f_{Qn} , except that we have $n \geq 2$ for f_{Qn} . A more important difference, however, is the position of these resonances with respect to f_T . The Bernstein resonance f_{Qn} always occurs at a frequency greater than f_T , whereas f_{Dn} is always less than f_T .

Oya (1971) explained the formation of the diffuse resonance f_{D1} by a theory in which the $2f_H$ and the Bernstein f_{Q3} waves played an important role. Some of the considerations underlying Oya's analysis were as follows: (1) the f_{D1} resonance corresponds to a frequency range where the warm plasma theory predicts instability, (2) there is a simple relationship between f_{D1} , f_{Q3} , and $2f_H$, namely $2f_H = f_{Q3} - f_{D1}$, (3) the resonances f_{D1} , $2f_H$, and f_{Q3} are seen simultaneously on mixed-mode ISIS 1 ionograms (i.e., a mode in which the sounder was operated at a fixed 0.82-MHz frequency while the receiver swept from 0.1 to 20 MHz), and (4) the theory must explain the long duration of the diffuse resonances.

According to Oya (1971) the sounder pulse creates an expanding turbulent region by increasing the electron energy mainly in the direction of the geomagnetic field vector. The disturbance produces the diffuse wave f_{D1} which can be returned to the sounder with relatively little attenuation provided f_{D1} propagates perpendicular to the magnetic field vector. Thus in Oya's model the observed diffuse resonance is generated in the portion of the turbulent region that propagated away from the sounder in a direction perpendicular to the magnetic field vector. The turbulence created by the sounder pulse, however, cannot last long enough to explain the duration of the diffuse resonance. To maintain the turbulence, Oya invoked a mechanism whereby f_{Q3} (also present in the disturbance) interacts with f_{D1} to produce the beat frequency $2f_H$ (according to the relation $2f_H = f_{Q3} - f_{D1}$). The $2f_H$ wave maintains the turbulence and the f_{D1} wave can continue to be generated. The work of Oya (1971) assumed $T_{\perp}/T_{\parallel} \geq 5$ where T_{\perp} is the temperature corresponding to electron motion normal to the magnetic field vector and T_{\parallel} is the temperature corresponding to electron motion parallel

to the magnetic field vector. Benson (1974a) published ηf_H resonance data from ISIS 1 showing that T_{\perp}/T_{\parallel} values greater than 5 could indeed exist.

Benson (1974b) suggested that the $2f_H$ wave (which is required in Oya's theory) is not created in the turbulent region, but present with sufficient energy in the sidebands of the transmitted rectangular pulse. Kiwamoto and Benson (1979) presented both theoretical arguments and experimental evidence showing further need for modifying Oya's theory. They pointed out that (1) the $2f_H$ wave cannot grow in the disturbance at the expense of the f_{Q3} and f_{D1} waves, (2) the relationship $2f_H = f_{Q3} - f_{D1}$ is only approximate, and (3) the presence of the $2f_H$, f_{Q3} and f_{D1} resonances on mixed-mode ionograms is no more significant than the presence of other resonances that are also seen in the mixed mode of operation. In the model developed by Kiwamoto and Benson, the sounder-stimulated $2f_H$ wave is the energy source for sustaining the f_{D1} wave, and the f_{Q3} wave is not involved in the theory. It is seen from the above discussion that the generation of the f_{D1} resonance involves a process that is quite different from the oblique echo or the velocity-matching mechanisms described in earlier sections.

3.2.9.5 Other Electron Plasma Resonances

Barry et al. (1967) suggested that some of the secondary resonances seen below f_H on the Alouette 2 ionograms were due to stimulated magnetic-dipole radiations from atmospheric constituents near the spacecraft. However, Barrington and Hartz (1968) showed that a significant number of these secondary resonances coincide with beats between the principal resonances (f_N , f_H , and f_T). Barrington and Hartz therefore suggested that the secondary resonances could be explained by the beat mechanism involving the stimulation of the principal resonances in the medium by the harmonics of the transmitter pulse.

A resonance, called the floating spike because it does not begin at zero range, was discovered in the Alouette 2 data by Hagg and Muldrew (1970). They observed that the floating spike occurs when the operating frequency

$$f = \frac{f_T}{2} = f_N - f_H$$

and they suggested that the second harmonic of f stimulates the f_T resonance, which in turn couples energy into the f_N and f_H resonances. The f_N and f_H resonances interact producing a beat frequency signal at the frequency $f_N - f_H$ which is detected after a short delay as a floating spike.

Ionograms exhibit occasionally (between f_H and f_N) a succession of short echoes separated approximately by the time t taken by the z-wave to propagate from the satellite to the z-wave reflection level and back. The display of these echoes on an ionogram resembles a string of beads. These echoes have been investigated by Muldrew and Hagg (1970) who called

them "ionospheric-resonance echoes." The explanation given by Muldrew and Hagg invokes a resonance mechanism produced in an ionospheric irregularity near the satellite by two pulses (a direct and reflected one) having a time separation t .

3.2.9.6 Electron Temperatures from Resonance Data

The explanations for the plasma, upper-hybrid, gyroharmonic ($n \geq 2$) and diffuse resonances are all based upon the theory of wave propagation in a warm plasma. These resonances have properties such as duration or amplitude modulation that are dependent upon the ambient electron temperature (T_e). Consequently, T_e information can be derived from these properties.

Feldstein and Graff (1972) have derived electron temperatures from the amplitude modulation observed on f_N and f_T resonances. Daytime and nighttime Alouette 2 data were used for this study. Since very reasonable values of T_e were obtained, these measurements can be viewed as providing further support for the oblique-wave theory of the f_N and f_T resonances.

Oya and Benson (1972) have derived electron temperatures from f_{D1} resonance data on Alouette 2 ionograms. The property of the f_{D1} resonance used for these measurements is the splitting of f_{D1} due to a Doppler effect caused by the satellite motion. Oya and Benson compared their measurements with T_e data obtained from the Alouette 2 electrostatic probe and found that the T_e values derived from the probe data were typically 50 percent greater than the T_e values measured from the f_{D1} resonance. The discrepancy was attributed to a departure of the electron motions from a Maxwellian distribution. This idea was explored further by Benson and Hoegy (1973), who computed the two-temperature plasma model that would be required to explain the discrepancy. They pointed out that the model (a superposition of two Maxwellian distributions) was difficult to reconcile with the current understanding of ionospheric plasmas. An additional study of the same problem (Benson, 1973) indicated that the discrepancy between the electrostatic probe and the f_{D1} resonance data seemed to be latitude dependent. Benson (1973) also considered the possibility that the discrepancy was due to a difference between electron temperatures corresponding respectively to motion parallel and perpendicular to the geomagnetic field. The required parallel vs. perpendicular anisotropy again appeared to be excessively large. The discrepancy has not yet been explained.

A third technique for deriving T_e from topside resonances was developed by Benson and Bitoun (1979). This technique is based upon the duration of the $3f_H$ resonance. (The $4f_H$ resonance could also be used for this purpose, but the $3f_H$ resonance is preferable because it has a longer time duration). The basic measurement required by the technique; i.e., the determination of a time duration, is easily performed. The derivation of electron temperatures from this measurement, however, requires an accurate knowledge of the sounder antenna orientation.

3.2.9.7 Proton Gyrofrequency Effects

Proton gyrofrequency effects were first detected on the Alouette 1 ionograms as spurs on the f_N resonance (see Section 1.2.9.5). Matuura and Nishizaki (1969) observed on Alouette 2 ionograms short-duration echoes at multiples of the proton cyclotron gyration period t_p . These echoes occurred primarily between f_H and f_N and they were not attached to any electron resonance. An extensive survey of the occurrence of both proton spurs and proton echoes was conducted by Horita (1974) using ionograms from 60 Alouette 2, ISIS 1, and ISIS 2 passes. Although based partly upon ISIS 1 and ISIS 2 data, Horita's study is given here under the Alouette 2 overview in order to summarize in chronological order the studies of proton gyrofrequency effects. The frequency ranges f of proton spurs and proton echoes were normalized to f_H and displayed as plots of f/f_H versus f_N/f_H . All the spurs studied by Horita were attached to the f_N resonance.

Benson (1975) found that the spurs can also be attached to the harmonics of nf_H ($n = 2, 3, 4, \dots$) of the electron gyrofrequency resonance, and occasionally to the resonance at the upper-hybrid frequency f_U . The spurs on the f_N resonance are very large when f_N overlaps with an nf_H resonance. Benson showed that proton spurs are observed on nf_H when the sounder can excite an unstable condition in the ambient plasma. The instability is caused by an anisotropic distribution of electron velocities. The observations suggest that coherent ion oscillations become possible when this unstable condition exists.

Oya (1978) determined the occurrence characteristics of unattached proton cyclotron echoes from a study based upon 800 Alouette 2 ionograms containing such echoes. He found that these echoes occurred only at magnetic dipole latitudes less than 25 deg. Oya suggested that the proton resonance echoes were due to a bunching of protons produced in the vicinity of the sounder antenna by the large negative excursions of the antenna potential. This bunching is repeated at the proton cyclotron period. In Oya's theory the echo-generating mechanism depends critically on the antenna orientation with respect to the geomagnetic field, and it requires that the satellite velocity be nearly parallel to the geomagnetic field. Oya's theoretical explanation was consistent with all the experimental evidence concerning unattached proton cyclotron echoes.

3.3 The Alouette 2 VLF Experiment

3.3.1 Introduction

As indicated in Section 1.3.1 the various VLF phenomena seen on the ground have also been observed in satellite VLF experiments. The use of the VLF data obtained from these two sources of observation has, however, been entirely different. The ground-based data have been used to establish the origin of VLF signals, to study their propagation characteristics and to calculate electron densities near the plasmopause. The phenomena of interest in the satellite data were primarily the phenomena that are not

seen in ground-based data, such as ion whistlers, LHR noise and ELF noise. The satellite VLF data, however, have yielded very little information on electron density because of the uncertainty concerning the propagation paths.

New information was obtained and new discoveries were made with the Alouette 2 VLF experiment because of the greater altitude range of Alouette 2 (compared with that of Alouette 1) and also because of improvements made to the VLF receiver on Alouette 2. The range of this receiver was extended downward to 50 Hz and upward to 30 kHz (compared to the 400-Hz to 10-kHz range of the Alouette 1 VLF experiment). The range of the Alouette 2 experiment included the following ITU bands:¹⁵ ELF (30 to 300 Hz), VF (voice frequencies, 300 to 3000 Hz), and VLF (3 to 30 kHz). However, most investigators studying radio emissions in the 30-Hz to 30-kHz frequency range do not split up this range into the three ITU bands. Instead, they include the lower portion of the VF band in the ELF band, and the upper portion of the VF band is included in the VLF band. The dividing line between ELF and VLF emissions is not sharply defined, but it is usually between 1 and 2 kHz. In certain contexts (such as the Alouette 2 VLF experiment), the term VLF includes the three ITU bands from 30 Hz to 30 kHz.

Whistler-mode noise emissions were also studied in the LF band (30 to 300 kHz) at a fixed frequency of 200 kHz. In this case the data were provided by the AGC voltage of the Alouette 2 sounder receiver, since this receiver swept from 0.1 to 15 MHz (see Section 3.4.4).

3.3.2 Ion Whistlers

The first ion whistler ever observed was a proton whistler discovered in the Alouette 1 VLF data. As indicated in Section 1.3.3 a proton whistler is a slowly rising tone that approaches asymptotically the ambient proton gyrofrequency. This frequency varied from 300 to 600 Hz at the Alouette 1 orbit. Since the low-frequency cutoff of the VLF receiver on Alouette 1 was 400 Hz, proton whistlers were observed only at high latitudes and usually only over the upper portion of their frequency range. In view of the importance of proton whistlers and of the possibility of detecting helium whistlers, the frequency range of the VLF receiver on Alouette 2 was lowered to 50 Hz. The extended low-frequency response of the Alouette 2 experiment has resulted in greatly improved proton whistler data, and it has led to the first observations of helium whistlers (Barrington et al., 1966). Proton whistlers were observed primarily at night at all geomagnetic latitudes less than about 65 deg and at altitudes from 500 to 3000 km, the height range of the Alouette 2 satellite. Helium whistlers were detected

¹⁵ The ITU bands have been defined by the International Telecommunication Union Radio Regulations, Article 2, Section II, Geneva, 1959.

under similar conditions but at altitudes less than 2000 km, probably because of the low concentration of helium ions above this height. The occurrence of helium whistlers was found to be less frequent than that of proton whistlers (McEwen and Barrington, 1968).

The crossover frequency between proton whistlers and their triggering fractional-hop whistlers yields a measurement of the local proton density (see Section 1.3.3). In a similar manner the local helium concentration can be derived from helium whistlers. An extensive study of hydrogen and helium whistlers was conducted by McEwen and Barrington (1968), using all the Alouette 2 VLF data recorded at the Ottawa telemetry station during 1966. Approximately one-fourth of the satellite passes yielded ion whistlers. From the available ion whistler data, over 575 proton whistlers were analyzed, yielding data for the full altitude range of the satellite and for invariant latitudes between 67 deg and 35 deg North. Helium whistlers were found for 61 of the above events but only at altitudes between 850 and 2100 km. The proton whistler data were used to determine the nighttime proton concentration as a function of altitude for four invariant latitude regions between 35 and 67 deg. The helium ion concentration was also determined as a function of altitude, but the data were divided into two latitude regions only.

Gurnett and Brice (1966) have derived a method for calculating the proton temperature from the abrupt decrease in amplitude of the proton whistler near its high-frequency cutoff. This method was first applied to VLF data from Injun 3 and Alouette 1. Lucas and Brice (1971) showed that the damping of the proton whistler is sensitive to irregularities in proton density. Taking this effect into consideration for an Alouette 2 proton whistler yielded a proton temperature greater by a factor of 2.

3.3.3 Whistler-Mode Noise Emissions

3.3.3.1 Introduction

Radio noise emissions in the ELF and VLF bands provide information concerning processes occurring in the ionosphere and the magnetosphere. The most intense and most frequent noise emission occurs at frequencies less than 1 kHz. It is called ELF noise (see comments in Section 3.3.1), and it has a bandwidth typically less than 500 Hz. Yet this noise is so strong that it can control the AGC level of the VLF receiver more than 50 percent of the time. This is remarkable since the ELF noise corresponds to less than 2 percent of the receiver bandwidth.

3.3.3.2 ELF Emissions

Holtet and Egeland (1969) have studied auroral ELF emissions observed simultaneously on the ground and by Alouette 2 in the frequency range 500 to 1000 Hz (called the 700-Hz band). The emission in the 700-Hz band was found surprisingly similar on the ground and at the satellite altitude

(2000 km), suggesting that the 700-Hz band must be generated above the ionosphere.

Harvey (1969) made a detailed analysis of the frequency spectrum of ELF noise recorded by the Alouette 2 receiver. He found that in many cases the ELF noise exhibited a sharply defined lower frequency cutoff, and whenever such a cutoff existed it occurred very close to the proton gyrofrequency. Occasionally another cutoff was observed at the second harmonic of the proton gyrofrequency. This study led Harvey (1969) to conclude that the ELF noise was due to electrostatic proton cyclotron harmonic waves.

The distribution of ELF noise as a function of invariant latitude and local mean time was investigated by Barrington et al. (1971). The Alouette 2 data showed that ELF noise occurred primarily during daylight hours and that its peak occurrence was centered roughly at local noon and at 50 deg invariant latitude. Barrington and Palmer (1972) compared the ELF noise distribution derived from the Alouette 2 data with ELF distributions derived from Injun 3 and OGO 3 data. Since the data obtained with the electric dipole on Alouette 2 yielded basically the same distribution as that obtained from studies made using magnetic loop antennas on Injun 3 and OGO 3, Barrington and Palmer concluded that the ELF noise was electromagnetic in nature.

Horita et al. (1975) showed that the Alouette 2 ELF emissions exhibited their maximum intensity over a region having a width of only a few degrees in latitude. The lower latitude termination of this region of maximum intensity was found to be very abrupt and to occur most frequently (for nighttime data) near the inner boundary of the plasma sheet.

3.3.3.3 VLF Emissions

The noise emission in the VLF range as a function of invariant latitude and local mean time was investigated by Barrington et al. (1971). They found that the VLF noise also exhibited a maximum intensity near noon. The center of the region of the most intense VLF noise was at 77 deg invariant latitude. This VLF noise was typically hiss, and it had a lower frequency cutoff at the LHR frequency of the ambient plasma (see Section 1.3.2).

3.3.4 Non-Guided Whistlers

As indicated in Section 1.3.1, evidence for non-guided (NG) whistlers was found in the Alouette 1 data. Similar evidence was observed in the OGO 2 and 4 data by Walter and Angerami (1969). A comprehensive study of NG whistlers based upon Alouette 2 data was conducted by Charcosset et al. (1973). The NG whistlers were observed for $L < 2.5$ at altitudes between 1000 and 1800 km. Non-guided whistlers exhibited a very unusual evolution in their spectral characteristics as a function of latitude. In a typical example shown by Charcosset et al., an NG whistler appeared initially near $L = 5$ as a fish-hook-shaped trace having its lower frequency cutoff near 11 kHz; i.e., at the lower electron hybrid frequency for the particular

location and time. Beginning at latitude L between 2 and 1.8, a separate low-frequency component appeared below the high-frequency hook trace. The low-frequency trace had a frequency dispersion corresponding to a guided whistler. The high- and low-frequency components merged gradually and became a single whistler at $L \leq 1.6$. A theory explaining all the observed features of NG whistlers was developed by Charcosset et al.

3.3.5 Rendezvous Experiments

A rocket VLF experiment was conducted from Fort Churchill, Canada, during a northbound pass of the Alouette 2 satellite (Barrington, 1969). The main objectives of the simultaneous measurements were (1) to compare VLF data from the two sources of observations and (2) to attempt the artificial stimulation and reception of VLF signals. Natural LHR noise was observed in both the Alouette 2 and rocket data. The low-frequency cutoff of the LHR noise as a function of time was consistent with the vertical trajectory for the rocket data. Specifically, the ion density derived from the LHR cutoff of the rocket was consistent with the vertical electron-density profile derived from the Alouette 2 topside ionograms. For the satellite data the LHR noise was consistent with the ambient conditions at the Alouette 2 altitude of about 800 km. The artificial stimulation and reception of VLF signals was undertaken in an attempt to overcome the major limitation of VLF experiments, namely the sporadic nature of VLF data. The value of LHR data, for example, would be enhanced considerably if LHR noise could be produced on request. The VLF stimulation experiment used a combination of high-voltage short-duration dc pulses and of 0- to 15-kHz swept-frequency impulses. Many, but not all, of the stimulating signals were followed by LHR noise. Thus the experiment was only partially successful.

Another rocket VLF experiment was conducted from Andoya, Northern Norway, during a Polar Cap Absorption (PCA) event and the results were compared to the closest available Alouette 2 data and ground-based data (Holtet et al., 1971). A high degree of correlation was found between the noise emissions observed at the satellite altitude of 1800 km and the emissions seen by the rocket experiment (the peak altitude was 216 km). The poor agreement with the ground-based data was explained by the strong PCA layer absorption (or upward reflection) of the noise emissions. There was a high degree of correspondence, however, between the ground, rocket and satellite data for the discrete ELF emissions seen in the 500- to 1500-Hz band. It was suggested that these ELF emissions had experienced relatively little attenuation because of strong guidance along geomagnetic field lines.

3.4 The Alouette 2 Cosmic Noise Experiment

3.4.1 Introduction

Since the AGC voltage of the sounder receiver provided the cosmic noise data, the improvements made to the Alouette 2 topside sounder experiment have resulted in corresponding improvements for the Alouette 2 cosmic noise experiment. Specifically, the extended low-frequency response of the

Alouette 2 receiver and the higher altitudes achieved by the Alouette 2 spacecraft have made it possible to obtain cosmic noise data at frequencies down to 0.6 MHz. By comparison the Alouette 1 receiver could not provide useful cosmic noise data at frequencies less than 1.5 MHz. The lower limit for cosmic noise measurements is approximately at the frequency f_T . The Alouette 1 data had provided evidence of unexpected high noise levels at frequencies below f_T but a systematic study of this noise could not be undertaken because of equipment limitation. The improved low-frequency response, selectivity, and resolution of the Alouette 2 sounder receiver have made it possible to investigate the noise at frequencies below f_T .

3.4.2 Galactic Noise

Data for galactic noise studies were obtained when the zenith of the Alouette 2 spacecraft was close to the North Galactic Pole (Hartz, 1969b). The previously known galactic noise spectrum (galactic brightness temperature versus frequency) was extended to include data in the frequency interval 0.6 to 1.5 MHz. Additional data points were also obtained in the frequency interval 4 to 12 MHz.

3.4.3 Solar Noise

Hartz (1969a) used Alouette 2 data to study type III solar bursts (see Section 1.4.3). He found that the bursts at hectometer wavelengths (0.6 MHz to 3.0 MHz) were quite similar to the higher frequency bursts at decametric and metric wavelengths, except that the burst duration was increased at the lower frequency. The electron temperatures in the coronal streamers where the bursts are assumed to originate were deduced from the burst decay rates. The calculated temperatures for the plasma within coronal streamers were found to be substantially lower than those of the background corona at similar distances from the sun. These findings together with the drift rate of the bursts led to an electron-density model for the coronal streamers one order of magnitude greater than those of the background corona. The average source drift velocity was found to be about $0.35c$, in substantial agreement with results obtained from ground-based measurements at metric and decametric wavelengths.

3.4.4 LF Emissions at 200 kHz

Hartz (1970) used data from the Alouette 2 cosmic noise experiment to obtain the distribution of LF noise at 200 kHz. Two principal regions of high-intensity noise were found. The first was centered at an invariant latitude of about 78 deg, and it extended from noon until about 10 p.m. The second was centered at an invariant latitude of 58 deg and extended through most of the night hours. Each region had a width of about 5 deg in latitude. A very pronounced minimum was found in the polar maximum region within the ring of high-intensity emission. The overall pattern of the first region followed that of the daytime auroral oval with a much suppressed nighttime portion. This spatial distribution led Hartz to conclude that the 200-kHz

emissions in the higher latitude region arose from Cerenkov radiation¹⁶ produced by fluxes of electrons having energies in the range 0.1 to 1.0 keV.

In a subsequent study, Hartz (1971) showed that the 200-kHz noise measured on ISIS 1 showed excellent correlation with the electron data in the 10-eV to 10-keV range from the ISIS 1 soft-particle spectrometer. This observation provided additional support for the Cerenkov mechanism of 200-kHz noise generation. The correlation was also taken as justification for interpreting the high-latitude 200-kHz noise data in terms of soft electron flux and for revising the particle precipitation pattern of Hartz and Brice (1967), described in Section 1.5.11. Hartz (1971) suggested that a third zone (corresponding to the high-intensity region of the 200-kHz noise) should be added to the two-zone pattern of Hartz and Brice.

3.5 The Alouette 2 Energetic Particle Experiment

3.5.1 Introduction

An energetic particle experiment, very similar to the one flown on Alouette 1, was included in the Alouette 2 payload. The Alouette 2 version consisted of several counters capable of detecting electrons with energies above 35 keV, 250 keV and 3.9 MeV, and protons above 500 keV, in the range 1 to 8 MeV, and above 100 MeV. Proton spectra could also be measured in the range 100 to 600 MeV. Most detectors were directional. With the Alouette 2 experiment it was possible to measure electron pitch-angle distribution, a measurement that could not be made with Alouette 1. Based on the publications resulting from this experiment, it would appear that the most useful electron data were obtained with the 35-keV detector. The published proton results, however, tend to be based upon the full selection of proton detectors.

3.5.2 High-Latitude Boundary for $E > 35$ keV Outer-Zone Electrons

3.5.2.1 Introduction

McDiarmid and Burrows (1968) have shown that electrons with energies above 35 keV are suitable tracers for identifying closed geomagnetic field lines. The latitude at which the 35-keV flux falls to cosmic-ray background gives approximately the high-latitude limit of closed field lines. This boundary latitude, designated Λ_b , was investigated as a function of local magnetic time (LMT), geomagnetic axis orientation (solar geomagnetic codeclination angle ϕ , the angle between the geomagnetic axis and the earth-sun direction), and interplanetary magnetic field (IMF) direction.

¹⁶ In the Cerenkov radiation process, emissions are generated by incoming electrons with velocities greater or comparable to phase velocity of radiation in the medium.

3.5.2.2 Boundary Latitude Λ_b vs. Local Magnetic Time

McDiarmid and Burrows (1968) used 35-keV data from 300 Alouette 2 passes between December 1965 and July 1966 to determine the dependence of Λ_b on LMT. This study was later extended by McDiarmid and Wilson (1968) using data from 450 Alouette 2 passes between December 1965 and October 1966. Only measurements taken when $K_p \leq 4+$ were used in this study. A quasi-sinusoidal variation was obtained, having a minimum near midnight with $\Lambda_b = 70$ deg and a maximum near noon with $\Lambda_b = 78$ deg. Since the variation of Λ_b vs. LMT correlated well with the high-latitude boundary of closed field lines versus LMT, it was concluded that Λ_b was a good indicator of this boundary.

3.5.2.3 Boundary Latitude Λ_b vs. Geomagnetic Axis Orientation

McDiarmid and Wilson (1968) investigated also the variation of Λ_b vs. the geomagnetic axis orientation. Their investigation was based on the same 35-keV data that had been used for their Λ_b vs. LMT study. It was found that Λ_b had a minimum value when ϕ was 90 deg. For the extreme values of ϕ (60 deg or 120 deg) the value of Λ_b was approximately 3 deg greater. These results were interpreted as indicating that more geomagnetic flux was swept back into the tail when $\phi = 90$ deg than at any other time. McDiarmid and Wilson (1968) showed that this behavior could not be explained by current theories for the interaction between the solar wind and the magnetosphere.

3.5.2.4 Boundary Latitude Λ_b vs. Interplanetary Magnetic Field

The 35-keV data from Alouette 2 were used by Hruska et al. (1972) to investigate the variation of Λ_b with the direction of the interplanetary magnetic field (IMF). The study of Hruska et al. was based on 118 polar passes of Alouette 2 observed in 1967 and 1968 during periods when IMF data were available from Explorers 33 and 35. Only passes for $K_p \leq 2$ were used in this study. When the IMF had a southward component, the 35-keV boundary was displaced poleward (with respect to its average position) in the time interval 2000 to 1000 MLT, and it was displaced equatorward from 1000 to about 2000 MLT. The opposite variation was observed when the IMF had a northward component.

3.5.2.5 Boundary Latitude Λ_b and the Auroral Oval

Feldstein and Starkov (1970) compared the boundaries of the auroral oval to the boundary of closed field lines given by Λ_b as defined by the 35-keV data from Alouette 2. The conclusion reached was that visual auroras are located on the poleward side of the boundary of closed field lines.

3.5.3 Outer Radiation Zone Morphology

3.5.3.1 Intensity of 35-keV Electrons During Magnetic Storms

McDiarmid et al. (1969a) made a study of outer zone electron intensities ($E > 35$ keV) at times of magnetic storms. Because of its near-polar orbit, Alouette 2 can provide data at the same invariant latitude at two local times that differ by about 12 hours. Measurements that are nearly simultaneous (within 20 to 30 minutes of each other) can be obtained when the above data pair is on the same orbit. The purpose of the study was to determine how well the two intensity measurements agreed. Any difference in the intensity-versus-latitude profiles was expected to yield information about acceleration mechanisms responsible for the outer-zone electrons. The 35-keV data from Alouette 2 in the invariant latitude range 50-72 deg obtained during 10 magnetic storms were used for this study. During the storms agreement was found to be very poor for latitudes as low as 55 deg. It was concluded from these observations that most of the storm-time acceleration for $E > 35$ -keV electrons takes place on the night and morning side of the earth.

3.5.3.2 Intensity of 35-keV Electrons During Magnetically Quiet Conditions

McDiarmid et al. (1969b) used 35-keV data from Alouette 2 to conduct a study of dawn-dusk asymmetries in the outer zone for magnetically quiet conditions. The data acquisition techniques were identical with those described in the previous paragraph (Section 3.5.3.1), except for the dawn-dusk restriction on local time and the low magnetic activity criterion. For $L > 5.5$ higher intensities were observed at dawn. The dawn-dusk difference increased with L . At $L = 7$ the dawn intensities were 40 percent higher than the dusk intensities. The results were used to place upper limits on the potential drop across the magnetosphere. These limits were found to be somewhat smaller than those implied by plasma convection models.

3.5.3.3 Location of Outer Zone Intensity Maximum

The outer radiation zone at altitudes less than a few thousand kilometers and for electron energies greater than 40 keV exhibits an intensity maximum at values of L between 3.5 and 6. Using data from Alouette 1, Alouette 2, and other satellites, McDiarmid and Burrows (1967) showed that the value of L corresponding to this intensity maximum was essentially independent of K_p for $E > 40$ keV. For more energetic electrons ($E > 250$ keV, $E > 1.5$ MeV) the L value increased from 3.5 to 4.7 over the period 1960 to 1966.

3.5.4 Solar Proton Profiles

McDiarmid and Wilson (1968) reported that the Alouette 2 particle data occasionally revealed the presence of solar protons with energies in the range 1 to 8 MeV. These solar protons appear in the data as a rise in intensity above the normally very low polar-plateau values (at latitudes well above the cutoff for trapped protons). The high-latitude cutoff for these

solar protons occurred approximately at Λ_b , the cutoff for $E > 35$ keV electrons. The flux of solar protons was found to extend to lower altitudes well into the region of closed field lines. The interpretation was that solar protons can diffuse across closed field lines and be temporarily trapped, giving rise to a small increase in intensity above the background values.

A more detailed study of 1 to 8 MeV solar proton profiles based on data from 100 Alouette 2 passes was conducted by McDiarmid and Burrows (1969). This study confirmed the preliminary results (discussed in the previous paragraph); namely, that the high-latitude cutoff of solar protons matches very well (on the average) the high-latitude cutoff for 35 keV outer-zone electrons.

3.5.5 Solar Electron Profiles

Occasionally when 1 to 8 MeV solar protons were observed in the Alouette 2 data, it was also possible to detect solar electrons over the polar cap (McDiarmid and Burrows, 1970). These solar electrons are revealed by a rise in intensity over the normal polar-cap background values in the $E > 35$ -keV data. Since a similar rise was not seen in the $E > 250$ -keV data, it was concluded that the solar electrons had energies between 35 and 250 keV. The latitude knee (low-latitude cutoff) for the solar electrons was found to be 5 to 8 deg above the knee for solar protons. The location of the solar electron knee agreed approximately with the high-latitude limit of 1 to 8 MeV solar protons which, as indicated in Section 3.5.4, is essentially the high-latitude cutoff for 35-keV outer-zone electrons.

3.5.6 Latitude Cutoff of Solar Particles vs. Rigidity¹⁷

The low-latitude cutoff (latitude knee) of solar particles can be calculated theoretically if the particle energy and charge are known and if an accurate model of the geomagnetic field is available. The results of such calculations are usually given in terms of latitude versus rigidity. McDiarmid et al. (1971) compared the Alouette 2 measurements of latitude knees to the best theoretical results available at that time; namely, the cutoff rigidity calculations of Smart et al. (1969). Fairly good agreement between measurements and calculations was obtained for 114-MeV protons. The measured knee latitudes for 33-MeV and 1-MeV protons were about 3 deg lower than the calculated values. The calculations of Smart et al. did not extend to sufficiently low rigidity values to permit a comparison with the observed latitude knee for 35-keV electrons.

¹⁷ "Magnetic rigidity" or momentum-to-charge ratio is a measure of a particle's ability to penetrate a magnetic field.

3.5.7 Solar Particles and Closed Field Lines

McDiarmid et al. (1972) used knee-latitude data for 35-keV solar electrons in an attempt to determine the dayside limit of closed geomagnetic field lines. The data used were obtained during the period 1966-1969 by Alouette 2 and during 1969 by ISIS 1. This investigation led McDiarmid et al. to suggest (1) that the limit of closed field lines under magnetically quiet conditions occurred at the position of the 35-keV solar electron knee latitude (78 deg invariant), and (2) that solar electrons diffuse across closed lines when the magnetic activity increases, causing the electron knee for high K_p values to be equatorward of the high-latitude limit of closed field lines.

3.6 Cylindrical Probe/Sounder Compatibility Test

Although the Alouette 1 mission represents a major step forward in the study of the topside ionosphere, a number of important parameters such as plasma temperatures and ion composition were not measured systematically¹⁸ with Alouette 1. One purpose of the ISIS X mission was to extend the scope of the ionospheric studies made with Alouette 1 by including the measurements of these additional ionospheric parameters. The principal techniques available for measuring plasma temperatures and composition involve the use of probes operating basically at or very close to the surface of a spacecraft. When such techniques are used, precautions must be taken to ensure that no serious errors are introduced in the measurements by the spacecraft disturbance of the ambient plasma.

On a spacecraft such as Alouette 2 a very severe disturbance would have been produced by the $\mathbf{V} \times \mathbf{B}$ potential induced on the long sounder antennas unless certain modifications had been made in the antenna design. The first attempt to solve this $\mathbf{V} \times \mathbf{B}$ problem was made on Explorer 20 (see Jackson, 1986, Section 4.2) where capacitive coupling was used between the antennas and the spacecraft. Although this was a step in the proper direction, it did not prove to be sufficient. A further improvement was attempted on Alouette 2 by adding a sheath guard on each sounder antenna. However, there was no assurance prior to flight that the Alouette 2 antenna design would solve the $\mathbf{V} \times \mathbf{B}$ problem. To ensure that the additional ionospheric parameters be measured accurately during the ISIS X mission a second satellite, Explorer 31, was launched simultaneously with Alouette 2 and essentially in the same orbit. To help resolve the question of the Alouette 2 compatibility with direct measurements, essentially identical cylindrical probes were placed on both satellites (Findlay and Brace, 1969). If compatibility had been achieved, the cylindrical probes on Alouette 2 and on Explorer 31 should have yielded the same data when the two spacecraft were in close proximity.

¹⁸ Some rough estimates of ion composition and temperature were occasionally derived from LHR noise data (see Section 1.3.2.3).

Although Alouette 2 and Explorer 31 drifted apart gradually, during the first 2 months after launch they were close enough to yield essentially simultaneous observations. Only data taken during this early period of near-proximity were used for the compatibility test (Brace and Findlay, 1969). This test led to the identification of three problem areas; namely, (1) the severe wake effects produced by the large sounder antennas, (2) the interference produced in the probe detection system by the sounder pulse and (3) the sounder pulse disturbance of the local plasma. Wake effects were avoided by rejecting data taken in the wake. The sounder interference varied as a function of sounder frequency and plasma density from a negligible level to a point where reduction of the data was impossible. Fortunately, the Alouette 2 sounder provided a 4-second off period between sounder sweeps. Cylindrical probe data taken during these 4-second off periods (and away from the wake) were essentially undisturbed and best suited for bulk analysis.

By careful selection of the data to avoid wake effects and sounder interference, it was found that there was no inherent incompatibility between the sounder experiment and direct measurement experiments. The electron temperature T_e and electron density N_e derived from the cylindrical probes on Alouette 2 and Explorer 31 generally agreed within 10 percent. Differences up to 15 percent in T_e and up to 40 percent in N_e were observed on rare occasions. The compatibility test indicated that direct experiments could be successfully combined with topside soundings on future satellites, if intermittent sounder operation and spacecraft attitude control are provided.

3.7 Ionospheric Studies with Alouette 2 Cylindrical Probe

Based upon the results of the compatibility test (see Section 3.6) it was concluded that reliable measurements could be made with the cylindrical probe on Alouette 2.

Nighttime electron density and temperature were measured by Mahajan and Brace (1969) at an altitude of 2500 ± 500 km over a geomagnetic latitude range of ± 60 degrees. Results were obtained for May, August, and December 1966 and March 1967 yielding essentially the seasonal variation. The electron density exhibited a pair of maxima at 30 degrees north and south with values ranging from $4 \times 10^3 \text{ cm}^{-3}$ in the fall to $8 \times 10^3 \text{ cm}^{-3}$ in the local summer. The electron temperature was found to exhibit a broad minimum of about 1800 K at low latitudes, and to increase rapidly at midlatitudes reaching values in excess of 3000 K at ± 60 degrees. No definite seasonal variation was observed in electron temperature. The cylindrical probes employed on Alouette 2 were identical to those used on several earlier satellites, including Explorer 22. Comparisons of Alouette 2 measurements with nearly simultaneous measurements made with Explorer 22 during the summer of 1966 revealed positive temperature gradients along field lines. Typical gradients at 1000 km were 0.6 K km^{-1} on the 35-deg field line and 1.2 K km^{-1} on the 50-deg field line.

The cylindrical probe on Alouette 2 was also used to measure small-scale electron-density irregularities in the topside ionosphere (Dyson, 1969). These irregularities are detected in cylindrical probe data as distortions in the current versus voltage curves. The resolution which depends upon the irregularity thickness and amplitude was typically 1 km for amplitudes greater than 10 percent and 5 km for amplitudes greater than 50 percent. The minimum resolution was 0.2 km for irregularity amplitudes greater than 5 percent. The maximum irregularity thickness that could be resolved was about 10 km and the amplitude of this irregularity had to be 100 percent. Thus the probe was best suited for the measurement of irregularities ranging in thickness from a few kilometers down to a few tenths of a kilometer. Irregularities of this size (referred to as fine structure) were observed primarily in the auroral and polar regions. Comparisons of the probe data with Alouette 2 ionograms obtained simultaneously showed that spread F occurred at the height of the satellite whenever fine structure was observed. However, particularly at midlatitudes spread F often occurred at the satellite when the probe did not detect fine structure. Dyson (1969) concluded that in such cases the irregularities had amplitudes less than 5 percent and thicknesses less than 0.5 km. This conclusion was based upon calculations of reflection coefficients as a function of frequency for a parabolic model of the electron concentration variation in field-aligned irregularities. Dyson (1969) concluded also from his study of irregularities that different irregularity production mechanisms must operate at different latitudes.

Dyson (1971) compared the relative sensitivities of electrostatic probe, sounder and scintillation techniques for the detection of electron-density irregularities at midlatitudes. The data used were obtained over Australia during March and April 1967 at times when the orbital planes of Alouette 2 and Explorer 22 were very closely aligned and when nearly simultaneous data were available from these two spacecraft. Cylindrical probe and sounder data were available from Alouette 2, scintillation data were available from the Beacon experiment on Explorer 22, and ground-based soundings were available from a network of six Australian ionosonde stations. The resulting comparisons led to the conclusion that topside sounding was the most sensitive technique for detecting midlatitude irregularities, followed by scintillation, bottomside sounding and electrostatic probe.

PAGE 82 INTENTIONALLY BLANK

4. EXPLORER 31 RESULTS

4.1 Introduction (General Objectives)

The Explorer 31 spacecraft had both technological and scientific objectives. The main technological objective was to provide data that would show whether or not the Alouette 2 spacecraft design was or could be made compatible with direct local measurements. Secondary objectives were to check the accuracy of various direct measurement techniques and in some cases to calibrate direct measurement instruments. The scientific objectives were to measure simultaneously the densities and temperatures of the most important ionospheric constituents. The Explorer 31 instrumentation made it possible for the first time to carry out such measurements with a high degree of accuracy. A number of geophysical studies and discoveries resulted from this new capability. The scientific results attributable to the Explorer 31 experiments include the worldwide distribution of electron and ion temperatures, the worldwide concentrations of the various ionic constituents, the first experimental observation of the polar wind, new information on ionospheric irregularities, a better understanding of conjugate point phenomena, a comprehensive and definitive investigation of spacecraft wake effects, the first measurement of suprathermal particles, and new insights concerning the applicability of the diffusive equilibrium theory.

4.2 Summary of Explorer 31 Experiments

The Explorer 31 spacecraft contained seven experiments designed to measure ambient electron density N_e , electron temperature T_e , ion density N_i , ion temperature T_i , ion composition and energetic electrons in the range 5 eV to 200 eV. Since each parameter was measured by at least two experiments and since many experiments had two or more similar names, it is sometimes difficult to identify the Explorer 31 experiment(s) associated with a given publication.

In view of the redundancy of measurements and the multiplicity of names for the Explorer 31 experiments, these experiments have been summarized in Table 1. The table is ordered according to the project name; i.e., the prelaunch designations. Since there were two Langmuir probes on Explorer 31 these were called C_1 and C_2 . The B_1 , B_A , B_D instruments were initially part of a "B" package that became separate experiments: B_1 for thermal electrons, B_A for suprathermal electrons (Analog data) and B_D for suprathermal electrons (Digital data). Detailed descriptions and typical results have been given by Donley (1969) for experiments A and B_1 , by Maier (1969) for experiments B_A and B_D , by Findlay and Brace (1969) for experiments C_1 and C_2 , by Hoffman (1969) for experiment D, and by Wrenn (1969) for experiments E and F. Analysis and calibration techniques are also discussed in the above references. Additional information on analysis techniques can be found in Moss and Hyman (1968) for experiments A and

PROJECT NAME	EXPERIMENT NAME (PI) (ALTERNATE NAMES)	MEASURED PARAMETERS					
		N _e	T _e	N _i	T _i	ION MASS	ENERGETIC ELECTRONS
A	Thermal Ion Probe (Donley) (Thermal Ion Trap; Planar Ion Trap; Thermal Ion Retarding Potential Analyzer)			X	X	Low Res.	> 15 eV
B ₁	Thermal Electron Probe (Donley) (Thermal Electron Trap; Planar Electron Trap; Thermal Electron Retarding Potential Analyzer)	X	X				> 5 eV
B _A , B _D	Energetic Electron Current Monitor (Maier) (Energetic Electron Sensor; Total Current Monitor; Planar Retarding Potential Analyzer)						2-200 eV
C ₁ , C ₂	Cylindrical Electrostatic Probes (Brace) (Electrostatic Probes)	X	X				
D	Magnetic Ion Mass Spectrometer (Hoffman) (High Resolution Ion Mass Spectrometer)			X		High Res.	
E	Electron Temperature Probe (Willmore) (UK Electron Temperature Probe; Electron Energy Probe; Langmuir Plate; Langmuir Probe; Planar Disk Langmuir Probe; Planar Probe; Electron Sensor)	X	X				
F	Spherical Ion Mass Spectrometer (Willmore) (Spherical Ion Probe)			X	X	Low Res.	

Table 1 EXPLORER 31 EXPERIMENTS

B_1 , in Brace et al. (1971) for experiment C_1 - C_2 , and in Bowen et al. (1964) for experiments E and F.

All the Explorer 31 experiments performed well in orbit except experiment B_D which was damaged just prior to launch by very severe rainstorms. Some useful data were nevertheless from experiment B_D , although it had lost several decades of sensitivity as a result of the excessive moisture. Explorer 31 yielded data for 3-1/2 years. On July 1, 1969, its data acquisition was terminated with five of the seven experiments still operational.

The redundancy of Explorer 31 experiments has led to a corresponding redundancy in the investigations performed with these experiments. For example, most of the Explorer 31 experiments were affected by the spacecraft wake and were therefore able to provide data on this topic. In such cases a more coherent presentation can be achieved by giving the results by topics rather than by experiments. There are, however, many cases in which results are uniquely associated with specific experiments. For consistency, the Explorer 31 results are presented by topic throughout. The experiments that have contributed to the results given under each section are indicated after the section title using the preflight designations.

4.3 Thermal Plasma Data from Explorer 31

Although direct measurement techniques had been used prior to the ISIS X mission, the absolute accuracy of such techniques had not been previously established. The ISIS X mission provided, for the first time, the opportunity to compare the measurements of various ionospheric parameters made simultaneously by many different techniques. During the first two months after launch the electron density and equivalently the ion density measurements on Explorer 31 could be checked also against the extremely accurate local electron densities provided by the topside sounder. As a result of such comparisons, it became possible, for example, to derive total ion concentration from the magnetic ion mass spectrometer, an instrument which otherwise would have yielded only relative concentrations. Since the spectrometer response was different for the various ion species, the calibration as a function of ion concentration was done in regions of nearly pure H^+ and also in regions of nearly pure O^+ (Hoffman, 1969). A similar calibration procedure was used in order to derive absolute concentrations from experiment F (Wrenn and Smith, 1969).

For the purpose of data intercomparison, a number of satellite passes were selected that occurred during the first two months in orbit (i.e., when Alouette 2 and Explorer 31 were in close proximity) at times when all experiments were operating and good aspect data were available (Donley et al., 1969). A wide variety of geographic locations and altitudes were included, but regions of rapidly varying ionospheric conditions were avoided. The plasma density measurements obtained by experiments A, B_1 , C_1 - C_2 , D and F

agreed with the sounder density values of N_e to within 20 percent for $N_e > 10^4 \text{ cm}^{-3}$. A slightly greater spread in results was obtained in the range $2 \times 10^3 < N_e < 10^4 \text{ cm}^{-3}$. No data were given for densities less than $2 \times 10^3 \text{ cm}^{-3}$. The electron temperature values obtained by experiments B, C₁-C₂, and E agreed within 10 percent on one pass and within 20 percent on other passes. The ion temperature from experiment A was consistently 500 to 1000 K higher than the values measured from experiment F. Both experiments (A and F) yielded ion temperatures considerably below the corresponding electron temperatures. Experiments A and F through retarding potential techniques served also as low-resolution spectrometers. Within this limitation the ion composition data from experiments A and F were consistent with the results of the high-resolution ion mass spectrometer (Experiment D). Experiment E (which was very similar to the successful experiment B₁) yielded electron density values that were too low by a factor of 2 to 5. The swept surface area of the sensor used for experiment B₁ was 55 cm² compared to a swept surface area of 12 cm² for experiment E, suggesting that the satellite sheath was not adequately penetrated in the case of the smaller area.

These intercomparisons indicated that there was no significant systematic disagreement between probes in the measurement of plasma density, electron temperature, and ion composition that could not be recognized as arising from sensitivity or other limiting considerations. One important conclusion was that correct plasma diagnostics could be achieved with flush sensors operating within the satellite ion sheath. The general agreement achieved indicated that large magnetic field orientation effects were not present. However, a small geomagnetic field effect upon the cylindrical probe data was detected at altitudes greater than 1000 km. This effect was investigated by Miller (1972) and found to be minimized when the probe axis was within 20 degrees from the geomagnetic field orientation.

4.4 Topside Morphology (Experiments A, B₁, and D)

Since direct measurement experiments yield data at the spacecraft only, the data corresponding to an eccentric orbit (such as that of Explorer 31) exhibit simultaneous altitude and latitude effects. Various techniques have been used to separate these effects in the Explorer 31 data: (1) the altitude variation could be minimized by making measurements near apogee (3000 km) or near perigee (500 km) which are locations where the altitude varies slowly as a function of latitude; (2) conversely, altitude effects could be made to dominate over the latitude effects at places along the orbit that were halfway between apogee and perigee; (3) altitude variations could also be obtained at a given latitude by taking advantage of the gradual rotation of the

line of apsides.¹⁹ This rotation causes the spacecraft to cross a given latitude at slightly different heights on successive days. This technique yields the most rapid daily height variation at locations halfway between apogee and perigee.

Goel et al. (1976) used a combination of techniques (2) and (3) to obtain vertical profiles of ion composition (Experiment A) and of plasma temperatures (Experiments A and B₁). The altitude variations were determined for daytime conditions at both low and middle latitudes. These results were obtained with September-October 1967 data during a period of medium solar activity and in the altitude range 700 to 2000 km. The transition heights where O⁺ and H⁺ densities are equal were found to be about 1600 and 1300 km at middle and low latitudes respectively. The results were used to derive a topside ionospheric composition model.

Hoffman (1970) used a combination of techniques (1) and (3) to obtain nighttime composition data near apogee versus geomagnetic latitude. The data were obtained with experiment D, and the altitude range used was actually from 2200 to 3000 km. At low and middle latitudes the H⁺ density was found to be about 3 orders of magnitude greater than the O⁺ density. At about 60 degrees geomagnetic, however, (in the local summer) an abrupt decrease in H⁺ density was observed with a corresponding rapid increase in O⁺, making O⁺ the dominant ion at latitudes greater than 60 degrees. In the polar regions the roll modulation seen in the ion spectrometer data revealed that H⁺ ions were flowing upward with a velocity of 10 to 15 km s⁻¹. This observation provided the first experimental evidence for the existence of the polar wind.

4.5 Conjugate Point Studies (Experiments A, B₁, B_A, and E)

4.5.1 Introduction

Theoretical considerations relating to electron temperature in the ionosphere led Hanson (1963) to conclude that photoelectrons released above 300 km and having energies in the range 5 eV to 50 eV could escape from their local source and travel along geomagnetic field lines to the magnetic conjugate point in the opposite hemisphere. Hanson calculated that the flux of these energetic photoelectrons should be about 10⁸ electrons cm⁻² s⁻¹. Indirect evidence for the existence of these non-local photoelectrons was provided by Cole (1965a) who showed theoretically that these photoelectrons could produce observed predawn enhancements of the

¹⁹ The line of apsides is a straight line from apogee to perigee. Since the actual apogee and perigee do not occur at the same time, the line of apsides actually connects the apogee and perigee of the "instantaneous" orbit.

6300-A airglow. Similar support for the concept of photoelectrons traveling along field lines was provided by Carlson (1966). Carlson showed that predawn increases in electron temperature observed at the Arecibo Ionospheric Observatory could be explained by photoelectrons coming from the sunlit magnetic conjugate ionosphere. The first experimental evidence and measurements of these energetic photoelectrons (also called eV electrons or suprathermal electrons) were obtained with Explorer 31 experiments A, B₁ and B_A.

4.5.2 Measurements of Conjugate Photoelectron Flux

Rao and Donley (1969) used experiments A and B₁ to measure suprathermal electrons when one end of the geomagnetic field line passing through the satellite was in darkness and when the other end was near sunrise. By making measurements at different locations and on different days, data were obtained at different times after conjugate sunrise, or equivalently for various values of the solar zenith angle χ . The values of χ at 300 km were taken as representative of sunrise in the ionosphere. The photoelectron flux was found to start increasing when χ was less than 102 deg (sunrise at 300 km). A maximum value of 2.5×10^8 electrons $\text{cm}^{-2} \text{s}^{-1}$ was reached when χ was about 60 deg. Simultaneous data from experiment B_A showed that the spectral distribution of these photoelectrons exhibited a broad maximum between 5 and 10 eV. Theoretical calculations by Shawhan et al. (1970) yielded values of photoelectron flux for values of χ between 80 and 110 deg that were in good agreement with the results of Rao and Donley (1969).

A concurrent study of conjugate point effects was conducted by Wrenn and Shepherd (1969) who used experiment E to measure electron temperature with the local ionosphere in darkness and varying degrees of solar illumination at the conjugate point. The electron temperature was found to increase from 1400 to 2400 K as the conjugate solar zenith angle (at 300 km) decreased from 98 to 90 deg. This enhancement was found to be remarkably insensitive to large changes of altitude, latitude, or longitude.

The investigations of conjugate point effects conducted by Rao and Donley (1969) were extended by Rao and Maier (1970) who measured the suprathermal flux both differentially and directionally with experiment B_A, the electron temperature with experiment B₁, and the ion temperature with experiment A. In the night hemisphere Rao and Maier (1970) found the electron temperature to increase from about 1500 to 3500 K as the solar zenith angle in the conjugate hemisphere decreased from 126 deg to 77 deg. The corresponding change in ion temperature was from 1500 to 3000 K while the change in the suprathermal flux was from 2×10^7 to 15×10^7 electrons $\text{cm}^{-2} \text{s}^{-1}$ for electrons with energies greater than 3.7 eV. Surprisingly, the measurements also revealed the presence of an appreciable return flow of photoelectrons from the night hemisphere back to the sunlit hemisphere.

4.6 Wake Effects (Experiments A, B₁, D, and E)

4.6.1 Introduction

The motion of a satellite creates a disturbed region around the satellite. In the ionospheric plasma the disturbance includes a positive ion sheath (typically a few centimeters in thickness for Explorer 31) and a downstream wake with an unequal depletion of both electrons and ions. At the Explorer 31 orbit the satellite velocity is roughly one order of magnitude greater than that of the ions and one order of magnitude smaller than that of the electrons. The spacecraft therefore sweeps out the ions and leaves a wake in which ions are depleted. The electrons are also depleted in the wake because electrostatic forces prevent a large electron-to-ion ratio from being created in the wake. Wake effects extend many spacecraft diameters downstream, but they are most pronounced close to the satellite surface.

These considerations have led to the following characteristics of the Explorer 31 spacecraft. The satellite was spin-stabilized at 3 revolutions per minute, the spin axis was maintained orthogonal to the orbital plane and the sensors were mounted perpendicular to the spin axis.²⁰ Thus each sensor faced forward once each roll period; i.e., once every 20 seconds. One important byproduct of this arrangement was a continuous variation in sensor orientation which permitted measurements at all angles with respect to the velocity vector from 0 deg (forward) to 180 deg (wake). These measurements (at various angles of attack) are the subject of Section 4.6.

4.6.2 Wake Effects on Electron and Ion Distributions

The first and perhaps the most spectacular demonstration of wake effects on an Explorer 31 experiment was provided by the magnetic ion-mass spectrometer data (experiment D). Hoffman (1967) showed that the spectrometer data were extremely sensitive to the angle of attack. The effects observed were also a function of mass, being much greater for heavy ions such as O⁺ than for light ions such as H⁺. For example, at an altitude of 650 km the amplitude variation as a function of angle of attack was one order of magnitude for H⁺, 2-1/2 orders of magnitude for He⁺ and more than 5 orders of magnitude for O⁺.

Samir and Wrenn (1969) used data from experiment E to investigate the variation of the electron density N_e as a function of the angle θ between the probe normal and the velocity vector (angle of attack). Wake effects were very small when θ was less than 60 deg. A rapid decrease in N_e was observed when θ was between 90 and 150 deg and the maximum effect was,

²⁰ The only exception was the sensor for experiment F, which was mounted on the spin axis about 50 cm away from the surface of the spacecraft.

as expected, at $\theta = 180$ deg. Although the satellite sheath introduced an error in the measurement of N_e (see Section 4.3), the error was at least one order of magnitude smaller than the wake effects at perigee. The wake effects became less pronounced at higher altitudes, but they could be detected up to apogee. The observed wake-to-front ratio

$$\delta = \frac{N_e \text{ (wake)}}{N_e \text{ (front)}}$$

was about 0.01 at 550 km, 0.1 at 800 km and 0.4 at 1000 km. The values of δ were found to correlate very well with the average ionic mass values M^+ obtained from experiment F. This result indicated that the measurements of δ were consistent and that such measurements could serve as a diagnostic tool to measure ion composition within a reasonable resolution. Samir (1970) used the above dependence of δ upon M^+ to explain the two orders of magnitude discrepancy between Explorer 8 and Ariel 1 electron-wake measurements. The Explorer 8 data were based upon measurements at 1000 km where δ should be about 0.4, and the Ariel 1 data were made in an ionosphere where O^+ was a major constituent; i.e., where δ should be about 0.01.

Samir and Jew (1972) published additional observations of wake effects as a function of θ . In this study the measured values of N_e (from experiment E) were normalized to N_e (front) and it was shown that the normalized data were in excellent agreement with corresponding normalized data from experiment B₁. It was therefore established that experiment E could yield accurate measurements of wake effects, although the absolute values of N_e from experiment E could be in error by as much as a factor of 5. The satellite sheath effect on experiment E appeared to be equivalent to a reduction of acceptance angle which remained essentially constant during a satellite spin, and would therefore reduce by the same factor all N_e values versus θ . The normalized wake data obtained at various altitudes were found to be in good agreement with the theoretical wake model of Liu and Jew (1968).

Samir et al. (1973) used data from experiment A to study wake effects upon N_i as a function of θ . The measured values of N_i were compared with N_e data from experiment E obtained under similar electron temperature and ionic mass conditions. In all cases the ion depletion was greater than the electron depletion. The ion density was smaller than the electron density, typically by one order of magnitude for $\theta = 90$ deg and by two orders of magnitude for $\theta = 150$ degrees. These observations provided the first experimental data showing quantitatively the ion-to-electron ratio in the wake as a function of the angle of attack.

Samir et al. (1975) compared the ion data of Samir et al. (1973) with the wake models of Liu and Jew (1968) and Gurevich et al. (1969). The model of Gurevich et al. was found to give better agreement with the data when at least 20 percent of the ions were H^+ and when the Mach number was low. For high Mach numbers the Liu and Jew model gave better agreement with the data.

4.6.3 Wake Effects on Electron Temperature

Samir and Wrenn (1972) used data from experiment E to investigate the variation of electron temperature T_e as a function of the angle of attack θ . The electron temperature was found to be relatively constant for θ less than 90 degrees. A monotonic increase in T_e was observed, however, when θ increased from 90 to 180 degrees. The maximum increase, which occurred at 180 degrees, was about 50 percent and relatively independent of ion composition.

Further investigations of wake effects on T_e were conducted by Troy et al. (1975) using data from experiments B₁ and E. A total of 139 sets of T_e versus θ curves was obtained under a variety of geophysical conditions. In most cases the results were in agreement with those of Samir and Wrenn (1972) in showing that (1) T_e usually varies as a function of θ , (2) when a variation exists a maximum value of T_e occurs at $\theta = 180$ degrees, and (3) the magnitude of the T_e enhancement in the wake does not correlate with the average positive ion mass. The study of Troy et al. (1975), however, yielded a number of cases in which T_e was essentially independent of θ . Troy et al. also found that T_e enhancements in the wake of 50 percent or greater were relatively rare. Enhancements of 20 percent or less were more common. The results of Troy et al. showed no clear evidence of either solar illumination or geomagnetic effects.

4.7 Rocket Rendezvous with ISIS X

A Javelin rocket was launched from Wallops Island, Virginia, on August 15, 1966, to rendezvous with passes of the Explorer 31 and Alouette 2 satellites (Hoffman et al., 1969). The rocket was instrumented with an ion-mass spectrometer identical to that used on Explorer 31. Rendezvous experiments between rockets and satellites have typically been performed to check or extend satellite data. However, in the case of the rocket experiment of August 15, 1966, the purpose of the rendezvous was to calibrate the ion-mass spectrometer used in the rocket experiment. This spectrometer had to be calibrated for the same reasons that the ion-mass spectrometer on Explorer 31 had to be calibrated (see Section 3.8.3). The calibration of the rocket instrument was done by comparisons with Experiment D on Explorer 31 and with the Alouette 2 sounder.

The rocket trajectory was due East at a latitude of 37.5 deg and the peak altitude was 723 km. The Explorer 31 altitude at the time of crossing was 972 km. However, because of the variation with latitude in the satellite altitude and because of the relatively uniform ionospheric conditions for a few degrees North and South of the rocket latitude, experiment D yielded representative composition data from about 800 km to 1100 km. The validity of the calibration procedure was established by noting that a smooth extrapolation of the rocket data was in good agreement with the 800- to 1100-km profile from Experiment D. This calibration of the rocketborne ion-mass spectrometer made it possible to obtain accurate measurements of ion composition at the rocket altitudes. In particular, it was shown that previous estimates of the H^+ concentration at altitudes between 200 and 400 km had been too high because the spectrometer was much more sensitive to H^+ than to O^+ .

4.8 Langmuir Probe vs. Incoherent Scatter Radar Data

Electron temperatures T_{es} (s for satellite data) obtained with the ISIS X cylindrical probes (cylindrical probes on Alouette 2; experiments C_1 and C_2 on Explorer 31) were compared with simultaneous observations of incoherent scatter radar temperatures T_{er} from Jicamarca, Peru, and Millstone, Massachusetts (Carlson and Sayers, 1970). A linear fit to the observations yielded the relationship

$$T_{er} = (5/6)T_{es} - 400 \text{ K}$$

For typical ionospheric temperatures this formula shows that $T_{es} - T_{er}$ ranges from less than 500 K to nearly 1500 K. Taylor and Wrenn (1970) found, however, that the T_{es} data from experiment E agreed with the T_{er} data from the incoherent scatter radar at Malvern, England. It was suggested by Carlson and Sayers (1970) that the good agreement obtained by Taylor and Wrenn (1970) might have been due to the rapid effective sweep rate used by experiment E. The slow sweep rate used by the cylindrical probe should theoretically have rendered this probe more sensitive to errors produced by the probe work function, yielding temperatures that would have been too high. Carlson and Sayers (1970) pointed out that laboratory plasma work had shown that probe work function could cause Langmuir probes to yield electron temperatures that are too high. Taylor and Wrenn (1970) also found that experiment F yielded values of ion temperatures and ion densities in agreement with corresponding data from the Malvern radar.

4.9 Vertical Temperature and Composition Profiles

A full description of the topside ionosphere requires not only the vertical distribution of electron density (which can be derived from topside soundings) but also the vertical distribution of other ionospheric parameters such as plasma temperatures and ion composition. Unfortunately, the satellite experiments that yield temperatures and ion composition do not

provide the vertical variation of these parameters. Thus the Explorer 31 measurements yield data only at the satellite location. Several attempts, based on theoretical considerations, have been made to overcome this limitation. The distribution of charged particles at any level in the ionosphere is represented by the equation of continuity which states simply that the time rate of change of particle density $\delta N_p / \delta t$ is equal to the production rate minus the (chemical + diffusion) loss rate. In spite of its apparent simplicity, the continuity equation can be solved only in very simple limiting cases. One limiting case is the diffusive equilibrium solution where for each ionospheric particle $\delta N_p / \delta t = 0$, production and chemical loss rates are negligible, and diffusion velocity = 0. Even under these conditions the theory must take into consideration all the major ionic constituents, their respective temperatures, and the Coulomb attraction between ions and electrons. A further assumption must be made, namely that all ions are at the same temperature. An excellent review of the diffusive equilibrium theory and of its applicability to the ionosphere has been given by Bauer (1969).

Several authors have used various forms of the diffusive equilibrium equations to derive vertical profiles of temperature and ion composition from local measurements made by the Explorer 31 and simultaneous $N(h)$ profiles obtained by the Alouette 2 sounder. The analysis that required the least number of assumptions was that of Smith (1968) who published one typical result showing vertical profiles of T_e , T_i , O^+ , and H^+ . Colin et al. (1969b), using a somewhat simpler approach in which T_e/T_i , was assumed to be constant for a given profile, obtained vertical profiles of ion composition and plasma temperatures

$$T_p = \frac{(T_e + T_i)}{2}$$

Regions of constant or slightly decreasing T_p with height were found on 35 of the 37 analyses performed. Mayr and Brace (1970) suggested, however, that the temperature results of Colin et al. (1969b) were incorrect because of the presence of significant proton fluxes (i.e., $\delta H^+ / \delta t \neq 0$). Mayr and Brace (1970) showed that an assumed proton flux of $1 \times 10^8 \text{ cm}^{-2} \text{ s}^{-1}$ yield results consistent with the Explorer 31 and Alouette 2 sounder data and a T_p profile that increases monotonically with altitude.

4.10 Suprathermal Electrons (Experiments B_A and B₁)

Explorer 31 was the first spacecraft to include experiments designed to measure the full range of suprathermal electrons; i.e., the range from 2 eV to 200 eV. Previous measurements were either for energies greater than 50 eV or in the thermal range (i.e., typically for energies less than 2 eV). Three of the Explorer 31 experiments were capable of measuring

suprathermal electrons. Experiment A could measure the integral flux of electrons with energies greater than 15 eV, experiment B₁ could measure the integral flux of electrons with energies greater than 5 eV, and experiment B_A was designed to measure the energetic electron fluxes at different threshold energies varying from about 2 volts to 200 volts.

Observations of suprathermal electron fluxes at high latitudes (Maier and Rao, 1970) in the altitude range 1700 to 3000 km during the winter of 1965-1966 revealed the existence of three distinct zones. The first zone (magnetic latitudes between 55 and 68 deg) exhibited a steady flux of photoelectrons (see Section 3.9.2 for a discussion of photoelectrons in the topside ionosphere). The second (or auroral) zone, corresponding to magnetic latitudes between 68 and 80 deg, was characterized by a high and variable flux containing precipitated particles in addition to photoelectrons. The third (or polar) zone was for magnetic latitudes greater than 80 deg. The flux in the polar zone was less variable than the flux in the auroral zone. The polar flux was about one order of magnitude smaller than the flux in the first zone. The observations of Maier and Rao (1970) also indicated that the magnetic field lines were closed up to $L = 7.7$ for the photoelectrons. The ambient electron temperature also appeared to depend on the level of flux in the auroral and polar regions.

The nighttime suprathermal flux at low magnetic latitudes (0 to 46 deg) was measured by Rao et al. (1974). These measurements represented background flux due to magnetospheric particles, since the photoelectrons are absent at night. The equatorial fluxes (magnetic latitudes less than 15 deg) revealed a large systematic variation as a function of pitch angle, with the maximum flux occurring for a pitch angle of 90 deg. The midlatitude flux (magnetic latitudes between 30 and 46 deg) varied randomly with pitch angle, and its amplitude was about one-fifth that of the maximum equatorial flux. It was shown that this nighttime flux made a significant contribution to the heating of the ambient (thermal) electrons.

REFERENCES

- ANGERAMI, J.J. THOMAS, J.O.
STUDIES OF PLANETARY ATMOSPHERES, 1. THE DISTRIBUTION OF ELECTRONS AND IONS IN THE EARTH'S EXOSPHERE
J. GEOPHYS. RES., 69, NO. 21, 4537-4560, NOV. 1964.
- ARENDDT, P.R.
COMPARISON OF THE TOPSIDE IONOSPHERE DURING MAGNETIC STORMS OF VARIOUS TYPES
PLANET. SPACE SCI., 17, 1993-1995, DEC. 1969.
- ARENDDT, P.R. PAPAYOANOU, A.
STRUCTURE AND VARIATION OF THE TOPSIDE IONOSPHERE CLOSE TO THE FORT MONMOUTH LONGITUDE
J. GEOPHYS. RES., 70, NO. 15, 3675-3685, AUG. 1965.
- ARENDDT, P.R. ROSATI, V. SOICHER, H.
QUICK LOOK SYSTEM FOR VIRTUAL REAL-TIME TELEMETRY RECEPTION OF TOPSIDE IONOGRAMS
PROC. OF THE IEEE, 57, 947-948, JUNE 1969.
- AXFORD, W.I.
POLAR WIND AND THE TERRESTRIAL HELIUM BUDGET
J. GEOPHYS. RES., 73, NO. 21, 6855-6859, NOV. 1968.
- BANKS, P.M. HOLZER, T.E.
HIGH-LATITUDE PLASMA TRANSPORT: THE POLAR WIND
J. GEOPHYS. RES., 74, NO. 26, 6317-6332, DEC. 1969.
- BANKS, P.M. DOUPNIK, J.R.
THERMAL PROTON FLOW IN THE PLASMASPHERE - THE MORNING SECTOR
PLANET. SPACE SCI., 22, NO. 1, 79-94, JAN. 1974.
- BARRINGTON, R.E.
PRELIMINARY ROCKET INVESTIGATION OF VERY LOW FREQUENCY IONOSPHERIC RESONANCES
SPACE RES., 9, 279-286, 1969. (PROCEEDINGS OF THE 11TH PLENARY MEETING OF COSPAR, TOKYO, JAPAN, MAY 9-21, 1968. EDS. K.S.W. CHAMPION, P.A. SMITH, R.L. SMITH-ROSE, NORTH-HOLLAND PUBLISHING CO., AMSTERDAM, NETHERLANDS).
- BARRINGTON, R.E. BELROSE, J.S.
PRELIMINARY RESULTS FROM THE VLF RECEIVER ABOARD CANADA'S ALOUETTE SATELLITE
NATURE, 198, NO. 4881, 651-656, MAY 1963.
- BARRINGTON, R.E. HERZBERG, L.
FREQUENCY VARIATION IN IONOSPHERIC CYCLOTRON HARMONIC SERIES OBTAINED BY THE ALOUETTE 1 SATELLITE
CAN. J. PHYS., 44, 987-994, MAY 1966.
- BARRINGTON, R.E. HARTZ, T.R.
SATELLITE IONOSONDE RECORDS - RESONANCES BELOW THE CYCLOTRON FREQUENCY
SCIENCE, 160, 181-184, APR. 1968.

- BARRINGTON, R.E. PALMER, F.H.
 DISTRIBUTION OF ELF/VLF NOISE IN THE POLAR IONOSPHERE
 IN -- MAGNETOS.-IONOS. INTERACTIONS, 97-104, B.M. MCCORMAC,
 UNIVERSITETSFORLAGET, OSLO, NORWAY, 1972.
- BARRINGTON, R.E. BELROSE, J.S. KEELEY, D.A.
 VERY LOW FREQUENCY NOISE BANDS OBSERVED BY THE ALOUETTE 1 SATELLITE
 J. GEOPHYS. RES., 68, NO. 23, 6539-6541, DEC. 1963.
- BARRINGTON, R.E. BELROSE, J.S. NELMS, G.L.
 ION COMPOSITION AND TEMPERATURES AT 1000 KM AS DEDUCED FROM
 SIMULTANEOUS OBSERVATIONS OF A VLF PLASMA RESONANCE AND TOPSIDE
 SOUNDING DATA FROM ALOUETTE 1 SATELLITE
 J. GEOPHYS. RES., 70, NO. 7, 1647-1664, APR. 1965.
- BARRINGTON, R.E. BELROSE, J.S. MATHER, W.E.
 HELIUM WHISTLER OBSERVED IN THE CANADIAN SATELLITE ALOUETTE 2
 NATURE, 210, 80-81, APR. 1966.
- BARRINGTON, R.E. HARTZ, T.R. HARVEY, R.W.
 DIURNAL DISTRIBUTION OF ELF, VLF, AND LF NOISE AT HIGH LATITUDES AS
 OBSERVED BY ALOUETTE 2
 J. GEOPHYS. RES., 76, NO. 22, 5278-5291, AUG. 1971.
- BARRY, J.D. COLEMAN, P.J., JR. LIBBY, W.F. LIBBY, L.M.
 RADIO REFLECTION BY FREE RADICALS IN EARTH'S ATMOSPHERE
 SCIENCE, 156, 1730-1732, JUNE 1967.
- BAUER, S.J.
 DIFFUSIVE EQUILIBRIUM IN THE TOPSIDE IONOSPHERE
 PROC. OF THE IEEE, 57, NO. 6, 1114-1118, JUNE 1969.
- BAUER, S.J. BLUMLE, L.J.
 MEAN DIURNAL VARIATION OF THE TOPSIDE IONOSPHERE AT MID-LATITUDES
 J. GEOPHYS. RES., 69, NO. 17, 3613-3618, SEPT. 1964.
- BAUER, S.J. KRISHNAMURTHY, B.V.
 BEHAVIOR OF THE TOPSIDE IONOSPHERE DURING A GREAT MAGNETIC STORM
 PLANET. SPACE SCI., 16, 653-663, MAY 1968.
- BAUER, S.J. BLUMLE, L.J. DONLEY, J.L. FITZENREITER, R.J. JACKSON, J.E.
 SIMULTANEOUS ROCKET AND SATELLITE MEASUREMENTS OF THE TOPSIDE
 IONOSPHERE
 J. GEOPHYS. RES., 69, NO. 1, 186-189, JAN. 1964.
- BECKER, W.
 FEW EXAMPLES OF ELECTRON DENSITY PROFILES FOR THE BOTTOMSIDE AND
 TOPSIDE IONOSPHERE
 KLEINHEUBACHER BERICHTE, 14, 145-154, 1971.
- BECKER, W.
 STANDARD PROFILE OF THE MID-LATITUDE F REGION OF THE IONOSPHERE AS
 DEDUCED FROM BOTTOMSIDE AND TOPSIDE IONOGRAMS
 SPACE RES., 12, 1241-1252, 1972. (PROC. OF THE 14TH COSPAR PLENARY MEETING,
 SEATTLE, WA, JUNE 21-JULY 2, 1971).

- BENSON, R.F.
 FREQUENCY SHIFTS OBSERVED IN THE ALOUETTE 2 CYCLOTRON HARMONIC PLASMA
 RESONANCES
 PROC. OF THE IEEE, 57, 1139-1142, JUNE 1969.
- BENSON, R.F.
 ANALYSIS OF ALOUETTE 1 PLASMA RESONANCE OBSERVATIONS
 IN -- PLASMA WAVES IN SPACE AND IN THE LAB., 2, 25-54, J.O. THOMAS, A.M.
 ELSEVIER PUBL. CO., NEW YORK, NY, 1970a.
- BENSON, R.F.
 FREQUENCY INTERPOLATION CORRECTION FOR ALOUETTE 2 IONOGRAMS
 PROC. OF THE IEEE, 58, NO. 12, 1959-1961, DEC. 1970b.
- BENSON, R.F.
 ALOUETTE 2 OBSERVATIONS SUPPORTING THE OBLIQUE ECHO MODEL FOR THE
 PLASMA FREQUENCY RESONANCE
 J. GEOPHYS. RES., 76, 1083-1087, FEB. 1971.
- BENSON, R.F.
 IONOSPHERIC PLASMA RESONANCES - TIME DURATIONS *VERSUS LATITUDE,
 ALTITUDE, AND FN/FH
 PLANET. SPACE SCI., 20, 683-706, MAY 1972a.
- BENSON, R.F.
 FREQUENCY SHIFTS OF IONOSPHERIC NF*SUB H RESONANCES
 J. ATMOS. TERR. PHYS., 34, 1201-1214, JULY 1972b.
- BENSON, R.F.
 SIMULTANEOUS IN SITU ELECTRON TEMPERATURE COMPARISON USING ALOUETTE 2
 PROBE AND PLASMA RESONANCE DATA
 NASA-GSFC, X-621-73-70, GREENBELT, MD., FEB. 1973.
- BENSON, R.F.
 STIMULATION OF THE HARRIS INSTABILITY IN THE IONOSPHERE
 PHYS. FLUIDS, 17, NO. 5, 1032-1037, MAY 1974a.
- BENSON, R.F.
 ON THE GENERATION OF THE SEQUENCE OF DIFFUSE RESONANCES OBSERVED ON
 TOP SIDE IONOGRAMS
 J. GEOPHYS. RES., 79, NO. 19, 2911-2912, JULY 1974b.
- BENSON, R.F.
 ION EFFECTS ON IONOSPHERIC ELECTRON RESONANT PHENOMENA
 RADIO SCI., 10, NO. 2, 173-185, FEB. 1975.
- BENSON, R.F.
 REMOTE DETECTION OF THE MAXIMUM ALTITUDE OF EQUATORIAL IONOSPHERIC
 PLASMA BUBBLES
 IN -- THE EFFECT OF THE IONOSPHERE ON RADIOWAVE SYSTEMS, APR. 14-16 1981,
 NRL, ONR, AFGL, UNDATED.
- BENSON, R.F. HOEGY, W.R.
 EFFECT OF AN ISOTROPIC NON-EQUILIBRIUM PLASMA ON ELECTRON
 TEMPERATURE MEASUREMENTS
 J. GEOPHYS. RES., 78, NO. 22, 4702-4706, AUG. 1973.

- BENSON, R.F. BITOUN, J.
 INTERPRETATION OF SATELLITE GYROHARMONIC RESONANCE OBSERVATIONS
 RADIO SCI., 14, NO. 1, 113-123, JAN.-FEB. 1979.
- BENT, R.B. WALLOCH, M.K. LLEWELLYN, S.K.
 DESCRIPTION AND EVALUATION OF THE BENT IONOSPHERIC MODEL
 DBA SYSTEMS INC., UNNUMBERED, MELBOURNE, FL, OCT. 1972.
- BERKNER, L.V. WELLS, H.W. SEATON, S.L.
 IONOSPHERIC EFFECTS ASSOCIATED WITH MAGNETIC DISTURBANCES
 TERR. MAGN. ATMOS. ELECTR., 44, 283-311, SEPT. 1939.
- BERNARD, R. TAIEB, C.
 STUDY OF THE LINK BETWEEN TOPSIDE AND BOTTOMSIDE SOUNDINGS
 PERFORMED AT OUAGADOUGOU (IN FRENCH)
 CNET, GRI-NT-78, ISSY-LES-MOULINEAUX, FRANCE, APR. 1970.
- BERNSTEIN, I.B.
 WAVES IN A PLASMA IN A MAGNETIC FIELD
 PHYS. REV., 109, NO. 1, 10-21, JAN. 1958.
- BILITZA, D.
 INTERNATIONAL REFERENCE IONOSPHERE: RECENT DEVELOPMENTS
 RADIO SCI., 21, NO. 3, 343-346, MAY-JUNE 1986.
- BITOUN, J. FLEURY, L. HIGEL, B.
 THEORETICAL STUDY OF GYRORESONANCES WITH APPLICATION TO ROCKET
 EXPERIMENTS
 RADIO SCI., 10, NO. 10, 875-889, OCT. 1975.
- BOOKER, H.G.
 THEORY OF SCATTERING BY NONISOTROPIC IRREGULARITIES WITH APPLICATION TO
 RADAR REFLECTIONS FROM THE AURORA
 J. ATMOS. TERR. PHYS., 8, NOS. 4-5, 204-221, MAY 1956.
- BOOKER, H.G. WELLS, H.W.
 SCATTERING OF RADIO WAVES BY THE F REGION OF THE IONOSPHERE
 TERR. MAGN. ATMOS. ELECTR., 43, NO. 3, 249-256, SEPT. 1938.
- BOURDEAU, R.E. CHAPMAN, J.H. MAEDA, K.
 IONOSPHERIC RESEARCH BY MEANS OF ROCKETS AND SATELLITES
 IN -- PROGRESS IN RADIO SCIENCE 1960-1963, VOL. 8, 5-70, K. MAEDA AND S. SILVER,
 ELSEVIER PUBL. CO., NEW YORK, NY, 1965.
- BOWEN, P.J. BOYD, R.L.F. HENDERSON, C.L. WILLMORE, A.P.
 MEASUREMENT OF ELECTRON TEMPERATURE AND CONCENTRATION FROM A
 SPACECRAFT
 ROY. SOC. OF LONDON, PROC. NO. 281, 514-525, 1964.
- BOWHILL, S.A.
 REVIEW ON IONOSPHERE
 SPACE RES., 10, 681-688, 1970. (PROC. OF THE 12TH COSPAR PLENARY MEET., PRAGUE,
 CZECHOSLOVAKIA, MAY 12-14, 1969).

- BRACE, L.H. FINDLAY, J.A.
 COMPARISON OF CYLINDRICAL ELECTROSTATIC PROBE MEASUREMENTS ON
 ALOUETTE 2 AND EXPLORER 31 SATELLITES
 PROC. OF THE IEEE, 57, 1057-1060, JUNE 1969.
- BRACE, L.H. CARIGNAN, G.R. FINDLAY, J.A.
 EVALUATION OF IONOSPHERIC ELECTRON TEMPERATURE MEASUREMENTS BY
 CYLINDRICAL ELECTROSTATIC PROBES
 SPACE RES., 11, 1079-1105, 1971. (PROC. OF THE 13TH PLENARY MEET. OF COSPAR,
 LENINGRAD, USSR, MAY 20-29, 1970).
- BRADFORD, H.M. HUGHES, V.A.
 EXCITATION AND DECAY OF LOW FREQUENCY TYPE 3 SOLAR RADIO BURSTS
 ASTRON. ASTROPHYS., 31, NO. 4, 419-429, APR. 1974.
- BRICE, N.M. SMITH, R.L.
 VERY LOW FREQUENCY PLASMA RESONANCE
 NATURE, 203, 4948, 926, AUG. 1964.
- BRICE, N.M. SMITH, R.L.
 LOWER HYBRID RESONANCE EMISSIONS
 J. GEOPHYS. RES., 70, NO. 1, 71-80, JAN. 1965.
- BRICE, N.M. SMITH, R.L. BELROSE, J.S. BARRINGTON, R.E.
 TRIGGERED VERY-LOW-FREQUENCY EMISSIONS
 NATURE, 203, 926-927, AUG. 1964.
- BURROWS, J.R. MCDIARMID, I.B.
 STUDY OF ELECTRONS ARTIFICIALLY INJECTED INTO THE GEOMAGNETIC FIELD IN
 OCTOBER, 1962
 CAN. J. PHYS., 42, 1529-1547, AUG. 1964.
- CALVERT, W.
 OBSERVATIONS OF IONOSPHERIC IRREGULARITIES AND PLASMA RESONANCES BY
 THE FIXED-FREQUENCY TOPSIDE SOUNDER SATELLITE
 IN -- ELECTRON DENSITY PROFILES IN IONOS. AND EXOS., 280-298, J. FRIHAGEN,
 NORTH-HOLLAND PUBL. CO., AMSTERDAM, THE NETHERLANDS, 1966a.
- CALVERT, W.
 STEEP HORIZONTAL ELECTRON-DENSITY GRADIENTS IN THE TOPSIDE F LAYER
 J. GEOPHYS. RES., 71, 3665-3669, AUG. 1966b.
- CALVERT, W.
 IONOSPHERIC TOPSIDE SOUNDING
 SCIENCE, 154, 228-234, OCT. 1966c.
- CALVERT, W.
 OBLIQUE Z MODE ECHOES IN THE TOPSIDE IONOSPHERE
 J. GEOPHYS. RES., 71, 5579-5583, DEC. 1966d.
- CALVERT, W. GOE, G.B.
 PLASMA RESONANCES IN THE UPPER IONOSPHERE
 J. GEOPHYS. RES., 68, NO. 22, 6113-6120, NOV. 1963.
- CALVERT, W. SCHMID, C.W.
 SPREAD F OBSERVATIONS BY THE ALOUETTE TOPSIDE SOUNDER SATELLITE
 J. GEOPHYS. RES., 69, NO. 9, 1839-1852, MAY 1964.

- CALVERT, W. VAN ZANDT, T.E.
FIXED FREQUENCY OBSERVATIONS OF PLASMA RESONANCES IN THE TOPSIDE IONOSPHERE
J. GEOPHYS. RES., 71, 1799-1813, APR. 1966.
- CALVERT, W. MCAFEE, J.R.
TOPSIDE SOUNDER RESONANCES
PROC. OF THE IEEE, 57, 1089-1096, JUNE 1969.
- CALVERT, W. VANZANDT, T.E. KNECHT, R.W. GOE, G.B.
EVIDENCE FOR FIELD-ALIGNED IONIZATION IRREGULARITIES BETWEEN 400 AND 1000 KM ABOVE THE EARTH'S SURFACE
PROC. OF THE INTERN. CONF. ON THE IONOS., 324-329, 1962.
- CALVERT, W. KNECHT, R.W. VAN ZANDT, T.E.
IONOSPHERE EXPLORER I SATELLITE, FIRST OBSERVATIONS FROM THE FIXED-FREQUENCY TOPSIDE SOUNDER
SCIENCE, 146, 391-395, OCT. 1964.
- CARLSON, H.C. SAYERS, J.
DISCREPANCY IN ELECTRON TEMPERATURES DEDUCED FROM LANGMUIR PROBES AND FROM INCOHERENT SCATTER RADARS
J. GEOPHYS. RES., 75, 4883-4886, SEPT. 1970.
- CARLSON, H.C., JR.
IONOSPHERIC HEATING BY MAGNETIC CONJUGATE-POINT PHOTOELECTRONS
J. GEOPHYS. RES., 71, NO. 1, 195-199, JAN. 1966.
- CARPENTER, D.L. DUNCKEL, N.
DISPERSION ANOMALY IN WHISTLERS RECEIVED ON ALOUETTE 1
J. GEOPHYS. RES., 70, NO. 15, 3781-3786, AUG. 1965.
- CARPENTER, D.L. DUNCKEL, N. WALKUP, J.F.
NEW VERY LOW FREQUENCY PHENOMENON, WHISTLERS TRAPPED BELOW THE PROTONOSPHERE
J. GEOPHYS. RES., 69, NO. 23, 5009-5017, DEC. 1964.
- CARPENTER, D.L. WALTER, F. BARRINGTON, R.E. MCEWEN, D.J.
ALOUETTE 1 AND 2 OBSERVATIONS OF ABRUPT CHANGES IN WHISTLER RATE AND OF VLF NOISE VARIATIONS AT THE PLASMAPAUSE-A SATELLITE-GROUND STUDY
J. GEOPHYS. RES., 73, NO. 9, 2929-2940, MAY 1968.
- CATHEY, E.H.
SOME MIDLATITUDE SPORADIC-E RESULTS FROM THE EXPLORER 20 SATELLITE
J. GEOPHYS. RES., 74, 2240-2247, MAY 1969.
- CHAN, K.L. COLIN, L.
GLOBAL ELECTRON DENSITY DISTRIBUTIONS FROM TOPSIDE SOUNDINGS
PROC. OF THE IEEE, 57, 990-1004, JUNE 1969.
- CHANDRA, S. KRISHNAMURTHY, B.V.
DAILY RESPONSE OF THE UPPER F REGION TO CHANGES IN UPPER ATMOSPHERIC TEMPERATURE AND GEOMAGNETIC ACTIVITY
J. ATMOS. TERR. PHYS., 30, 47-54, JAN. 1968.
- CHANDRA, S. MAIER, E.J. TROY, B.E., JR. RAO, B.C.N.
SUBAURORAL RED ARCS AND ASSOCIATED IONOSPHERIC PHENOMENA
J. GEOPHYS. RES., 76, NO. 4, 920-925, FEB. 1971.

- CHAPMAN, J.H.
 TOPSIDE IONOSPHERE
 IN -- ELECTRON DENSITY PROFILES IN IONOS. AND EXOS., 264-269, J. FRIHAGEN,
 NORTH-HOLLAND PUBL. CO., AMSTERDAM, THE NETHERLANDS, 1966.
- CHAPMAN, J.H. MOLOZZI, A.R.
 INTERPRETATION OF COSMIC NOISE MEASUREMENTS AT 3.8 MC/S FROM SATELLITE
 1960 ETA
 NATURE, 191, 480, JULY 1961.
- CHAPMAN, J.H. WARREN, E.S.
 TOPSIDE SOUNDING OF THE EARTH'S IONOSPHERE
 SPACE SCI. REV., 8, 846-865, DEC. 1968.
- CHARCOSSET, G. TIXIER, M. CORCUFF, Y. GARNIER, M.
 EXPERIMENTAL AND THEORETICAL STUDY OF NONGUIDED WHISTLERS RECEIVED
 ON BOARD OF THE ALOUETTE 2 SATELLITE AT LOW LATITUDES
 ANN. DE GEOPHYS., 29, NO. 2, 279-291, APR.-JUNE 1973.
- CHIA, R.C. FUNG, A.K. MOORE, R.K.
 HIGH FREQUENCY BACKSCATTER FROM THE EARTH MEASURED AT 1000 KM
 ALTITUDE
 RADIO SCI., 69D, NO. 4, 641-649, APR. 1965.
- CHIVERS, H.J.A. BURROWS, J.R.
 SIMULTANEOUS SATELLITE AND GROUND-BASED OBSERVATIONS OF SOLAR
 PROTONS
 PLANET. SPACE SCI., 14, 131-142, 1966.
- CLARK, W.L., JR. MCAFEE, J.R. NORTON, R.B. WARNOCK, J.M.
 RADIO WAVE REFLECTIONS FROM LARGE HORIZONTAL GRADIENTS IN THE TOPSIDE
 IONOSPHERE
 PROC. OF THE IEEE, 57, 493-496, APR. 1969.
- COGGER, L.L.
 SOME CONTRIBUTIONS OF THE ISIS PROGRAM TOWARDS ADVANCES IN KNOWLEDGE
 OF LOW LATITUDE IONOSPHERIC PHENOMENA
 SPACE SCI. REV., 31, NO. 4, 437-452, 1982.
- COHEN, R. VAN ZANDT, T.E.
 SYSTEMATIC HEIGHT DISCREPANCY BETWEEN SIMULTANEOUS ALOUETTE 1 AND
 INCOHERENT SCATTER ELECTRON CONCENTRATION PROFILES
 IN -- THOMSON SCATTER STUDIES OF THE IONOSPHERE, 189-191, ILL. U., URBANA, IL,
 MAY 1967.
- COLE, K. D.
 PREDAWN ENHANCEMENT OF 6300 A AIRGLOW
 ANN. GEOPHYS., TOME 21, NO. 1, 156-158, JAN. 1965a.
- COLE, K.D.
 STABLE AURORAL RED ARCS, SINKS FOR ENERGY OF DST MAIN PHASE
 J. GEOPHYS. RES., 70, NO. 7, 1689-1706, APR. 1965b.
- COLE, K.D.
 FORMATION OF FIELD-ALIGNED IRREGULARITIES IN THE MAGNETOSPHERE
 J. ATMOS. TERR. PHYS., 33, 741-750, MAY 1971.

- COLIN, L. DUFOUR, S.W.
CHARGED PARTICLE TEMPERATURES AND CONCENTRATIONS IN THE EARTH'S
EXOSPHERE
J. GEOPHYS. RES., 73, 2967-2984, NO. 9, MAY 1968.
- COLIN, L. CHAN, K.L.
MODEL STUDIES OF THE KINKED Z TRACE IN TOPSIDE IONOGRAMS
PROC. OF THE IEEE, 57, 1143-1147, JUNE 1969.
- COLIN, L. SHMOYS, J. MCCULLEY, G.
RAY TRACING STUDIES FOR THE TOPSIDE IONOSPHERE
J. GEOPHYS. RES., 74, NO. 3, 809-814, FEB. 1969a.
- COLIN, L. DUFOUR, S.W. WILLOUGHBY, D.S.
TEMPERATURE AND ION ABUNDANCE PROFILES DEDUCED FROM SIMULTANEOUS
EXPLORER 31 AND ALOUETTE 2 DATA
PROC. OF THE IEEE, 57, 1154-1158, JUNE 1969b.
- CRAWFORD, F.W. HARP, R.S. MANTEI, T.D.
ON THE INTERPRETATION OF IONOSPHERIC RESONANCES STIMULATED BY
ALOUETTE 1
J. GEOPHYS. RES., 72, NO. 1, 57-68, JAN. 1967.
- DAVIES, F.T.
ALOUETTE TOPSIDE IONOSPHERE STUDIES
IG BULL., NO. 79, 1-7, JAN. 1964.
- DAVIES, K.
USE OF TOPSIDE SOUNDERS IN IONOSPHERIC RESEARCH
TELECOMMUN. J., 32, NO. 3, 116-123, MAR. 1965.
- DAVIES, K.
IONOSPHERIC RADIO PROPAGATION
DOVER PUBLICATIONS, INC., NEW YORK, NY, 1966.
- DAYHARSH, T.I. FARLEY, W.W.
ELECTRON DENSITY VARIATIONS AT 1000 KILOMETERS
J. GEOPHYS. RES., 70, NO. 21, 5361-5368, NOV. 1965.
- DONLEY, J.L.
THERMAL ION AND ELECTRON TRAP EXPERIMENTS ON THE EXPLORER 31 SATELLITE
PROC. OF THE IEEE, 57, 1061-1063, JUNE 1969.
- DONLEY, J.L. BRACE, L.H. FINDLAY, J.A. HOFFMAN, J.H. WRENN, G.L.
COMPARISON OF RESULTS OF EXPLORER 31 DIRECT MEASUREMENT PROBES
PROC. OF THE IEEE, 57, 1078-1084, JUNE 1969.
- DOT, M. FAYNOT, J.M.
ELECTRON DENSITY PROFILES OBTAINED OVER FRANCE USING TOPSIDE AND
GROUND BASED IONOSPHERIC SOUNDINGS
GROUPE DE RECH. IONOSPHERIQUES, GRI/NT/50, PARIS, FRANCE, DEC. 1965.
- DOUGHERTY, J.P. MONAGHAN, J.J.
THEORY OF RESONANCES OBSERVED IN IONOGRAMS TAKEN BY SOUNDERS ABOVE
THE IONOSPHERE
PROC. OF THE ROY. SOC., SERIES A, 289, NO. 1417, 214-234, JAN. 1966.

- DOUPNIK, J.R. SCHMERLING, E.R.
REDUCTION OF IONOGRAMS FROM THE BOTTOMSIDE AND TOPSIDE
J. ATMOS. TERR. PHYS., 27, 917-941, SEPT. 1965.
- DU CASTEL, F.
CONCERNING GUIDED ECHOES OBSERVED BY IONOSPHERIC SOUNDINGS FROM A
SATELLITE
SPACE RES., 5, 216-228, 1965. (PROC. 5TH INT. SPACE SCI. SYMP., FLORENCE, ITALY,
MAY 12-16, 1964.)
- DU CASTEL, F. FAYNOT, J.M. VASSEUR, G.
OBSERVATION OF IONOSPHERIC IRREGULARITIES IN THE BOTTOMSIDE AND
TOPSIDE IONOSPHERE
IN -- ELECTRON DENSITY PROFILES IN IONOS. AND EXOS., 579-586, J. FRIHAGEN,
NORTH-HOLLAND PUBL. CO., AMSTERDAM, THE NETHERLANDS, 1966.
- DYSON, P.L.
COMPARISON OF IRREGULAR FEATURES APPEARING ON IONOGRAMS RECORDED BY
TOPSIDE AND GROUND-BASED SOUNDERS
J. ATMOS. TERR. PHYS., 29, 881-886, JULY 1967a.
- DYSON, P.L.
MAGNETIC FIELD ALIGNED IRREGULARITIES AT MID GEOMAGNETIC LATITUDES
J. ATMOS. TERR. PHYS., 29, 857-869, JULY 1967b.
- DYSON, P.L.
ELECTRON DENSITIES AND SCALE HEIGHTS IN THE MID-LATITUDE TOPSIDE
IONOSPHERE
AUST. J. PHYS., 20, 401-405, AUG. 1967c.
- DYSON, P.L.
TOPSIDE REFRACTIVE IRREGULARITIES AND TRAVELLING IONOSPHERIC
DISTURBANCES
AUSTRALIAN J. PHYS., 20, 467-469, AUG. 1967d.
- DYSON, P.L.
TOPSIDE SPREAD F AT MIDLATITUDES
J. GEOPHYS. RES., 73, NO. 7, 2441-2446, APR. 1968.
- DYSON, P.L.
DIRECT MEASUREMENTS OF THE SIZE AND AMPLITUDE OF IRREGULARITIES IN THE
TOPSIDE IONOSPHERE
J. GEOPHYS. RES., 74, 6291-6303, DEC. 1969.
- DYSON, P.L.
COMPARISON OF SCINTILLATION, SPREAD F AND ELECTROSTATIC PROBE
OBSERVATIONS OF ELECTRON DENSITY IRREGULARITIES
J. ATMOS. TERR. PHYS., 33, NO. 8, 1185-1192, AUG. 1971.
- DYSON, P.L. BENSON, R.F.
TOPSIDE SOUNDER OBSERVATIONS OF EQUATORIAL BUBBLES
GEOPHYS. RES. LETT., 5, NO. 9, 795-798, SEPT. 1978.
- ECCLES, D. KING, J.W.
IONOSPHERIC PROBING USING VERTICAL INCIDENCE SOUNDING TECHNIQUES
J. ATMOS. TERR. PHYS., 32, 517-538, APR. 1970.

- ELKINS, T.J.
EMPIRICAL MODEL OF THE POLAR IONOSPHERE
AFCRL, TR-73-0331, BEDFORD, MA, MAY 1973.
- ETKIN, B. HUGHES, P.C.
EXPLANATION OF THE ANOMALOUS SPIN BEHAVIOR OF SATELLITES WITH LONG
FLEXIBLE ANTENNAE
J. SPACECR. ROCKETS, 4, 1139-1145, SEPT. 1967.
- FATKULLIN, M.N.
SEASONAL ANOMALY IN THE ELECTRON DENSITY OF THE TOPSIDE F2-REGION
J. ATMOS. TERR. PHYS., 32, NO. 6, 1067-1075, JUNE 1970a.
- FATKULLIN, M.N.
DIURNAL DEVELOPMENT OF THE SEASONAL ANOMALY PHENOMENON IN THE
MIDDLE LATITUDE TOPSIDE F2-REGION
J. ATMOS. TERR. PHYS., 32, 1989-1994, DEC. 1970b.
- FATKULLIN, M.N.
STORMS AND THE SEASONAL ANOMALY IN THE TOPSIDE IONOSPHERE
J. ATMOS. TERR. PHYS., 35, NO. 3, 453-468, MAR. 1973.
- FEJER, J.A. CALVERT, W.
RESONANCE EFFECTS OF ELECTROSTATIC OSCILLATIONS IN THE IONOSPHERE
J. GEOPHYS. RES., 69, NO. 23, 5049-5062, DEC. 1964.
- FEJER, J.A. YU, W.
DIPOLE IN A WEAKLY INHOMOGENEOUS PLASMA
J. GEOPHYS. RES., 75, NO. 10, 1919-1925, APR. 1970.
- FELDSTEIN, R. GRAFF, P.
DAYTIME AND NIGHTTIME ELECTRON TEMPERATURES FROM TOPSIDE RESONANCES
J. GEOPHYS. RES., 77, 1896-1904, APR. 1972.
- FELDSTEIN, YA.I. STARKOV, G.V.
AURORAL OVAL AND THE BOUNDARY OF CLOSED FIELD LINES OF GEOMAGNETIC
FIELD
PLANET. SPACE SCI., 18, 501-508, APR. 1970.
- FERGUSON, E.E. GREEN, R.G.
SIMPLE RECEIVING AND DISPLAY SYSTEM FOR ALOUETTE 1 IONOGRAMS
PROC. OF THE IEEE, 57, 945-947, JUNE 1969.
- FINDLAY, J.A. BRACE, L.H.
CYLINDRICAL ELECTROSTATIC PROBES EMPLOYED ON ALOUETTE 2 AND EXPLORER
31 SATELLITES
PROC. OF THE IEEE, 57, 1054-1056, JUNE 1969.
- FITZENREITER, R.J. BLUMLE, L.J.
ANALYSIS OF TOPSIDE SOUNDER RECORDS
J. GEOPHYS. RES., 69, NO. 3, 407-415, FEB. 1964
- FLEURY, L. TAIEB, C.
SIMULTANEOUS MEASUREMENTS OF ELECTRONIC DENSITY USING TOPSIDE
SOUNDINGS AND INCOHERENT SCATTER SOUNDINGS
J. ATMOS. TERR. PHYS., 33, NO. 6, 909-918, JUNE 1971.

- FRANKLIN, C.A. MACLEAN, M.A.
DESIGN OF SWEEP-FREQUENCY TOPSIDE SOUNDERS
PROC. OF THE IEEE, 57, NO. 6, 897-929, JUNE 1969.
- FRANKLIN, C.A. BIBBY, R.J.
ACCURACY OF RANGE MARKERS ON CRC/DRTE IONOGRAMS
MINUTES OF THE 19TH MEETING OF THE ISIS WORKING GROUP, APPENDIX E, NASA-
GSFC, GREENBELT, MD, SEPT. 9-10, 1969.
- FRANKLIN, C.A. BIBBY, R.J. HITCHCOCK, N.S.
DATA ACQUISITION AND PROCESSING SYSTEM FOR MASS PRODUCING TOPSIDE
IONOGRAMS
PROC. OF THE IEEE, 57, NO. 6, 929-944, JUNE 1969
- GLEDHILL, J.A. TORR, D.G.
IONOSPHERIC EFFECTS OF PRECIPITATED ELECTRONS IN THE SOUTH RADIATION
ANOMALY
SPACE RES., 6, 222-229, 1966 (PROC. OF THE 6TH INT. SPACE SCI. SYMP., MAR DEL
PLATA, ARGENTINA, MAY 11-19, 1965).
- GLEDHILL, J.A. TORR, D.G. TORR, M.R.
IONOSPHERIC DISTURBANCE AND ELECTRON PRECIPITATION FROM THE OUTER
RADIATION BELT
J. GEOPHYS. RES., 72, NO. 1, 209-214, JAN. 1967.
- GOEL, M.K. RAO, B.C.N. CHANDRA, S. MAIER, E.J.
SATELLITE MEASUREMENTS OF ION COMPOSITION AND TEMPERATURES IN THE
TOPSIDE IONOSPHERE DURING MEDIUM SOLAR ACTIVITY
J. ATMOS. TERR. PHYS., 38, NO. 4, 389-394, APR. 1976.
- GOLDBERG, R.A.
REVIEW OF THE THEORIES CONCERNING THE EQUATORIAL F2 REGION IONOSPHERE
PROC. OF THE IEEE, 57, NO. 6, 1119-1126, JUNE 1969.
- GONDHALEKAR, P.M.
BEHAVIOR OF THE TOPSIDE IONOSPHERE DURING MAGNETICALLY DISTURBED
CONDITIONS
J. ATMOS. TERR. PHYS., 35, 1293-1298, JULY 1973.
- GONDHALEKAR, P.M. KING, J.W.
LATITUDINAL VARIATION OF THE ELECTRON CONCENTRATION IN THE TOPSIDE
IONOSPHERE IN WINTER
J. ATMOS. TERR. PHYS., 35, 1299-1308, JULY 1973.
- GRAFF, P.
GENERAL EXPRESSION OF THE FREQUENCIES OF THE OBLIQUE ECHOES AT THE
PLASMA RESONANCE
J. GEOPHYS. RES., 76, NO. 4, 1060-1064, FEB. 1971.
- GREENER, J.G. GLEDHILL, J.A.
ELECTRON FLUXES OBSERVED NEAR SANAE, ANTARCTICA, BY THE SATELLITE
ALOUETTE 1 DURING 1962-1963
S. AFRICAN J. ANTARCTIC RES., NO. 2, 35-39, JUNE 1972.
- GROSS, S.H.
VLF DUCT ASSOCIATED WITH THE LOWER-HYBRID-RESONANCE FREQUENCY IN A
MULTI-ION UPPER IONOSPHERE
J. GEOPHYS. RES., 75, NO. 22, 4235-4247, AUG. 1970.

- GROSS, S.H. LAROCCA, N.
PHENOMENOLOGICAL STUDY OF LHR HISS
J. GEOPHYS. RES., 77, NO. 7, 1146-1156, MAR. 1972.
- GUREVICH, A.V. PITAEVSKI, L.P. SMIRNOVA, V.V.
IONOSPHERIC AERODYNAMICS
SPACE SCI. REV., 9, NO. 6, 805-871, SEPT. 1969.
- GURNETT, D.A. SHAWHAN, S.D.
DETERMINATION OF HYDROGEN ION CONCENTRATION, ELECTRON DENSITY, AND
PROTON GYROFREQUENCY FROM THE DISPERSION OF PROTON WHISTLERS
J. GEOPHYS. RES., 71, NO. 3, 741-754, FEB. 1966.
- GURNETT, D.A. BRICE, N.M.
ION TEMPERATURE IN THE IONOSPHERE OBTAINED FROM CYCLOTRON DAMPING OF
PROTON WHISTLERS
J. GEOPHYS. RES., 71, 3639-3652, AUG. 1966.
- GURNETT, D.A. SHAWHAN, S.D. BRICE, N.M. SMITH, R.L.
ION CYCLOTRON WHISTLERS
J. GEOPHYS. RES., 70, NO. 7, 1665-1688, APR. 1965.
- HAGG, E.L.
PRELIMINARY STUDY OF THE ELECTRON DENSITY AT 1000 KILOMETERS
CAN. J. PHYS., 41, 195-199, JAN. 1963.
- HAGG, E.L.
REMOTE CYCLOTRON RESONANCE PHENOMENON OBSERVED BY THE ALOUETTE
SATELLITE
NATURE, 210, 927-929, MAY 1966.
- HAGG, E.L.
ELECTRON DENSITIES OF 8-100 ELECTRONS CM⁻³ DEDUCED FROM ALOUETTE 2 HIGH-
LATITUDE IONOGRAMS
CAN. J. PHYS., 45, 27-36, JAN. 1967.
- HAGG, E.L. MULDREW, D.B.
NOVEL SPIKE OBSERVED ON ALOUETTE 2 IONOGRAMS
IN -- PLASMA WAVES IN SPACE AND IN THE LAB., 2, 69-75, J.O. THOMAS, A.M.
ELSEVIER PUBL. CO., NEW YORK, NY 1970.
- HAGG, E.L. HEWENS, E.J. NELMS, G.L.
INTERPRETATION OF TOPSIDE SOUNDER IONOGRAMS
PROC. OF THE IEEE, 57, 949-960, JUNE 1969.
- HANSON, W.B.
ELECTRON TEMPERATURES IN THE UPPER ATMOSPHERE
SPACE RES., 3, 282-302, 1963 (PROC. OF THE 3RD INT. SPACE SCI. SYMP., WASH., DC,
MAY 2-8, 1962).
- HANSON, W.B. SANATANI, S.
LARGE ION CONCENTRATION GRADIENTS BELOW THE EQUATORIAL F PEAK
J. GEOPHYS. RES., 78, 1167-1173, MAR. 1973.
- HARTZ, T.R.
STUDY OF INTERFERENCE ON THE ALOUETTE TOP-SIDE SOUNDER RECORDS
DEF. RES. TELECOMMUN. ESTABL., REP. NO. 1123, OTTAWA, CAN., OCT. 1963.

- HARTZ, T.R.
SOLAR NOISE OBSERVATIONS FROM THE ALOUETTE SATELLITE
ANN. D'ASTROPHYS., 27, 831-836, NOV.-DEC. 1964a.
- HARTZ, T.R.
OBSERVATIONS OF THE GALACTIC RADIO EMISSION BETWEEN 1.5 AND 10MHZ
FROM THE ALOUETTE SATELLITE
ANN. D'ASTROPHYS., 27, 823-830, NOV.-DEC. 1964b.
- HARTZ, T.R.
TYPE 3 SOLAR RADIO NOISE BURSTS AT HECTOMETER WAVELENGTHS
PLANET. SPACE SCI., 17, NO. 2, 267-287, FEB. 1969a.
- HARTZ, T.R.
RADIO NOISE LEVELS WITHIN AND ABOVE THE IONOSPHERE
PROC. OF THE IEEE, 57, 1042-1050, JUNE 1969b.
- HARTZ, T.R.
LOW FREQUENCY NOISE EMISSIONS AND THEIR SIGNIFICANCE FOR ENERGETIC
PARTICLE PROCESSES IN THE POLAR IONOSPHERE
IN -- POLAR IONOS. AND MAGNETOS. PROCESSES, 151-160, GUNNAR SKOVLI, GORDON
AND BREACH SCI. PUBL., INC., NEW YORK, 1970.
- HARTZ, T.R.
PARTICLE PRECIPITATION PATTERNS
IN -- RADIATING ATMOS., UNNUMBERED, 225-238, 1971.
- HARTZ, T.R.
MORPHOLOGY OF RADIO-RADAR POLAR PROPAGATION EFFECTS
IN -- RADAR PROPAGATION IN THE ARCTIC, AGARD-CP-97, 1-1 THRU 1-18, JON
FRIHAGEN, AGARD, PARIS, FRANCE, 1972.
- HARTZ, T.R. ROGER,R.S.
EFFECTIVE ANTENNA BEAM WIDTH FOR A SATELLITE-BORNE RADIO TELESCOPE
CAN. J. PHYS., 42, 2146-2152, NOV. 1964.
- HARTZ, T.R. BRICE,N.M.
GENERAL PATTERN OF AURORAL PARTICLE PRECIPITATION
PLANET. SPACE SCI., 15, 301-329, FEB. 1967.
- HARVEY, R.W.
EVIDENCE OF ELECTROSTATIC PROTON CYCLOTRON HARMONIC WAVES FROM
ALOUETTE 2 SATELLITE DATA
J. GEOPHYS. RES., 74, 3969-3978, AUG. 1969.
- HERZBERG, L. NELMS, G.L.
IONOSPHERIC CONDITIONS FOLLOWING THE PROTON FLARE OF 7 JULY 1966 AS
DEDUCED FROM TOPSIDE SOUNDINGS
IN -- ANNALS OF THE IQSY - THE PROTON FLARE PROJECT (THE JULY 1966 EVENT),
VOL. 13, PAPER 57, 426-436, A. C. STRICKLAND, MIT PRESS, CAMBRIDGE, MA, 1969.
- HERZBERG, L. NELMS, G.L. DYSON, P.L.
TOPSIDE OBSERVATION OF ELECTRON DENSITY VARIATIONS (G-CONDITION) AT
TIMES OF LOW MAGNETIC ACTIVITY
CAN. J. PHYS., 47, NO. 23, 2683-2689, DEC. 1969.

- HICE, J.D. FRANK, B.
 OCCURRENCE PATTERNS OF TOPSIDE SPREAD F ON ALOUETTE IONOGRAMS
 J. GEOPHYS. RES., 71, NO. 15, 3653-3664, AUG. 1966.
- HOFFMAN, J.H.
 COMPOSITION MEASUREMENTS OF THE TOPSIDE IONOSPHERE
 SCIENCE, 155, 322-324, JAN. 1967.
- HOFFMAN, J.H.
 ION COMPOSITION MEASUREMENTS IN THE POLAR REGION FROM THE EXPLORER 31
 SATELLITE
 TRANS. AM. GEOPHYS. UNION, 49, NO. 1, 253, MARCH 1968.
- HOFFMAN, J.H.
 ION MASS SPECTROMETER ON EXPLORER 31 SATELLITE
 PROC. OF THE IEEE, 57, 1063-1067, JUNE 1969.
- HOFFMAN, J.H.
 STUDIES OF THE COMPOSITION OF THE IONOSPHERE WITH A MAGNETIC
 DEFLECTION MASS SPECTROMETER
 IN -- SPACE SYST. AND THERMAL TECH. FOR THE 70'S, AMER. SOC. OF MECH. ENG.,
 PT. 1, 1970.
- HOFFMAN, J.H. JOHNSON, C.Y. HOLMES, J.C. YOUNG, J.M.
 DAYTIME MIDLATITUDE ION COMPOSITION MEASUREMENTS
 J. GEOPHYS. RES., 74, 6281-6290, DEC. 1969.
- HOJO, A. NISHIZAKI, R.
 REDUCTION OF TOPSIDE IONOGRAMS FOR FIELD-ALIGNED PROPAGATION PATHS
 NATURE PHYS. SCI., 233, NO. 41, 121-123, OCT. 1971.
- HOLTET, J. EGELAND, A.
 SIMULTANEOUS GROUND AND SATELLITE MEASUREMENTS OF THE ENHANCED
 ELECTROMAGNETIC BAND EMISSION BETWEEN 500 AND 1000 HZ
 IN -- ATMOS. EMISSIONS, 175-180, VAN NOSTRAND REINHOLD CO., NEW YORK, NY,
 1969.
- HOLTET, J. EGELAND, A. MAYNARD, N.C.
 ROCKET GROUND AND SATELLITE MEASUREMENTS OF ELF EMISSIONS DURING A PCA
 IN -- RADIATING ATMOS., UNNUMBERED, 345-354, D. REIDEL PUB. CO., DORDRECHT,
 NETH., 1971.
- HORITA, R.E.
 PROTON CYCLOTRON FREQUENCY PHENOMENA IN THE TOPSIDE IONOSPHERE
 PLANET. SPACE SCI., 22, 793-799, MAY 1974.
- HORITA, R.E. SMITH, B.P. WATANABE, T. BARRINGTON, R. PALMER, F.H.
 ELF EMISSIONS OBSERVED NEAR THE PLASMAPAUSE AND PLASMA SHEET
 J. ATMOS. TERR. PHYS., 37, 1263-1269, -SEPT. 1975.
- HRUSKA, A. BURROWS, J.B. MCDIARMID, I.B.
 HIGH LATITUDE LOW ENERGY ELECTRON FLUXES AND VARIATION OF THE
 MAGNETOSPHERIC STRUCTURE WITH THE DIRECTION OF THE INTERPLANETARY
 MAGNETIC FIELD AND WITH THE GEOMAGNETIC ACTIVITY
 J. GEOPHYS. RES., 77, 2770-2779, JUNE 1972.

- HUGHES, P.C. CHERCHAS, D.B.
SPIN DECAY OF EXPLORER 20
J. SPACECR. ROCKETS, 7, NO. 1, 92-94, JAN. 1970.
- JACKSON, J.E.
REDUCTION OF TOPSIDE IONOGRAMS TO ELECTRON-DENSITY PROFILES
PROC. OF THE IEEE, 57, 960-976, JUNE 1969a.
- JACKSON, J.E.
COMPARISONS BETWEEN TOPSIDE AND GROUND-BASED SOUNDINGS
PROC. OF THE IEEE, 57, 976-985, JUNE 1969b.
- JACKSON, J.E.
P PRIME (F) TO N(H) INVERSION PROBLEM IN IONOSPHERIC SOUNDING
IN -- MATHEMATICS OF PROFILE INVERSION, NASA-TM-X-62150, 4-2 THRU 4-14, L.
COLIN, WASH., DC, AUG. 1972.
- JACKSON, J.E.
ALOUETTE-ISIS PROGRAM SUMMARY
NSSDC/WDC-A-R+S, 86-09, GREENBELT, MD, AUG. 1986.
- JACKSON, J.E.
CALIBRATIONS AND IDENTIFICATION OF ALOUETTE AND TOPSIDE IONOGRAMS
NSSDC, WDC-A-R&S, 88-06, GREENBELT, MD, FEB. 1988.
- JACKSON, J.E. WARREN, E.S.
OBJECTIVES, HISTORY, AND PRINCIPAL ACHIEVEMENTS OF THE TOPSIDE SOUNDER
AND ISIS PROGRAMS
PROC. OF THE IEEE, 57, 861-865, JUNE 1969.
- JACKSON, J.E. SCHMERLING, E.R. WHITTEKER, J.H.
MINI REVIEW ON TOPSIDE SOUNDING
IEEE TRANS. ON ANTENNAS AND PROPAG., AP-28, NO. 2, 284-288, MAR. 1980.
- JANSKY, K.G.
ELECTRICAL DISTURBANCES APPARENTLY OF EXTRATERRESTRIAL ORIGIN
PROC. OF THE I.R.E., 21, NO. 10, 1387-1398, OCT. 1933.
- JELLY, D.H. BRICE, N.
CHANGES IN VAN ALLEN RADIATION ASSOCIATED WITH POLAR SUBSTORMS
J. GEOPHYS. RES., 72, NO. 23, 5919-5931, DEC. 1967.
- JELLY, D.H. PETRIE, L.E.
HIGH LATITUDE IONOSPHERE
PROC. OF THE IEEE, 57, 1005-1012, JUNE 1969.
- JELLY, D.H. MCDIARMID, I.B. BURROWS, J.R.
CORRELATION BETWEEN INTENSITIES OF AURORAL ABSORPTION AND PRECIPITATED
ELECTRONS
CAN. J. PHYS., 42, 2411-2418, DEC. 1964.
- JENSEN, D.C. CAIN, J.C.
INTERIM GEOMAGNETIC FIELD
J. GEOPHYS. RES., 67, NO. 9, 3568-3569, AUG. 1962.
- JOHNSON, F.S.
ION DISTRIBUTION ABOVE THE F2 MAXIMUM
J. GEOPHYS. RES., 65, NO. 2, 577-584, FEB. 1960.

- JORGENSEN, T.S. BELL, F.T.
OBSERVATIONS OF NATURALLY OCCURRING VLF AND MAN-MADE HF PLASMA WAVES
IN AURORAL REGIONS OF THE IONOSPHERE
IN -- PLASMA WAVES IN SPACE AND IN THE LAB. 2, 377-387, J.O. THOMAS, AM.
ELSEVIER PUBL. CO., NEW YORK, NY, 1970.
- KELLEY, M.C. HAERENDEL, G. KAPPLER, H. VALENZUELA, A. BALSLEY, B.B. CARTER, D.A.
ECKLUND, W.L. CARLSON, C.W. HAUSLER, B. TORBERT, R.
EVIDENCE FOR A RAYLEIGH-TAYLOR TYPE INSTABILITY AND UPWELLING OF
DEPLETED DENSITY REGIONS DURING EQUATORIAL SPREAD F
GEOPHYS. RES. LETT., 3, NO. 8, 448-450, AUG. 1976.
- KING, J.W.
REVIEW OF THE LARGE-SCALE STRUCTURE OF THE IONOSPHERIC F-LAYER
IN -- ANNALS OF THE IQSY, 5, PAPER 6, 131-165, A.C. STRICKLAND, MIT PRESS,
CAMBRIDGE, MA, 1969a.
- KING, J.W.
IQSY DATA REVIEW. IONOSPHERE 4 -- THE TOPSIDE SOUNDER SATELLITE DATA
IN -- ANNALS OF THE IQSY, SURVEY OF IQSY OBS. AND BIBL., 6, PAPER NO. 9, 167-185,
A. C. STRICKLAND, MIT PRESS, CAMBRIDGE, MA, 1969b.
- KING, J.W. PREECE, D.M.
OBSERVATIONS OF PROTON GYRO-EFFECTS IN THE TOPSIDE IONOSPHERE
J. ATMOS. TERR. PHYS., 29, 1387-1390, NOV. 1967.
- KING, J.W. REED, K.C.
RELATIONSHIP BETWEEN 10 CM SOLAR FLUX AND ELECTRON CONCENTRATION IN
THE TOPSIDE IONOSPHERE
J. ATMOS. TERR. PHYS., 30, 431-437, MAR. 1968.
- KING, J.W. ECCLES, D.
EFFECT OF A SOLAR ECLIPSE ON THE DEVELOPMENT OF THE IONOSPHERIC
EQUATORIAL ANOMALY
J. ATMOS. TERR. PHYS., 30, 1715-1718, SEPT. 1968.
- KING, J.W. SMITH, P.A. ECCLES, D. FOOKS, G.F. HELM, H.
PRELIMINARY INVESTIGATIONS OF THE STRUCTURE OF THE UPPER IONOSPHERE AS
OBSERVED BY THE TOPSIDE SOUNDER SATELLITE, ALOUETTE
PROC. OF THE ROY. SOC. OF LONDON, SERIES A, 281, 464-487, OCT. 1964.
- KING, J.W. SMITH, P.A. REED, K.C. SEABROOK, C.
TOPSIDE SOUNDER STUDIES OF CORPUSCULAR RADIATION EFFECTS ON THE
IONOSPHERE DURING QUIET AND DISTURBED CONDITIONS
J. ATMOS. TERR. PHYS., 29, 1327-1336, NOV. 1967a.
- KING, J.W. LEGG, A.J. REED, K.C.
OBSERVATIONS OF THE TOPSIDE IONOSPHERE DURING THREE SOLAR ECLIPSES
J. ATMOS. TERR. PHYS., 29, 1365-1371, NOV. 1967b.
- KING, J.W. REED, K.C. OLATUNJI, E.O. LEGG, A.J.
BEHAVIOR OF THE TOPSIDE IONOSPHERE DURING STORM CONDITIONS
J. ATMOS. TERR. PHYS., 29, 1355-1363, NOV. 1967c.

- KING, J.W. ECCLES, D. REED, K.C.
 TIME OF THE SUNRISE EFFECT IN THE TOPSIDE IONOSPHERE IN SUMMER
 J. ATMOS. TERR. PHYS., 30, 423-430, MAR. 1968a.
- KING, J.W. HAWKINS, G.L. RIX, H.G.
 STUDIES OF RESONANCES AND OTHER PHENOMENA ON THE FIXED-FREQUENCY
 TOPSIDE SOUNDER RECORDS
 J. ATMOS. TERR. PHYS., 30, 621-626, APR. 1968b.
- KING, J.W. HAWKINS, G.L. SEABROOK, C.
 SEASONAL BEHAVIOR OF THE TOPSIDE IONOSPHERE
 J. ATMOS. TERR. PHYS., 30, 1701-1706, SEPT. 1968c.
- KING, J.W. RIX, H.G. SEABROOK, C.
 BEHAVIOR OF THE TOPSIDE IONOSPHERE AT MIDDLE LATITUDES AT NIGHT
 J. ATMOS. TERR. PHYS., 30, 1605-1613, SEPT. 1968d.
- KIWAMOTO, Y. BENSON, R.F.
 NONLINEAR LANDAU DAMPING IN THE IONOSPHERE
 J. GEOPHYS. RES., 84, NO. A8, 4165-4174, AUG. 1979.
- KNECHT, R.W. RUSSELL, S.
 PULSED RADIO SOUNDING OF THE TOP-SIDE OF THE IONOSPHERE IN THE
 PRESENCE OF SPREAD F
 J. GEOPHYS. RES., 67, NO. 3, 1178-1182, MAR. 1962.
- KNECHT, R.W. VAN ZANDT, T.E.
 SOME EARLY RESULTS FROM THE IONOSPHERIC TOP-SIDE SOUNDER SATELLITE
 NATURE, 197, NO. 4868, 641-644, FEB. 1963.
- KNECHT, R.W. VAN ZANDT, T.E. RUSSELL, S.
 FIRST PULSED RADIO SOUNDING OF THE TOPSIDE IONOSPHERE
 J. GEOPHYS. RES., 66, NO. 9, 3078-3081, SEPT. 1961.
- KOHNLEIN, W.
 ELECTRON DENSITY MODELS OF THE IONOSPHERE
 REV. GEOPHYS. SPACE PHYS., 16, NO. 3, 341-354, AUG. 1978.
- KRISHNAMURTHY, B.V.
 BEHAVIOR OF TOPSIDE AND BOTTOMSIDE SPREAD F AT EQUATORIAL LATITUDES
 J. GEOPHYS. RES., 71, NO. 19, 4527-4533, OCT. 1966.
- LAWRENCE, R.S. HALLENBECK, M.J.
 METHOD FOR OBTAINING THE PARAMETERS OF ELECTRON DENSITY PROFILES FROM
 TOPSIDE IONOGRAMS
 NATL. BUR. OF STANDARDS, CENT. RADIO PROPAG. LAB., TECH. NOTE 315, BOULDER,
 CO, AUG. 1965.
- LEGG, A.J. NEWMAN, W.S.
 RECEPTION OF GROUND-BASED LORAN TRANSMISSIONS BY THE FIXED-FREQUENCY
 TOPSIDE SOUNDER SATELLITE
 J. ATMOS. TERR. PHYS., 29, 1383-1386, NOV. 1967.
- LEGG, A.J. KING, J.W. PREECE, F.M.
 DIURNAL VARIATIONS OF THE ELECTRON CONCENTRATION IN THE TOPSIDE
 IONOSPHERE AT LOW AND MIDDLE LATITUDES
 J. ATMOS. TERR. PHYS., 29, 1397-1401, NOV. 1967.

- LIN, W.C. MCDIARMID, I.B. BURROWS, J.R.
ELECTRON FLUXES AT 1000-KM ALTITUDE ASSOCIATED WITH AURORAL SUBSTORMS
CAN. J. PHYS., 46, 80-83, JAN. 1968.
- LIU, V.C. JEW, H.
NEAR WAKE OF THE RAREFIED PLASMA FLOWS AT MESOTHERMAL SPEEDS
AIAA, PAPERS, 68-169, NEW YORK, NY, 1968.
- LOCKWOOD, G.E.K.
PLASMA AND CYCLOTRON SPIKE PHENOMENA OBSERVED IN TOP-SIDE IONOGRAMS
CAN. J. PHYS., 41, 190-194, JAN. 1963.
- LOCKWOOD, G.E.K.
EXCITATION OF CYCLOTRON SPIKES IN THE IONOSPHERIC PLASMA
CAN. J. PHYS., 43, 291-297, FEB. 1965.
- LOCKWOOD, G.E.K.
COMPUTER AIDED SYSTEM FOR SCALING TOPSIDE IONOGRAMS
PROC. OF THE IEEE, 57, 986-989, JUNE 1969.
- LOCKWOOD, G.E.K.
MODIFIED ITERATION TECHNIQUE FOR USE IN COMPUTING ELECTRON DENSITY
PROFILES FROM TOPSIDE IONOGRAMS
RADIO SCI., 5, NO. 3, 575-577, MAR. 1970.
- LOCKWOOD, G.E.K.
CALCULATION OF ELECTRON DENSITY PROFILES FROM TOPSIDE IONOGRAMS
METHOD AND APPLICATIONS
IN -- MATHEMATICS OF PROFILE INVERSION, NASA-TM-X-62150, 4-15 THRU 4-26, L.
COLIN, WASH., DC, AUG. 1972.
- LOCKWOOD, G.E.K. PETRIE, L.E.
LOW LATITUDE FIELD ALIGNED IONIZATION OBSERVED BY THE ALOUETTE TOPSIDE
SOUNDER
PLANET. SPACE SCI., 11, 327-330, MAR. 1963.
- LOCKWOOD, G.E.K. NELMS, G.L.
TOPSIDE SOUNDER OBSERVATIONS OF THE EQUATORIAL ANOMALY IN THE 75
DEGREE W LONGITUDINAL ZONE
J. ATMOS. TERR. PHYS., 26, 569-580, MAY 1964.
- LOFTUS, B.T. VANZANDT, T.E. CALVERT, W.
OBSERVATIONS OF CONJUGATE DUCTING BY THE FIXED-FREQUENCY TOPSIDE-
SOUNDER SATELLITE
ANN. DE GEOPHYS., 22, 530-537, OCT-DEC. 1966.
- LUCAS, C. BRICE, N.
IRREGULARITIES IN PROTON DENSITY DEDUCED FROM CYCLOTRON DAMPING OF
PROTON WHISTLERS
J. GEOPHYS. RES., 76, 92-99, JAN. 1971.
- LUND, D.S. HUNSUCKER, R.D.
EXCITATION OF STABLE AURORAL RED ARCS - SIMULTANEOUS HF RADAR,
PHOTOMETER AND ALOUETTE 1 OBSERVATIONS
J. ATMOS. TERR. PHYS., 33, NO. 8, 1177-1183, AUG. 1971.

- LUND, D.S. HUNSUCKER, R.D. BATES, H.F. MURCRAY, W.B.
ELECTRON NUMBER DENSITIES IN AURORAL IRREGULARITIES, COMPARISON OF
BACKSCATTER AND SATELLITE DATA
J. GEOPHYS. RES., 72, 1053-1059, FEB. 1967.
- MAHAJAN, K.K. BRACE, L.H.
LATITUDINAL OBSERVATIONS OF THE THERMAL BALANCE IN THE NIGHTTIME
PROTONOSPHERE
J. GEOPHYS. RES., 74, 5099-5112, OCT. 1969.
- MAHAJAN, K.K. PANDEY, V.K.
ESTIMATION OF H⁺ FLUXES IN THE POLAR REGION
SPACE RES., 14, 347-352, 1974.(PROC. OF THE 14TH COSPAR PLENARY MEET.,
KONSTANZ, WEST GERMANY, MAY 23-JUNE 5, 1974.)
- MAIER, E.J.
EXPLORER 31 TOTAL CURRENT MONITOR EXPERIMENTS
PROC. OF THE IEEE, 57, 1068-1071, JUNE 1969.
- MAIER, E.J. RAO, B.C.N.
OBSERVATIONS OF THE SUPRATHERMAL ELECTRON FLUX AND THE ELECTRON
TEMPERATURE AT HIGH LATITUDES
J. GEOPHYS. RES., 75, 7168-7174, DEC. 1970.
- MAR, J. GARRETT, T.
MECHANICAL DESIGN AND DYNAMICS OF THE ALOUETTE SPACECRAFT
PROC. OF THE IEEE, 57, 882-896, JUNE 1969.
- MATUURA, N. ONDOH, T.
STRUCTURE OF THE TOPSIDE IONOSPHERE DEDUCED FROM ALOUETTE DATA
PROC. OF THE IEEE, 57, NO. 6, 1150-1153, JUNE 1969.
- MATUURA, N. NISHIZAKI, R.
PROTON CYCLOTRON ECHOES IN THE TOPSIDE IONOSPHERE
J. GEOPHYS. RES., 74, 5169-5172, OCT. 1969.
- MAYR, H.G. BRACE, L.H.
SIGNIFICANCE OF THE IONOSPHERE-PROTONOSPHERE COUPLING FOR THE
INTERPRETATION OF TOPSIDE SOUNDER PROFILES
J. GEOPHYS. RES., 75, NO. 13, 2608-2610, MAY 1970.
- MCAFEE, J.R.
RAY TRAJECTORIES IN AN ANISOTROPIC PLASMA NEAR PLASMA RESONANCE
J. GEOPHYS. RES., 73, 5577-5583, SEPT. 1968.
- MCAFEE, J.R.
TOPSIDE RESONANCES AS OBLIQUE ECHOES
J. GEOPHYS. RES., 74, NO. 3, 802-808, FEB. 1969a.
- MCAFEE, J.R.
TOPSIDE RAY TRAJECTORIES NEAR THE UPPER HYBRID RESONANCE
J. GEOPHYS. RES., 74, 6403-6408, DEC. 1969b.
- MCAFEE, J.R.
TOPSIDE PLASMA FREQUENCY RESONANCE BELOW THE CYCLOTRON FREQUENCY
J. GEOPHYS. RES., 75, NO. 22, 4287-4290, AUG. 1970.

- MCAFEE, J.R.
ELECTRON PLASMA RESONANCES IN THE TOPSIDE IONOSPHERE
FUNDAM. COSMIC PHYS., 1, NO. 1-2, 71-117, 1974.
- MCAFEE, J.R. THOMPSON, T.L. CALVERT, W. WARNOCK, J.M.
ROCKET OBSERVATION OF TOPSIDE RESONANCES
J. GEOPHYS. RES., 77, NO. 28, 5542-5550, OCT. 1972.
- MCCLURE, J.P. HANSON, W.B. HOFFMAN, J.H.
PLASMA BUBBLES AND IRREGULARITIES IN THE EQUATORIAL IONOSPHERE
J. GEOPHYS. RES., 82, 2650-2656, JULY 1977.
- MCCULLEY, L.
NUMERICAL METHODS FOR REDUCTION OF TOPSIDE IONOGRAMS
IN -- MATHEMATICS OF PROFILE INVERSION, NASA-TM-X-62150, 4-27 THRU 4-36, L.
COLIN, WASH., DC, AUG. 1972.
- MCDIARMID, I.B. BURROWS, J.R.
HIGH LATITUDE BOUNDARY OF THE OUTER RADIATION ZONE AT 1000 KM
CAN. J. PHYS., 42, 616-626, APR. 1964a.
- MCDIARMID, I.B. BURROWS, J.R.
DIURNAL INTENSITY VARIATIONS IN THE OUTER RADIATION ZONE AT 1000 KM
CAN. J. PHYS., 42, 1135-1148, JUNE 1964b.
- MCDIARMID, I.B. BURROWS, J.R.
ELECTRON FLUXES AT 1000 KILOMETERS ASSOCIATED WITH THE TAIL OF THE
MAGNETOSPHERE
J. GEOPHYS. RES., 70, NO. 13, 3031-3043, JULY 1965.
- MCDIARMID, I.B. BURROWS, J.R.
TEMPORAL VARIATIONS OF OUTER RADIATION ZONE ELECTRON INTENSITIES AT 1000
KM
CAN. J. PHYS., 44, 1361-1379, JAN. 1966.
- MCDIARMID, I.B. BURROWS, J.R.
DEPENDENCE OF THE POSITION OF THE OUTER RADIATION ZONE INTENSITY
MAXIMA ON ELECTRON ENERGY AND MAGNETIC ACTIVITY
CAN. J. PHYS., 45, 2873-2878, SEPT. 1967.
- MCDIARMID, I.B. BURROWS, J.R.
LOCAL TIME ASYMMETRIES IN THE HIGH-LATITUDE BOUNDARY OF THE OUTER
RADIATION ZONE FOR THE DIFFERENT ELECTRON ENERGIES
CAN. J. PHYS., 46, 49-57, JAN. 1968.
- MCDIARMID, I.B. WILSON, M.D.
DEPENDENCE OF THE HIGH LATITUDE ELECTRON (E GREATER THAN 35 KEV)
BOUNDARY ON THE ORIENTATION OF THE GEOMAGNETIC AXIS
J. GEOPHYS. RES., 73, NO. 23, 7237-7244, DEC. 1968.
- MCDIARMID, I.B. BURROWS, J.R.
RELATION OF SOLAR PROTON LATITUDE PROFILES TO OUTER RADIATION ZONE
ELECTRON MEASUREMENTS
J. GEOPHYS. RES., 74, 6239-6246, DEC. 1969.
- MCDIARMID, I.B. BURROWS, J.R.
LATITUDE PROFILES OF LOW-ENERGY SOLAR ELECTRONS
J. GEOPHYS. RES., 75, 3910-3914, JULY 1970.

- MCDIARMID, I.B. BURROWS, J.R. BUDZINSKI, E.E. ROSE, D.C.
 SATELLITE MEASUREMENTS IN THE 'STARFISH' ARTIFICIAL RADIATION ZONE
 CAN. J. PHYS., 41, 1332-1345, AUG. 1963a.
- MCDIARMID, I.B. BURROWS, J.R. BUDZINSKI, E.E. WILSON, M.D.
 SOME AVERAGE PROPERTIES OF THE OUTER RADIATION ZONE AT 1000 KM
 CAN. J. PHYS., 41, 2064-2079, DEC. 1963b.
- MCDIARMID, I.B. BURROWS, J.R. WILSON, M.D.
 MORPHOLOGY OF OUTER RADIATION ZONE ELECTRON ACCELERATION MECHANISMS
 J. GEOPHYS. RES., 74, 1749-1758, APR. 1969a.
- MCDIARMID, I.B. BURROWS, J.R. WILSON, M.D.
 DAWN DUSK ASYMMETRIES IN THE OUTER RADIATION ZONE AT MAGNETICALLY
 QUIET TIMES
 J. GEOPHYS. RES., 74, 3554-3560, JULY 1969b.
- MCDIARMID, I.B. BURROWS, J.R. WILSON, M.D.
 STRUCTURE OBSERVED IN SOLAR PARTICLE LATITUDE PROFILES AND ITS
 DEPENDENCE ON RIGIDITY
 J. GEOPHYS. RES., 76, 227-231, JAN. 1971.
- MCDIARMID, I.B. BURROWS, J.R. WILSON, M.D.
 SOLAR PARTICLES AND THE DAYSIDE LIMIT OF CLOSED FIELD LINES
 J. GEOPHYS. RES., 77, 1103-1108, MAR. 1972.
- MCEWEN, D.J. BARRINGTON, R.E.
 SOME CHARACTERISTICS OF THE LOWER HYBRID RESONANCE NOISE BANDS
 OBSERVED BY THE ALOUETTE 1 SATELLITE
 CAN. J. PHYS., 45, 13-19, JAN. 1967.
- MCEWEN, D.J. BARRINGTON, R.E.
 ION COMPOSITION BELOW 3000 KM DERIVED FROM ION WHISTLER OBSERVATIONS
 SPACE RES., 8, 396-404, 1968. (PROC. OF THE 10TH COSPAR PLENARY MEETING,
 LONDON, ENGLAND, JULY 25-28, 1967).
- MCILWAIN, C.E.
 COORDINATES FOR MAPPING THE DISTRIBUTION OF MAGNETICALLY TRAPPED
 PARTICLES
 J. GEOPHYS. RES., 66, 3681-3691, NOV. 1961.
- MILLER, N.J.
 SOME IMPLICATIONS OF SATELLITE SPIN EFFECTS IN CYLINDRICAL PROBE
 MEASUREMENTS
 J. GEOPHYS. RES., 77, 2851-2861, JUNE 1972.
- MOLOZZI, A.R. RICHARDSON, J.R.
 MEASURED IMPEDANCE OF A DIPOLE ANTENNA IN THE IONOSPHERE
 SPACE RES., 7, 1, 489-505, 1967. (PROC. OF THE 7TH INTERN. SPACE SCI. SYMP.,
 VIENNA, AUSTRIA, MAY 10-18, 1966, R.L. SMITH-ROSE, NORTH-HOLLAND PUBL. CO.,
 AMSTERDAM, NETHERLANDS).
- MOLOZZI, A.R. FRANKLIN, C.A. TYAS, J.P.I.
 COSMIC NOISE MEASUREMENTS FROM 1960 *ETA 1 AT 3.8 MC./S.
 NATURE, 190, NO. 4776, 616-617, MAY 1961.

- MOSS, S.J. HYMAN, E.
 MINIMUM VARIANCE TECHNIQUE FOR THE ANALYSIS OF IONOSPHERIC DATA
 ACQUIRED IN SATELLITE RETARDING POTENTIAL ANALYZER EXPERIMENTS
 J. GEOPHYS. RES., 73, 4315-4323, JULY 1968.
- MULDREW, D.B.
 RADIO PROPAGATION ALONG MAGNETIC FIELD-ALIGNED SHEETS OF IONIZATION
 OBSERVED BY THE ALOUETTE TOPSIDE SOUNDER
 J. GEOPHYS. RES., 68, NO. 19, 5355-5370, OCT. 1963.
- MULDREW, D.B.
 F LAYER IONIZATION TROUGHS DEDUCED FROM ALOUETTE DATA
 J. GEOPHYS. RES., 70, NO. 11, 2635-2650, JUNE 1965.
- MULDREW, D.B.
 DELAYED GENERATION OF AN ELECTROMAGNETIC PULSE IN THE TOPSIDE IONOSPHERE
 J. GEOPHYS. RES., 72, NO. 15, 3777-3794, AUG. 1967a.
- MULDREW, D.B.
 MEDIUM FREQUENCY CONJUGATE ECHOES OBSERVED ON TOPSIDE-SOUNDER DATA
 CAN. J. PHYS., 45, 3935-3944, DEC. 1967b.
- MULDREW, D.B.
 ELECTROSTATIC RESONANCES ASSOCIATED WITH THE MAXIMUM FREQUENCIES OF
 CYCLOTRON-HARMONIC WAVES
 J. GEOPHYS. RES., 77, NO. 10, 1794-1801, APR. 1972a.
- MULDREW, D.B.
 ELECTRON RESONANCES OBSERVED WITH TOPSIDE SOUNDERS
 RADIO SCI., 7, NO. 8-9, 779-789, AUG.-SEPT. 1972b.
- MULDREW, D.B.
 FORMATION OF DUCTS AND SPREAD F AND THE INITIATION OF BUBBLES BY FIELD
 ALIGNED CURRENTS
 J. GEOPHYS. RES., 85, NO. A2, 613-625, FEB. 1980.
- MULDREW, D.B. HAGG, E.L.
 NOVEL IONOSPHERIC CYCLOTRON RESONANCE PHENOMENON OBSERVED ON
 ALOUETTE 1 DATA
 CAN. J. PHYS., 44, 925-939, MAY 1966.
- MULDREW, D.B. HAGG, E.L.
 PROPERTIES OF HIGH-LATITUDE IONOSPHERIC DUCTS DEDUCED FROM ALOUETTE 2
 TWO-HOP ECHOES
 PROC. OF THE IEEE, 57, 1128-1134, JUNE 1969.
- MULDREW, D.B. HAGG, E.L.
 STIMULATION OF IONOSPHERIC-RESONANCE ECHOES BY THE ALOUETTE II
 SATELLITE
 IN -- PLASMA WAVES IN SPACE AND IN THE LAB., 2, 55-68, J.O. THOMAS, AM. ELSEVIER
 PUBL. CO., NEW YORK, NY, 1970.
- MULDREW, D.B. ESTABROOKS, M.F.
 COMPUTATION OF DISPERSION CURVES FOR A HOT MAGNETOPLASMA WITH
 APPLICATION TO THE UPPER-HYBRID AND CYCLOTRON FREQUENCIES
 RADIO SCI., 7, NO. 5, 579-586, MAY 1972.

- MULDREW, D.B. LITWACK, M.D. TIMLECK, P.L.
 INTERPRETATION OF THE STATISTICS OF OCCURRENCE OF ALOUETTE 1 EARTH
 ECHOES
 PLANET. SPACE SCI., 15, 611-618, APR. 1967.
- MUZZIO, J.L.R. RAMINEZ PARDO, P. DE MENDONCA, F.
 MEASUREMENTS OF THE EARTH'S TOTAL MAGNETIC FIELD AT HEIGHTS OF 1000 KM
 IN THE BRAZILIAN ANOMALY
 SPACE RES., 6, 217-221, 1966 (PROC. OF THE 6TH INT. SPACE SCI. SYMP., MAR DEL
 PLATA, ARGENTINA, MAY 11-19, 1965).
- NELMS, G.L.
 IONOSPHERIC RESULTS FROM THE TOPSIDE SOUNDER SATELLITE ALOUETTE
 SPACE RES., 4, 437-448, 1964. (PROC. OF THE 4TH INTERN. SPACE SCI. SYMP.,
 WARSAW, POLAND, JUNE 4-10, 1963).
- NELMS, G.L.
 SEASONAL AND DIURNAL VARIATIONS OF THE DISTRIBUTION OF ELECTRON
 DENSITY IN THE TOPSIDE OF THE IONOSPHERE
 IN -- ELECTRON DENSITY PROFILES IN IONOS. AND EXOS., 358-386, J. FRIHAGEN,
 NORTH-HOLLAND PUBL. CO., AMSTERDAM, THE NETHERLANDS, 1966.
- NELMS, G.L. LOCKWOOD, G.E.K.
 EARLY RESULTS FROM THE TOPSIDE SOUNDER IN THE ALOUETTE 2 SATELLITE
 SPACE RES., 7, 604-623, 1967. (PROC. OF THE 7TH INTERN. SPACE SCI. SYMP.,
 VIENNA, AUSTRIA, MAY 10-18, 1966).
- NELMS, G.L. CHAPMAN, J.H.
 HIGH LATITUDE IONOSPHERE - RESULTS FROM ALOUETTE/ISIS TOPSIDE SOUNDERS
 IN -- POLAR IONOSPHERE AND MAGNETOSPHERIC PROCESSES, 233-269, GORDON AND
 BREACH, SCI. PUBL., NEW YORK, NY, 1970.
- NISBET, J.S.
 ON THE CONSTRUCTION AND USE OF A SIMPLE IONOSPHERIC MODEL
 RADIO SCI., 6, NO. 4, 437-464, APR. 1971.
- NISHIDA, A.
 AVERAGE STRUCTURE AND STORM-TIME CHANGE OF THE POLAR TOPSIDE
 IONOSPHERE AT SUNSPOT MINIMUM
 J. GEOPHYS. RES., 72, NO. 23, 6051-6061, DEC. 1967.
- NORTON, R.B. FINDLAY, J.A.
 ELECTRON DENSITY AND TEMPERATURE IN THE VICINITY OF THE 29 SEPTEMBER
 1967 MIDDLE LATITUDE RED ARC
 PLANET. SPACE SCI., 17, 1867-1877, NOV. 1969.
- ONDOH, T.
 MORPHOLOGY OF DISTURBED TOPSIDE IONOSPHERE FOR 1962-1964
 RADIO RES. LAB. J., 14, 267-279, NOV. 1967.
- OYA, H.
 SEQUENCE OF DIFFUSE PLASMA RESONANCES OBSERVED ON ALOUETTE II
 IONOGRAMS
 J. GEOPHYS. RES., 75, 4279-4285, AUG. 1970.

- OYA, H.
 VERIFICATION OF THEORY ON WEAK TURBULENCE RELATING TO THE SEQUENCE OF
 DIFFUSE PLASMA RESONANCES IN SPACE
 PHYS. FLUIDS, 14, NO. 11, 2487-2499, NOV. 1971.
- OYA, H.
 GENERATION MECHANISM OF PROTON CYCLOTRON ECHOES DUE TO PULSED RADIO
 FREQUENCY WAVES IN SPACE PLASMA
 J. GEOPHYS. RES., 83, NO. A5, 1991-2008, MAY 1978.
- OYA, H. BENSON, R.F.
 NEW METHOD FOR IN-SITU ELECTRON TEMPERATURE DETERMINATIONS FROM
 PLASMA WAVE PHENOMENA
 J. GEOPHYS. RES., 77, 4272-4276, AUG. 1972.
- PAGHIS, I.
 IONOSPHERIC RESONANCE PHENOMENA AT VHF AND HF, AND THEIR EFFECTS ON
 SPACE TELECOMMUNICATIONS
 IN -- PROPAGATION FACTORS IN SPACE COMMUNICATIONS, 133159, W. T.
 BLACKLAND, AGARD, PARIS, FRANCE, 1967.
- PAGHIS, I. FRANKLIN, C.A. MAR, J.
 ALOUETTE 1 THE FIRST THREE YEARS IN ORBIT
 DEF. RES. TELECOMMUN. ESTABL., REP. NO. 1159, OTTAWA, CAN., MAR. 1967.
- PANDEY, V.K. MAHAJAN, K.K.
 LATITUDINAL DISTRIBUTION OF ELECTRON CONCENTRATION FROM THE ALOUETTE II
 TOPSIDE SOUNDER
 INDIAN J. RADIO SPACE PHYS., 2, 134-138, JUNE 1973.
- PARKES, E.J.
 ANALYTICAL STUDY OF THE OBLIQUE ECHO MODEL FOR THE TOPSIDE PLASMA
 RESONANCE
 J. PLASMA PHYS., 12, PT. 2, 199-216, OCT. 1974.
- PETRIE, L.E.
 TOPSIDE SPREAD ECHOES
 CAN. J. PHYS., 41, 194-195, JAN. 1963.
- PETRIE, L.E.
 PRELIMINARY RESULTS ON MID AND HIGH LATITUDE TOPSIDE SPREAD F
 IN -- SPREAD F AND ITS EFFECTS ON RADIOWAVE PROPAG. AND COMMUN., 67-77, P.
 NEWMAN, TECHNIVISION, MAIDENHEAD, ENGL., 1966.
- PETRIE, L.E. LOCKWOOD, G.E.K.
 ON THE PREDICTION OF F-LAYER PENETRATION FREQUENCIES
 PROC. OF THE IEEE, 57, 1025-1028, JUNE 1969.
- POEVERLEIN, H.
 RAY PATHS OF RADIO WAVES IN THE IONOSPHERE
 Z. ANGEW. PHYS., 1, NO. 11, 517-525, OCT. 1949.
- RAMASASTRY, J.
 CHARACTERISTICS OF MAGNETOSPHERIC DUCTS OBSERVED BY THE ALOUETTE-2
 TOPSIDE SOUNDER
 J. GEOPHYS. RES., 76, NO. 22, 5352-5357, AUG. 1971.

- RAMASASTRY, J. WALSH, E.J.
 CONJUGATE ECHOES OBSERVED BY ALOUETTE 2 TOPSIDE SOUNDER AT THE
 LONGITUDES OF SINGAPORE
 J. GEOPHYS. RES., 74, NO. 24, 5665-5674, NOV. 1969.
- RAO, B.C.N. DONLEY, J.L.
 PHOTOELECTRON FLUX IN THE TOPSIDE IONOSPHERE MEASURED BY RETARDING
 POTENTIAL ANALYZERS
 J. GEOPHYS. RES., 74, 1715-1719, APR. 1969.
- RAO, B.C.N. MAIER, E.J.R.
 PHOTOELECTRON FLUX AND PROTONOSPHERIC HEATING DURING THE CONJUGATE
 POINT SUNRISE
 J. GEOPHYS. RES., 75, 816-822, FEB. 1970.
- RAO, B.C.N. SINGH, R. MAIER, E.J.
 OBSERVATIONS OF THE NIGHTTIME ELECTRON VOLT RANGE ELECTRON FLUXES IN
 THE EQUATORIAL REGION
 J. GEOPHYS. RES., 79, 305-306, JAN. 1974.
- REINISCH, B.W. HUANG, X.
 AUTOMATIC CALCULATION OF ELECTRON DENSITY PROFILES FROM DIGITAL
 IONOGRAMS 1. AUTOMATIC O AND X TRACE IDENTIFICATION FOR TOPSIDE
 IONOGRAMS
 RADIO SCI., 17, NO. 2, 421-434, APR. 1982.
- ROBLE, R.G. HAYS, P.B. NAGY, A.F.
 COMPARISON OF CALCULATED AND OBSERVED FEATURES OF A STABLE
 MIDLATITUDE RED ARC
 J. GEOPHYS. RES., 75, 4261-4265, AUG. 1970.
- ROBLE, R.G. NORTON, R.B. FINDLAY, J.A. MAROVICH, E.
 CALCULATED AND OBSERVED FEATURES OF STABLE AURORAL RED ARCS DURING
 THREE GEOMAGNETIC STORMS
 J. GEOPHYS. RES., 76, 7648-7662, NOV. 1971.
- RUSH, C.M. RUSH, S.V. LYONS, L.R. VENKATESWARAN, S.V.
 EQUATORIAL ANOMALY DURING A PERIOD OF DECLINING SOLAR ACTIVITY
 RADIO SCI., 4, NO. 9, 829-841, SEPT. 1969.
- RUSSELL, S. ZIMMER, F.C.
 DEVELOPMENT OF THE FIXED-FREQUENCY TOPSIDE-SOUNDER SATELLITE
 PROC. OF THE IEEE, 57, 876-881, JUNE 1969.
- RYCROFT, M.J. THOMAS, J.O.
 MAGNETOSPHERIC PLASMAPAUSE AND ELECTRON DENSITY TROUGH AT ALOUETTE 1
 ORBIT
 PLANET. SPACE SCI., 18, NO. 1, 65-80, JAN. 1970.
- RYCROFT, M.J. BURNELL, S.J.
 STATISTICAL ANALYSIS OF MOVEMENTS OF THE IONOSPHERIC TROUGH AND THE
 PLASMAPAUSE
 J. GEOPHYS. RES., 75, NO. 28, 5600-5604, OCT. 1970.
- SAMIR, U.
 POSSIBLE EXPLANATION OF AN ORDER OF MAGNITUDE DISCREPANCY IN
 ELECTRON-WAKE MEASUREMENTS
 J. GEOPHYS. RES., 75, 855-858, FEB. 1970.

- SAMIR, U. WRENN, G.L.
DEPENDENCE OF CHARGE AND POTENTIAL DISTRIBUTION AROUND A SPACECRAFT
ON IONIC COMPOSITION
PLANET. SPACE SCI., 17, 693-706, APR. 1969.
- SAMIR, U. WRENN, G.L.
EXPERIMENTAL EVIDENCE OF AN ELECTRON TEMPERATURE ENHANCEMENT IN THE
WAKE OF AN IONOSPHERIC SATELLITE
PLANET. SPACE SCI., 20, 899-904, JUNE 1972.
- SAMIR, U. JEW, H.
COMPARISON OF THEORY WITH EXPERIMENT FOR ELECTRON DENSITY
DISTRIBUTION IN THE NEAR WAKE OF AN IONOSPHERIC SATELLITE
J. GEOPHYS. RES., 77, NO. 34, 6819-6827, DEC. 1972.
- SAMIR, U. MAIER, E.J. TROY, B.E., JR.
ANGULAR DISTRIBUTION OF ION FLUX AROUND AN IONOSPHERIC SATELLITE
J. ATMOS. TERR. PHYS., 35, 513-519, MAR. 1973.
- SAMIR, U. FIRST, M. MAIER, E.J. TROY, B., JR.
COMPARISON OF THE GUREVICH ET AL. AND THE LIU-JEW WAKE MODELS FOR THE
ION FLUX AROUND A SATELLITE
J. ATMOS. TERR. PHYS., 37, 577-586, APR. 1975.
- SATO, T.
ELECTRON CONCENTRATION VARIATIONS IN THE TOPSIDE IONOSPHERE BETWEEN 60
DEGREES NORTH AND 60 DEGREES SOUTH GEOMAGNETIC LATITUDE ASSOCIATED
WITH GEOMAGNETIC DISTURBANCES
J. GEOPHYS. RES., 73, NO. 19, 6225-6241, OCT. 1968.
- SATO, T. COLIN, L.
MORPHOLOGY OF ELECTRON CONCENTRATION ENHANCEMENT AT A HEIGHT OF 1000
KILOMETERS AT POLAR LATITUDES
J. GEOPHYS. RES., 74, NO. 9, 2193-2207, MAY 1969.
- SCHMID, P.E. BENT, R.B. LLEWELLYN, S.K. NESTERCZUK, G., RANGASWAMY, S.
NASA-GSFC IONOSPHERIC CORRECTIONS TO SATELLITE TRACKING DATA
NASA GSFC, TM-X-70608, X-591-73-281, GREENBELT, MD, DEC. 1973.
- SHARMA, R.P. MULDREW, D.B.
LUNAR EFFECT IN THE OCCURRENCE OF CONJUGATE ECHOES ON TOPSIDE SOUNDER
IONOGRAMS
J. GEOPHYS. RES., 78, NO. 34, 8251-8260, DEC. 1973.
- SHARMA, R.P. MULDREW, D.B.
SEASONAL AND LONGITUDINAL VARIATIONS IN THE OCCURRENCE FREQUENCY
OF MAGNETOSPHERIC IONIZATION DUCTS
J. GEOPHYS. RES., 80, NO. 7, 977-984, MAR. 1975.
- SHARMA, R.P. HEWENS, E.J.
STUDY OF THE EQUATORIAL ANOMALY AT AMERICAN LONGITUDES DURING
SUNSPOT MINIMUM
J. ATMOS. TERR. PHYS., 38, NO. 5, 475-484, MAY 1976.
- SHAWHAN, S.D. BLOCK, L.P. FALTHAMMAR, C.G.
CONJUGATE PHOTOELECTRON IMPACT IONIZATION
J. ATMOS. TERR. PHYS., 32, 1885-1900, DEC. 1970.

- SHKAROFSKY, I.P.
HIGHER ORDER CYCLOTRON HARMONIC RESONANCES AND THEIR OBSERVATION IN
THE LABORATORY AND IN THE IONOSPHERE
J. GEOPHYS. RES., 73, NO. 15, 4859-4867, AUG. 1968.
- SHMOYS, J.
MULTIPATH EFFECTS IN TOPSIDE SOUNDING IN IONOSPHERIC DUCTS
J. GEOPHYS. RES., 74, NO. 9, 2265-2270, MAY 1969.
- SINGLETON, D.G.
MORPHOLOGY OF SPREAD-F OCCURRENCE OVER HALF A SUNSPOT CYCLE
J. GEOPHYS. RES., 73, NO. 1, 295-308, JAN. 1968.
- SMART, D.F. SHEA, M.A. GALL, R.
DAILY VARIATION OF TRAJECTORY-DERIVED HIGH-LATITUDE CUTOFF RIGIDITIES IN
A MODEL MAGNETOSPHERE
J. GEOPHYS. RES., 74, NO. 19, 4731-4738, SEPT. 1969.
- SMITH, P.A.
DETERMINATION OF VERTICAL DISTRIBUTIONS OF PLASMA TEMPERATURE AND
COMPOSITION FROM SATELLITE MEASUREMENTS
J. ATMOS. TERR. PHYS., 30, 1203-1209, JUNE 1968.
- SMITH, P.A. KAISER, B.A.
ESTIMATES OF IONOSPHERIC COMPOSITION AND TEMPERATURE DERIVED FROM
TOPSIDE SOUNDER ELECTRON SCALE HEIGHT DATA
J. ATMOS. TERR. PHYS., 29, 1345-1353, NOV. 1967.
- SMITH, P.A. KING, J.W.
CHANGES IN THE TOPSIDE IONOSPHERE DURING SOLAR ECLIPSES
IN -- SOLAR ECLIPSES AND THE IONOSPHERE, UNNUMBERED, 285-298,
M ANASTASSIADES, PLENUM PRESS, NEW YORK, NY, 1969.
- SMITH, R.L.
PROPERTIES OF THE OUTER IONOSPHERE DEDUCED FROM NOSE WHISTLERS
J. GEOPHYS. RES., 66, NO. 11, 3709-3716, NOV. 1961.
- SMITH, R.L. BRICE, N.M. KATSUFRAKIS, J. GURNETT, D.A. BARRINGTON, R.E. SHAWHAN,
S.D. BELROSE, J.S.
ION GYROFREQUENCY PHENOMENON OBSERVED IN SATELLITES
NATURE, 204, NO. 4955, 274-275, OCT. 1964.
- SMITH, R.L. KIMURA, I. VIGNERON, J. KATSUFRAKIS, J.
LOWER HYBRID RESONANCE NOISE AND A NEW IONOSPHERIC DUCT
J. GEOPHYS. RES., 71, NO. 7, 1925-1927, APR. 1966.
- SOICHER, H.
TOPSIDE IONOSPHERE AT MIDLATITUDES DURING LOCAL SUNRISE
J. ATMOS. TERR. PHYS., 35, 657-668, APR. 1973.
- STIX, T.H.
THEORY OF PLASMA WAVES
MCGRAW HILL, NEW YORK, NY, 1962.

- TAYLOR, G.N. WRENN, G.L.
COMPARISONS OF SIMULTANEOUS SATELLITE AND GROUND-BASED
MEASUREMENTS OF IONOSPHERIC PARAMETERS
PLANET. SPACE SCI., 18, 1663-1666, NOV. 1970.
- THOMAS, J.A. SMITH, E.K.
SURVEY OF THE PRESENT KNOWLEDGE OF SPORADIC-E IONIZATION
J. ATMOS. TERR. PHYS., 13, 295-314, FEB. 1959.
- THOMAS, J.O. SADER, A.Y.
ALOUETTE TOPSIDE SOUNDINGS MONITORED AT STANFORD UNIVERSITY
STANFORD U., RADIO SCI. LAB., ELECTRON LAB., TECH. REPT. NO. 6, SEL-64-007,
STANFORD, CA, DEC. 1963.
- THOMAS, J.O. SADER, A.Y.
ELECTRON DENSITY AT THE ALOUETTE ORBIT
J. GEOPHYS. RES., 69, NO. 21, 4561-4581, NOV. 1964.
- THOMAS, J.O. DUFOUR, S.W.
ELECTRON DENSITY IN THE WHISTLER MEDIUM
NATURE, 206, NO. 4984, 567-571, MAY 1965.
- THOMAS, J.O. ANDREWS, M.K.
TRANSPOLAR EXOSPHERIC PLASMA, 3 - A UNIFIED PICTURE
PLANET. SPACE SCI., 17, 433-446, MAR. 1969.
- THOMAS, J.O. RYCROFT, M.J.
EXOSPHERIC PLASMA DURING THE INTERNATIONAL YEARS OF THE QUIET SUN
PLANET. SPACE SCI., 18, NO. 1, 41-63, JAN. 1970.
- THOMAS, J.O. LONG, A.R. WESTOVER, D.
CALCULATION OF ELECTRON DENSITY PROFILES FROM TOPSIDE SOUNDER RECORDS
J. GEOPHYS. RES., 68, NO. 10, 3237-3242, MAY 1963.
- THOMAS, J.O. RYCROFT, M.J. COLIN, L. CHAN, K.L.
TOPSIDE IONOSPHERE
IN -- ELECTRON DENSITY PROFILES IN IONOS. AND EXOS., 298-357, J. FRIHAGEN,
NORTH-HOLLAND PUBL. CO., AMSTERDAM, THE NETHERLANDS, 1966.
- TIMLECK, P.L. NELMS, G.L.
ELECTRON DENSITIES LESS THAN 100 ELECTRON CM-3 IN THE TOPSIDE IONOSPHERE
PROC. OF THE IEEE, 57, 1164-1171, JUNE 1969.
- TITHERIDGE, J.E.
PLASMA TEMPERATURES FROM ALOUETTE 1 ELECTRON DENSITY PROFILES
PLANET. SPACE SCI., 24, 247-259, MAR. 1976a.
- TITHERIDGE, J.E.
ION TRANSITION HEIGHTS FROM TOPSIDE ELECTRON DENSITY PROFILES
PLANET. SPACE SCI., 24, 229-245, MAR. 1976b.
- TITHERIDGE, J.E.
DIRECT ESTIMATES OF SCALE HEIGHT FROM TOPSIDE IONOGRAMS
J. ATMOS. TERR. PHYS., 38, 623-626, JUNE 1976c.
- TITHERIDGE, J.E.
IONOSPHERIC HEATING BENEATH THE MAGNETOSPHERIC CLEFT
J. GEOPHYS. RES., 81, NO. 19, 3221-3226, JULY 1976d.

- TITHERIDGE, J.E.
 PLASMAPAUSE EFFECTS IN THE TOP SIDE IONOSPHERE
 J. GEOPHYS. RES., 81, NO. 19, 3227-3233, JULY 1976e.
- TROY, B.E., JR. MAIER, E.J. SAMIR, U.
 ELECTRON TEMPERATURES IN THE WAKE OF AN IONOSPHERIC SATELLITE
 J. GEOPHYS. RES., 80, NO. 7, 993-997, MARCH 1975.
- VASSEUR, G. FELSTEIN, R.
 CALCULATION OF IONIZATION PROFILES FROM TOPSIDE AND BOTTOMSIDE
 IONOSPHERIC SOUNDINGS
 ANN. DES TELECOMM., 23, 183-194, JULY-AUG. 1968.
- VILA, P.
 INTERTROPICAL F2 IONIZATION DURING JUNE AND JULY 1966
 RADIO SCI., 6, NO. 7, 689-697, JULY 1971.
- WALKER, G.O. CHAN, C.S.
 DIURNAL VARIATION OF THE EQUATORIAL ANOMALY IN THE TOPSIDE IONOSPHERE
 AT SUNSPOT MAXIMUM
 J. ATMOS. TERR. PHYS., 38, NO. 7, 699-706, JULY 1976.
- WALTER, F. ANGERAMI, J.J.
 NONDUCTED MODE OF VLF PROPAGATION BETWEEN CONJUGATE HEMISPHERES -
 OBSERVATIONS ON OGO'S 2 AND 4 OF THE 'WALKING-TRACE' WHISTLER AND OF
 DOPPLER SHIFTS IN FIXED FREQUENCY TRANSMISSIONS
 J. GEOPHYS. RES., 74, 6352-6370, DEC. 1969.
- WARNOCK, J.M. MCAFEE, J.R. THOMPSON, T.L.
 ELECTRON TEMPERATURE FROM TOPSIDE PLASMA RESONANCE OBSERVATIONS
 J. GEOPHYS. RES., 75, 7272-7275, DEC. 1970.
- WARREN, E.S.
 PERTURBATION OF THE LOCAL ELECTRON DENSITY BY ALOUETTE SATELLITE
 CAN. J. PHYS., 41, 188-189, JAN. 1963.
- WARREN, E.S. HAGG, E.L.
 OBSERVATION OF ELECTROSTATIC RESONANCES OF THE IONOSPHERIC PLASMA
 NATURE, 220, NO. 5166, 466-468, NOV. 1968.
- WATT, T.M.
 ION DISTRIBUTION AND TEMPERATURE IN THE TOPSIDE IONOSPHERE OBTAINED
 FROM THE ALOUETTE SATELLITE
 J. GEOPHYS. RES., 70, NO. 23, 5849-5859, DEC. 1965.
- WATT, T.M.
 CORRELATION OF PLASMA SCALE HEIGHT WITH KP IN THE TOPSIDE IONOSPHERE
 J. GEOPHYS. RES., 71, NO. 13, 3131-3140, JULY 1966.
- WATT, T.M.
 OBTAINING LOCAL VALUES OF PLASMA SCALE HEIGHT WITH THE ALOUETTE 1
 TOPSIDE SOUNDER
 J. GEOPHYS. RES., 72, NO. 16, 3843-3853, AUG. 1967.

- WATT, T.M.
VERTICAL INCIDENCE PULSE DISPERSION WITH APPLICATIONS TO THE ALOUETTE 1
TOPSIDE SOUNDER
J. GEOPHYS. RES., 74, NO. 11, 2972-2981, JUNE 1969.
- WATT, T.M.
TOPSIDE IONOSPHERE AT SUNRISE
J. GEOPHYS. RES., 76, NO. 13, 3095-3105, MAY 1971.
- WHITTEKER, J.H.
COMPARISON OF THE BEAT METHOD OF DETERMINING LOW ELECTRON DENSITIES
FROM TOPSIDE IONOGRAMS WITH THE PLASMA-FREQUENCY RESONANCE METHOD
RADIO SCI., 13, NO. 6, 1047-1051, NOV.-DEC. 1978.
- WRENN, G.L.
LANGMUIR PLATE AND SPHERICAL ION PROBE EXPERIMENTS ABOARD EXPLORER 31
PROC. OF THE IEEE, 57, 1072-1077, JUNE 1969.
- WRENN, G.L. SMITH, P.A.
RESULTS DERIVED FROM SIMULTANEOUS MEASUREMENTS USING THE LANGMUIR
PLATE AND SPHERICAL ION PROBE ON EXPLORER 31 AND THE IONOSONDE ON
ALOUETTE 2
PROC. OF THE IEEE, 57, 1085-1089, JUNE 1969.
- WRENN, G.L. SHEPHERD, G.G.
CONJUGATE POINT EFFECT OBSERVED FOR ELECTRON TEMPERATURES IN THE 1000-
2500 KM HEIGHT RANGE
J. ATMOS. TERR. PHYS., 31, 1383-1389, DEC. 1969.



